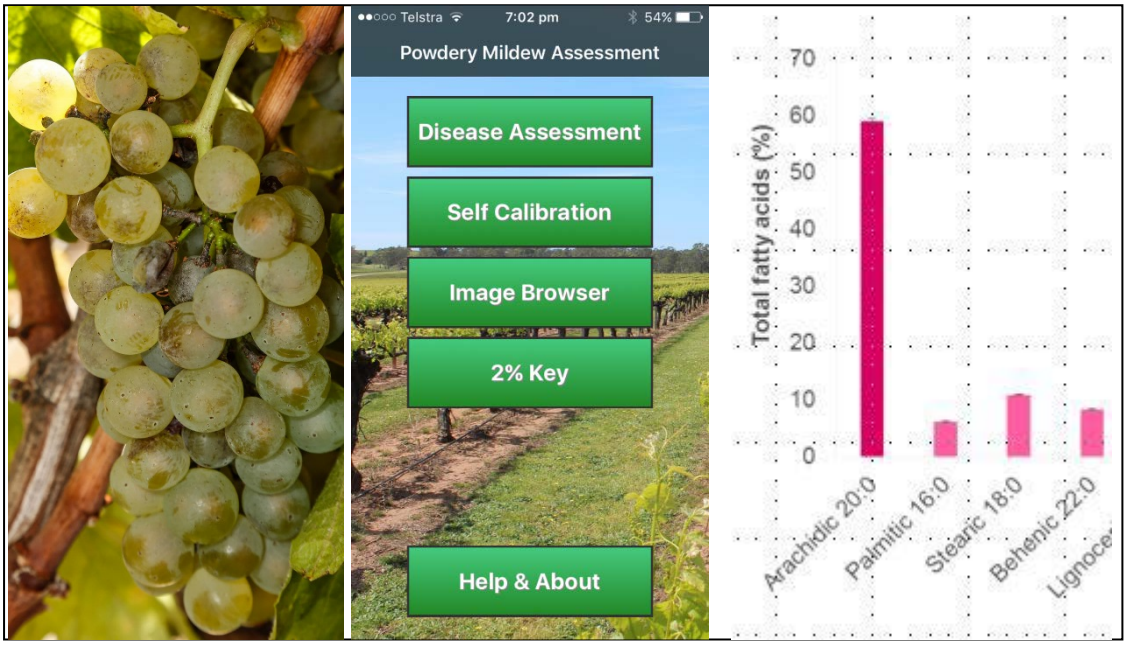
Australian Government

Australian Grape and Wine Authority

THE UNIVERSITY of ADELAIDE

OBJECTIVE MEASURES FOR POWDERY MILDEW



FINAL REPORT to

AUSTRALIAN GRAPE AND WINE AUTHORITY

Project Number: **UA1202**

Principal Investigator: **Eileen Scott**

Research Organisation: **The University of Adelaide**

Date: **December 2016**

Objective measures for powdery mildew

Authors

Prof Eileen S. Scott, Dr Tijana Petrovic, Dr Olena Kravchuk and Mr Timothy Zanker
School of Agriculture, Food and Wine, Waite Campus, The University of Adelaide, PMB 1, Glen Osmond, SA 5064

Dr Robert W. Emmett, RW Emmett Horticultural Pathology Research Pty Ltd, Mildura, Victoria

Dr Katherine J. Evans, Tasmanian Institute of Agriculture and University of Tasmania, Hobart, Tasmania

Corresponding author

Eileen S. Scott

Email: eileen.scott@adelaide.edu.au

Telephone: +61 8 8313 7266

Citing this report

This report may be cited as Scott ES et al. (2016) Objective measures for powdery mildew. Final report to the Australian Grape and Wine Authority, UA1202. The University of Adelaide, 100 pp

Disclaimer

This publication may be of assistance to you but the authors and their employers do not guarantee that the publication is without flaw of any kind or is wholly appropriate for your particular purposes and therefore disclaim all liability for any error, loss or other consequence which may arise from you relying on any information in this publication.

Copyright

© The University of Adelaide 2016

Acknowledgements

Research in the project reported here was supported by Wine Australia and the School of Agriculture, Food and Wine of The University of Adelaide, both of which are gratefully acknowledged. Wine Australia project managers Sharon Harvey, Elise Heyes, Adrian Loschiavo and Liz Waters provided valuable advice and support and at least one of them took part in each Project Steering Group meeting.

The extensive in-kind support provided by Accolade Wines was greatly appreciated. Thanks to Warren Birchmore, Chris Bevin and other staff who participated in the Project Steering Group, arranged and collected grape samples from commercial vineyards, and tested prototypes of PMapp and the supporting online resource.

Wade Perry, Lemur Software, developed the software for PMapp, created the software to generate diagrams of bunches, provided valuable guidance on content and managed release of the app. Milos Novakovic developed a proof-of-concept version of the area assessment tool component of the online resource. Petros Bakopoulos and Harry Lucas, GrapeBrain (then trading as Seer Insights), developed the code for the online resource and Bruno Carrocci, Edward Bittner and Bahareh Dehghanian of Arris Pty Ltd assisted with refining the materials and hosting the site. We also thank the following for photographs taken for the online resource: Eric Wilkes, Tijana Petrovic, Timothy Zanker, Bob Emmett, Katherine Evans, Warren Birchmore and Suzanne Leong-Scott.

Daniel Cozzolino provided guidance and logistical support for MIR spectroscopy and suggested lipids as possible biochemical markers for powdery mildew. Wies Cynkar and Bob Dambergs provided guidance and assistance with NIR analysis. Belinda Stummer and Paul Harvey provided advice on qPCR. Dilhani Perera and Jessamy Bennett assisted with research on fatty acids, John Carragher, Liu Ge and colleagues at Waite Lipid Analysis Service conducted fatty acid analysis and David Jeffery advised on confirmation of identity of arachidic acid. Ben Pike and Phillip Earl kindly allowed the research team to propagate powdery mildew in selected areas of the Coombe and Alverstoke vineyards at Waite Campus.

Members of the Project Steering Group are gratefully acknowledged. Their contribution was immensely valuable in guiding the research and ensuring that the outcomes were relevant to the grape and wine sector. Thanks to members of the Steering Group who contributed their time and expertise when available: Chris Bevin, Warren Birchmore, Alex Sas, Adam Steer (Accolade Wines), Ian Macrae, Nicole Pitman (CCW Cooperative Ltd), Andrew Weeks (CCW Cooperative Ltd and Vignerons Australia), Philip Deverell, Michael Sandercock (Pernod-Ricard Winemakers), Suzanne McLoughlin, Jana Shepherd, Gioia Small (Treasury Wine Estates), Paul Petrie (Treasury Wine Estates and AWRI/SARDI), Amanda Mader, Glynn Muster (Yalumba), Mary Retallack (Retallack Viticulture), Bruce Henderson (Henderson Vineyard Technical and Advisory Services), Chris Dundon (Food and Beverage Australia Ltd), Barbara Hall, Lee Bartlett, Trevor Wicks (SARDI), Marcel Essling, Mardi Longbottom (AWRI), Belinda Stummer (CSIRO), Phillip Earl, Ben Pike, Philip Sweeney (University of Adelaide), Sharon Harvey, Elise Heyes, Adrian Loschiavo, Liz Waters (Wine Australia)

Eileen Scott thanks the research team and collaborators for their hard work, dedication and for working together effectively through a challenging and wide-ranging project. Tijana Petrovic, Tim Zanker, Olena Kravchuk and Warren Birchmore contributed to both improvement of in-field assessment and development of objective measures. Bob Emmett and Kathy Evans contributed to improvement of in-field assessment and Daniel Cozzolino, Dilhani Perera, Bob Dambergs and Wies Cynkar contributed to development of objective measures.

Table of Contents

1. Abstract ……..4
2. Executive summary ……....4
3. Background ……....7
4. Project aims and performance targets ……..9
5. Improving visual assessment of powdery mildew ……11
   - 1.1 Diagrammatic key and vineyard assessment guide ……..11
   - 1.2 Review of sampling strategies ……...22
   - 1.3 Smart-phone app ……24
   - 1.4 Online resource ……..29
6. Development of objective measures for powdery mildew ……....35
   - 6.1 Quantitative polymerase chain reaction assay ……..35
   - 6.2 MIR spectroscopic analysis ……52
   - 6.3 NIR spectroscopic analysis ……63
   - 6.4 MIR and fatty acid analysis of individual berries……67
7. Outcomes and recommendations ……..88
8. Recommendations ……90
9. Appendix 1. Communications ……....91
   - 9.1 Publications ……..91
   - 9.2 Presentations ……91
10. Appendix 2. Intellectual property ……..92
11. Appendix 3. References ……..92
12. Appendix 4. Staff ……92
13. Appendix 5. Other materials ……..94
   - 5.1 Diagrammatic key with 2% increments at low severity ……...94
   - 5.2 Best practice guide for vineyard powdery mildew assessment .95
   - 5.3 Media release November 2016 ……..98

1. Abstract

Powdery mildew compromises wine quality. Visual inspection, currently used to estimate disease severity, is subjective and prone to inaccuracy. Research was undertaken to improve visual assessment and to develop objective measures. A diagrammatic key and smartphone app, with supporting online training resource, were developed, trialled in Australia in 2015 and released globally in 2016. A DNA-based assay (qPCR) was developed for absolute quantification of powdery mildew fungus in grapes. Mid- and near-infrared spectroscopy proved insufficiently sensitive to discriminate levels of powdery mildew severity critical to the sector. Arachidic fatty acid was identified as a potential biomarker for quantifying powdery mildew on grapes.

2. Executive summary

Powdery mildew, caused by the fungus *Erysiphe necator*, occurs in most viticultural regions of Australia and worldwide, and causes loss of yield and quality if not adequately controlled. Many Australian wineries have thresholds for powdery mildew contamination, such that grapes that exceed 3-5% of the surface area affected (disease severity) may be rejected or downgraded. Assessment of disease severity is based on visual inspection in the vineyard and/or at the winery. Visual assessment or estimation of disease severity is subjective and prone to variation depending on the assessor and the conditions of assessment. Uncertainty about visual assessments can lead to confusion and disputes about quality and pricing, so objective, quantitative and reliable measures for powdery mildew are required to allow better-informed decisions. Preliminary research that preceded this project suggested that near infrared spectroscopy and DNA-based methods had potential to provide objective measurement of powdery mildew. The research reported in this document was undertaken to develop (i) tools to improve the accuracy and reliability of visual assessment and (ii) objective measures for powdery mildew.

The development of tools to improve in-field visual assessment is described in Chapter 5 of this report. The concepts, components and features of the tools were discussed and refined at a series of six meetings of the Project Steering Group from January 2013 to September 2016. The main outputs from this work are: a new diagrammatic key, a smartphone application (app) and a supporting online resource to provide training in field assessment of powdery mildew. The diagrammatic key features standard area diagrams of grape bunches with increments in shading to represent powdery mildew in increments of 2% in the range 2-12% severity. The app, PMapp, was made available in Australia in December 2015 and globally in November 2016 as a free download for Apple and Android devices. PMapp has four components; assessment data entry, image browser, self calibration test for visual assessment and the diagrammatic key with 2% increments. The assessment screen allows the user to enter the score for each bunch by tapping the button which represents the best-fit severity category. The emphasis is on categories at the low end of the severity scale. The date, time and location (latitude and longitude) are recorded. The user can review cumulative disease incidence and severity as they go and toggle between data for the row and patch being assessed. On completion of the patch assessment, results can be sent in a csv or xml format to a designated email account for analysis. The image browser contains computer-generated images of bunches of various configurations with pale blue shading to represent powdery mildew, comprising 25 severity categories. The self calibration function allows the user to test their skills in estimating area, presenting 10 or 20 images for assessment followed by results for accuracy and bias. The online resource was developed in response to requests from the Steering Group to provide training in recognising and assessing powdery mildew in the field to support PMapp, and is designed for pre-vintage training for new staff and refreshing skills of experienced assessors. This free-to-access resource (pmassessment.com.au) comprises; a best practice guide for assessing powdery mildew, an exercise to assist recognition of powdery mildew, an area assessment training tool and the diagrammatic key. The vineyard assessment guide is presented as a stepwise dichotomous key that allows the user to identify his/her training needs and link directly to PMapp, the disease recognition exercise and the area assessment training tool. It also provides guidance about sampling strategy for use when a winery protocol is not available. The disease recognition exercise features high definition photographs of bunches of white and black grapes, which can be enlarged, and the user is asked to identify which have powdery mildew symptoms outlined correctly. The area assessment training tool features the images used in PMapp and the user can choose to assess 20 images spanning 0.5-15% severity or 30 images spanning 0.5-90% severity, and provides the user with information about the accuracy, repeatability and speed with which they assessed area shaded to represent powdery mildew.

A specific, sensitive and reliable quantitative polymerase chain reason (qPCR) assay was developed for the absolute quantification of biomass of *E. necator* on grape berries, based on DNA content, to serve as a means of calibrating a spectroscopic or biochemical assay. The qPCR assay was applied to homogenates of Chardonnay, Riesling, Grenache and Pinot Noir grapes which had been manufactured, by mixing homogenates of healthy and fully-infected berries, to represent various degrees of powdery mildew severity (weight:weight), as well as to homogenates of composite samples (surface area affected) and individual bunches of selected visual disease severity. The qPCR data, expressed as pathogen coefficient (log of ratio of quantification cycle for *V. vinifera* and *E. necator*), were used to develop statistical models for quantifying powdery mildew severity in these four varieties and predicting the visual severity by assuming a spherical berry shape and taking into

account the decrease in weight between healthy and infected berries. There was no obvious relationship between the amount of *E. necator* as measured by qPCR and disease severity as estimated by visual assessment of bunches and individual berries using a magnifying lamp and dissecting microscope, respectively. This can be attributed in part to variation in the density of the fungus (mycelium, spores) on the surface of infected berries, and further confirms the subjective nature of visual assessment.

Mid-infrared spectroscopy was applied to homogenised individual berries, individual bunches and composite bunches for which *E. necator* biomass had been determined by qPCR. Differences attributed to powdery mildew were observed in the spectral region 1800-1185 cm^{-1}, indicative of a mixture of lipid moieties, amide I and II, protein carboxyls, nucleic acids and fatty acid esters. Soluble and insoluble proteins in the spectral region 1695-1300 cm^{-1} contributed to the separation of some individual bunches and berries of Chardonnay with diverse *E. necator* biomass measured by qPCR. Principal component analysis followed by partial least squares analyses identified the optimal number of PCs (factors) that covered relevant spectral information related to powdery mildew, leading to development of a good calibration model for Grenache ($R^2 = 0.83$). This model needs to be validated in the future. However, the calibration models established for Chardonnay and Riesling demonstrated poor predictive performance in validation using separate test samples. The calibration model for Pinot Noir was informative only for samples from healthy grapes. MIR spectroscopy was therefore limited in terms of practical implementation. Near infrared spectroscopy was not informative at the levels of discrimination required and calibration models could not be obtained for Chardonnay, Riesling or Pinot Noir.

Fatty acid profiling of spores of *E. necator* and of powdery mildew-affected Chardonnay berries identified arachidic acid (C20:0) as a potential biomarker for powdery mildew. It was the predominant fatty acid in spores of *E. necator* but was not detected in *Botrytis cinerea* (botrytis bunch rot) or *Plasmopara viticola* (downy mildew). Arachidic acid concentration increased as powdery mildew severity increased from healthy through half-infected to fully-infected berries, and correctly classified 90% of healthy berries. Analysis of arachidic acid and three other medium-long-chain fatty acids (behenic, myristic and pentadecanoic) correctly classified 97% of healthy berries and 75% of half- and fully-infected berries. Fatty acid analysis offers a routine, accurate and potentially rapid means of measuring powdery mildew and can be conducted in a standard analytical laboratory with minimal sample preparation. Further research is required to determine if analysis of fatty acids will allow discrimination of powdery mildew severity levels with sufficient sensitivity.

Fatty acids are known to affect the sensory qualities of food and beverages and the increase in particular fatty acids with increasing disease severity observed here offers insights into the mechanism(s) by which powdery mildew may affect wine quality and, in particular, cause the oily/viscous mouth-feel identified in previous research. Research to identify the concentrations of arachidic and other fatty acids that compromise wine may lead to an objective measure for wine quality that can be adopted for routine use in the wine sector.

Project outcomes have been communicated through articles submitted to scientific journals (two) and the Australian and New Zealand Grapegrower and Winemaker magazine (two), 10 conference proceedings, workshops at the Australian Wine Industry Technical Conference 2016 and the National Wine and Grape Industry Centre, and the McLaren Vale Grape Wine and Tourism Association Technical Viticulture Conference in 2016. Two additional scientific papers are in preparation. PMapp was used to improve the reliability of disease assessment in vintage 2016 and the app and supporting resources have been used in teaching viticulture and oenology students at the University of Adelaide and Charles Sturt University.

Wine Australia and the School of Agriculture, Food and Wine of the University of Adelaide provided financial and in-kind support. Collaborators include RW Emmett Horticultural Pathology Research, the Tasmanian Institute of Agriculture, Accolade Wines, Lemur Software, Arris Pty Ltd, the Australian Wine Research Institute, Wine TQ and Fraunhofer (Germany). This project benefited immensely from an engaged and enthusiastic Project Steering Group that comprised personnel of large and small wine sector companies, research organisations and Wine Australia.

3. Background

Powdery mildew, caused by the fungus *Erysiphe necator* (formerly *Uncinula necator*), is an important disease of grapevines in Australia and world-wide. If not adequately controlled, the disease can reduce yield and quality of grapes and the resulting wines. Research commissioned by the then Grape and Wine Research and Development Corporation estimated that powdery mildew costs the Australian wine industry $76 million per annum in terms of increased cost and reduced income (Scholefield and Morison 2010). Widespread crop loss occurred in 2010/2011 when conditions were particularly conducive for development of powdery mildew and other diseases. The adverse effects of powdery mildew on wine quality include off-flavours and aromas (Ough and Berg 1979, Darriet et al. 2002). Wines made from Chardonnay grapes with as little as 1-5% of the bunch surface affected by powdery mildew had increased phenolic content and a more pronounced viscous/oily mouth feel, as perceived by a trained sensory panel, than did wines made from powdery mildew-free grapes (Stummer et al. 2003, 2005).

Many wineries in Australia have thresholds for powdery mildew, typically 3-5% (Viti-Notes 2005) or 3-6% (Birchmore et al. 2015) of the surface of the bunches with visible signs or symptoms of the disease. These values reflect severity (the percentage of the bunch surface area affected), whereas if disease incidence (percentage of bunches affected of the number of bunches assessed) is used, values are larger. However, the assessment criterion (incidence or severity) is not always clearly articulated in contractual negotiations, potentially leading to misunderstandings. Consignments of grapes with powdery mildew exceeding the threshold set by the winery may be downgraded or rejected. Powdery mildew is generally assessed in the vineyard in the weeks before harvest and again at the weighbridge to make decisions about quality, pricing and use of grapes.

Assessment is typically made on the basis of visual inspection. Powdery mildew can be difficult to assess because the disease typically appears as numerous small, scattered patches of fungal colonies that are non-descript and, if the fungus is not sporulating, are particularly hard to see. This contrasts with botrytis bunch rot, where entire berries or clumps of berries may appear discoloured, often pink or brown, and symptoms are more readily discerned (Emmett et al. 2015). Diagrammatic keys may be used to facilitate assessment but, although such keys have been developed for powdery mildew on bunches by researchers, e.g. Emmett and Wicks, they have not been published. Various in-house keys are in use in the wine sector, however, a standardised approach to visual assessment is lacking. Visual assessment is acknowledged to be subjective and estimates of disease can be variable among assessors or even during repeated assessments made by a single assessor. Training has been shown to improve visual assessment of disease severity (Bock et al. 2010), however intrinsic factors such as grape variety and colour, as well as extrinsic factors such as lighting and time of day, can influence assessment and visual inspection, at best, gives an estimate of disease severity.

Uncertainty about assessments, and even which estimate is used (incidence or severity), can lead to confusion and disputes about quality and pricing, so objective, quantitative measures are required. Preliminary research in the Cooperative Research for Viticulture (CRV 99/23, CRCV Project 1.5.2) suggested that near infrared (NIR) spectroscopy had potential for detecting and quantifying powdery mildew in homogenised grapes (Scott et al. 2006). In a subsequent scoping study (UA 05/08), analysis of homogenised Chardonnay berries from two South Australian regions generally resulted in good agreement between DNA content of the powdery mildew fungus, NIR spectra and visual classification. Grapes were assigned to five powdery mildew severity categories (<1%, 1-10%, 11-30%, 31-60% and >60%) and principal component analysis (PCA) of the resulting spectral data revealed clustering according to severity category determined by visual assessment and confirmed by DNA analysis. Linear discriminant analysis of the first three PCA scores identified a good classification rate, only one of 38 samples incorrectly classified. DNA data, obtained by use of a radioactive probe, provided a more reliable reference for NIR than did visual classification of powdery mildew severity (Scott et al. 2007, Scott et al. 2010). The DNA probe was used to develop a quantitative polymerase chain reaction (qPCR) assay by the Australian Genome Research Facility, Waite Campus, in 2007 but standardisation proved problematic and the assay was never validated.

Spectroscopic approaches are used to assess quality parameters of a wide range of crops, from cereals to coffee beans, including contamination by fungi and mycotoxins, and are currently used to measure anthocyanin and alcohol content in wine (Cozzolino and Dambergs 2010). Spectroscopic measurement of contamination requires calibration using an independent measure, such as qPCR to measure fungal DNA or the quantification of a chemical component of the contaminant. Hill et al. (2013) investigated the use of NIR and mid-infrared (MIR) spectroscopy to quantify botrytis bunch rot

on Chardonnay and Riesling grapes assigned to relatively broad categories by visual assessment, and concluded that further calibration was required to achieve accurate quantification of disease at low severity. They suggested that calibration using 1% intervals of bunch rot severity might improve accuracy. Hill et al. (2014) subsequently, and after research on objective measures for powdery mildew was well-underway, compared NIR and MIR spectroscopy, qPCR and image analysis with visual estimation of botrytis bunch rot severity and concluded that digital image analysis was the most practical alternative to visual assessment, whereas qPCR was deemed accurate but not cost-effective for routine use in a vineyard setting and spectroscopy was insufficiently sensitive.

Porep et al. (2014a) showed ergosterol, a component of fungal cell membranes, to be a quantitative biomarker for fungal rots of grape bunches, including those caused by mycotoxigenic *Aspergillus* and *Penicillium* species, and proposed NIR/VIS spectroscopy as a rapid means of quantifying ergosterol and other components that increase in rotten fruit compared with sound fruit (Porep et al. 2014b). While *E. necator* does not contain ergosterol (Porep et al. 2014a) it is possible that analogous fungal components may prove useful in measuring powdery mildew.

The primary aim of the research reported here was to develop objective methods for measuring powdery mildew severity on grapes close to harvest. Recognising that visual assessment is the current practice in the wine sector and widespread adoption of any objective measures would be some time off, a secondary aim was to improve methods for visual assessment of powdery mildew in the interim. During the course of the project, the secondary aim was expanded from the initial concept of improving diagrammatic keys and developing a user-friendly iPhone application (app) to include modification of the app for use with iPads and android hand-held devices, and to develop a suite of online resources to support the app.

A Project Steering Group was established during the first month of the project and met between one and three times per year. This group, which comprised representatives of wine companies, including disease assessors, independent consultant disease assessors and researchers, provided valuable guidance throughout the project.

References cited in this section

Bock CH, Poole GH, Parker PE and Gottwald TR (2010) Critical disease severity measured visually, by digital photography and image analysis, and by hyperspectral imaging. Critical Reviews in Plant Sciences **29**, 59-107

Cozzolino D and Dambergs RG (2010) Instrumental analysis of grape, must and wine. In: Reynolds AG (ed) Managing Wine Quality: Viticulture and Wine Quality (Volume 1), Woodhead Publishing Ltd, Cambridge, UK, pp 134-188

Darriet P, Pons M, Henry R, Dumont O, Findeling V, Cartolaro P, Calonnec A and Dubourdieu D (2002) Impact odorants contributing to the fungus type aroma from grape berries contaminated by powdery mildew (*Uncinula necator*); incidence of enzymatic activities of the yeast *Saccharomyces cerevisiae*. Journal of Agricultural and Food Chemistry **50**, 3277-82

Emmett R, Scott E, Petrovic T, Zanker T, Evans K, Kravchuk O, Perry W (2015) A diagrammatic key to assist assessment of powdery mildew severity on grape bunches. The Australian and New Zealand Grapegrower and Winemaker **623**, 46-9

Hill GN, Evans KJ, Beresford RM and Dambergs RG (2013) Near and mid-infrared spectroscopy for the quantification of botrytis bunch rot in white wine grapes. Journal of Near Infrared Spectroscopy **21**, 467-75

Hill GN, Evans KJ, Beresford RM and Dambergs RG (2014) Comparison of methods for the quantification of botrytis bunch rot in white grapes. Australian Journal of Grape and Wine Research **20**, 432–41

Ough CS and Berg HW (1979) Powdery mildew sensory effect on wine. American Journal of Enology and Viticulture **30**, 321

Porep JU, Erdmann ME, Korzendorfer A, Kammerer DR and Carle R (2014a) Rapid determination of ergosterol in grape mashes for grape rot indication and further quality assessment by means of an industrial near infrared/visible (NIR/VIS) spectrometer - a feasibility study. Food Control **43**, 142-49

Porep JU, Walter R, Kortekamp A and Carle R (2014b) Ergosterol as an objective indicator for grape rot and fungal biomass in grapes. Food Control **37**, 77-84

Scholefield P and Morison J (2010) Assessment of economic cost of endemic pests & diseases on the Australian grape and wine industry. GWRDC Project GWR 08/04 (www.wineaustralia.com).

Scott ES, Stummer BE and Leong SL (2006) Fungal contaminants and their impact on wine quality GWRDC project CRV 99/23 (http://research.wineaustralia.com/completed_projects/fungal-contaminants-and-their-impact-on-wine-quality-1-5-2/)
Scott ES, Stummer BE and Dambergs RG (2007) Application of NIR for disease assessment. GWRDC Project UA 05/08 (http://research.wineaustralia.com/completed_projects/application-of-nir-for-disease-assessment/)
Scott ES, Dambergs RG, Stummer BE (2010) Fungal contaminants in the vineyard and wine quality. In: Reynolds AG (ed) Managing Wine Quality: Viticulture and Wine Quality (Volume 1), Woodhead Publishing Ltd, Cambridge, UK, pp 481-514
Stummer BE, Francis IL, Markides AJ and Scott ES (2003) The effect of powdery mildew infection of grape berries on juice and wine composition and on sensory properties of Chardonnay wines. Australian Journal of Grape and Wine Research **9**, 28-39
Stummer BE, Francis IL, Zanker T, Lattey KA and Scott ES (2005) Effects of powdery mildew on the sensory properties and composition of Chardonnay juice and wine when grape sugar ripeness is standardised. Australian Journal of Grape and Wine Research **11**, 66-78
Viti-Notes (2005), What wineries want …and why: winegrape assessment in the vineyard and at the winery. Grape purity 1. Diseases – powdery mildew, downy mildew, Botrytis and other moulds and rots. www.crcv.com.au/viticare/vitinotes

4. Planned Project Outputs and activities

2012 (December)–13 [1]

Output	Activities
Sampling strategies and training for in-field assessment of powdery mildew documented.	- Compile and review literature on sampling strategies for in-field disease assessment. - Consult industry practitioners about practical sampling strategies and methods for calculation of contamination with powdery mildew.
Powdery mildew severity assessment key and implementation strategy assembled.	- Compile pictorial keys and protocols for sampling and interpretation of results and training of industry practitioners. - Convene workshop in early vintage involving Industry Reference Group (IRG) and leading practitioners, as available, to evaluate keys and protocols.
Powdery mildew severity assessment key and implementation strategy evaluated (vintage 1).	- Refine key, sampling strategy and training options in workshop with IRG after vintage 1. - Begin development of iPhone app. - Adoption strategy developed in consultation workshop with IRG, industry practitioners and GWRDC Program Manager(s).

2013–14

Output	Activities
Development of reference method for NIR/MIR initiated using detached leaf cultures and frozen grapes.	- Preliminary investigation of relationship between disease severity category, amount of DNA (via qPCR) and other fungal components, such as chitin and ergosterol, using detached leaf cultures and frozen grapes from vintage 1.
Potential reference method for calibrating NIR/MIR identified.	- Vintage 2 evaluation underway.
In-field powdery mildew severity assessment protocol deployed and reviewed for vintage 2.	- Review diagrammatic keys with IRG, GWRDC program manager(s) and industry practitioners pre-vintage and discuss adoption strategy.

2014–15 [2]

Output	Activities
NIR and MIR evaluated for specificity and accuracy.	- Use independent data from vintage 2 to validate NIR/MIR results from vintage 1, using frozen grapes. - Compare calibration protocols and NIR/MIR using grapes of two white and red varieties with powdery mildew and other diseases, to determine specificity. - Test in industry setting.
In-field powdery mildew severity assessment protocol deployed and reviewed for vintage 3.	- Begin development of smart phone app. - Test agreed disease assessment protocol with assessors in SA. - Pre-vintage workshop with Industry Reference Group and practitioners to review smart phone app and disease severity assessment protocol.
Training package for in-field assessment of powdery mildew severity refined.	- Post-vintage workshop to review and refine training package (pictorial key, sampling and interpretation) and smart phone app at workshop with Industry Reference Group.

2015–16 (December) [3]

Output	Activities
Online resource to support PMapp released to industry.	- Researchers work with chosen provider to develop and test the online resource. - Fine-tune in response to feedback from industry reference group.
Training package for in-field assessment of powdery mildew severity refined.	- 'Early adopters' and 'early majority' assessors use disease assessment protocol during vintage 4. - Post-vintage workshop with Industry Reference Group and practitioners to review disease assessment protocol and utility of online resource.
Visual assessment competency verified using objective measurements.	- In-field disease severity assessments verified by comparison with standard reference method and NIR/MIR.
Sampling protocols for NIR/MIR assay verified.	- Refine protocols for sampling, application and calibration of NIR/MIR methods in vintage 4, in research and industry settings.
Reference method for NIR/MIR defined.	- Compare data for NIR, qPCR, other fungal component(s) and visual assessment, and relationships between variety, Baume, pH and NIR spectra. - Validate NIR/MIR using independent data from vintage 4.
Objective measure for powdery mildew available to industry.	- Finalise calibrations and comparisons of reference methods and NIR/MIR.
Results published in scientific journals and industry publications.	- Collate and publish results on in-field powdery mildew severity assessment and objective measurements for contamination.

[1] Outputs and activities in all years were delayed when the designated research fellow took a position elsewhere, the position was advertised and Dr Petrovic was appointed (beginning July 2013).
[2] Output 2 was varied to make the app available for Android as well as Apple devices.
[3] Output 1 was added to address the Project Steering Group's recommendation to develop an online resource to support the app.

5. Improving visual assessment of powdery mildew

Summary

Visual assessment of powdery mildew severity (proportion of surface area affected) on grape bunches in the vineyard is subjective, prone to error and labour intensive. A new diagrammatic key to assist area assessment was developed as a result of workshops with the Project Steering Group. Of six keys tested (having I, 2, 3, 4, 5, 6% increments in the low range of severity), the key with 2% increments in the range 2-12% provided the most accurate, repeatable and reproducible assessment of area on diagrams shaded to represent powdery mildew on bunches. However, there was no compelling evidence that the use of keys improved assessment of powdery mildew on detached bunches in the laboratory or bunches in the vineyard. A smart-phone app, PMapp, was developed to facilitate in-field assessment of powdery mildew. PMapp comprises an assessment screen for entering observations of powdery mildew severity, image browser and self calibration functions to assist with area assessment and the 2% increment key. The app was released in Australia in December 2015 for use in vintage 2016 and worldwide in November 2016. An online resource was developed to support PMapp, comprising a vineyard powdery mildew assessment guide, disease recognition exercise, area assessment training tool and the 2% increment key. The step-wise vineyard assessment guide allows the user to identify skill development needs and access the above components to undertake the training required.

5.1 Development of a key for assessing powdery mildew

Robert W. Emmett, Olena Kravchuk, Tijana Petrovic, Warren Birchmore, Timothy Zanker, Katherine J. Evans, Eileen S. Scott

Introduction

Powdery mildew is assessed in the vineyard to allow growers to make decisions about disease management during the growing season and, closer to harvest, to make decisions about the quality of grapes for winemaking. Disease may be quantified or, more correctly, estimated, as incidence (the number of units, e.g. vines, bunches, diseased out of the total number of units assessed, usually expressed as a percentage) and severity (the proportion of area of the units diseased out of the total area assessed, usually expressed as a percentage) (Seem 1984, Nutter et al. 1991). Powdery mildew severity is typically assessed on bunches close to harvest as it is directly related to the quality of grapes for making wine (Stummer et al. 2003, 2005, Calonnec et al. 2004, Gadoury et al. 2007). Disease symptoms on bunches at this time are sometimes difficult to discern from other damage. Powdery mildew is often easiest to detect at earlier crop stages when fungal colonies are actively producing spores (propagules). Visual assessment of severity in the vineyard is often guided by the use of diagrammatic keys.

Bock et al. (2010) reviewed approaches used for assessing disease, including sources of variation in estimating severity, the use of diagrammatic keys (termed interval or category scales) and training to improve the quality of visual assessment. They used the term “estimate” for visual assessments of disease severity and “measurement” for assessments made using image analysis, and that convention will be used in this report. Factors such as the innate skill and experience of the assessor, repeatability of assessments made by a single assessor and the reproducibility of assessments made of the same specimen by several assessors, and statistical tests that may be applied to evaluate the quality of severity estimates were considered. One common approach in estimating disease severity is the use of categories or intervals of severity in linear or logarithmic increments, although the logarithmic approach has fallen out of favour (Bock et al. 2010). The use of ratio scales, i.e., a continuous percentage from 0 to 100%, is another approach widely used in estimating disease severity. The use of categories rather than a continuous percentage may have benefits for efficiency when assessing large areas in the field (Bock et al. 2010). Training in the field, laboratory or through computer programs, and the use of diagrammatic keys can be used to improve the quality of visual assessment of disease severity. Diagrammatic keys comprise standard area diagrams (SAD) which comprise plant parts shaded or coloured to depict various areas or severities of disease symptoms and can be used to assist assessment based on categories or continuous percentages.

Diagrammatic keys or SAD have been shown to improve the reliability and accuracy of the human eye in assessing numerous diseases on leaves (Nutter et al. 1993, Bock et al., 2010), including downy and powdery mildew on grape leaves (Emmett et al. 1997, Nutter et al. 2000, Nutter et al. 2006) and on fruit (Braido et al. 2014). However, few diagrammatic keys are designed specifically for disease on grape bunches. An exception is the key for botrytis bunch rot published by Hill et al. (2010, see https://www.nzpps.org/journal/63/nzpp_631740.pdf), in which SAD depict patterns typical of botrytis rot, where entire berries and contiguous clusters are shaded black to denote disease. The appearance of powdery mildew on grapes is much more subtle, in that diseased tissues can be difficult to discern and there may be several to numerous independent infections on a bunch, often with individual berries that are partially covered in fungal growth. Also, it has been noted that severity tends to be over-estimated when disease manifest as multiple small lesions rather than fewer larger lesions (Sherwood et al. 1983, Bock et al. 2008). Nevertheless, anecdotal evidence suggests that diagrammatic keys for botrytis bunch rot are being used to assess powdery mildew. In addition, various keys, typically based on previous research by RW Emmett and TJ Wicks (unpublished), are used by wine sector personnel to assess powdery mildew on grape bunches. Some of those keys depict bunches containing entire berries only (e.g. Figure 5.1.1), rather than parts of berries, affected by disease. A standardised key for assessing powdery mildew on bunches had not been published prior to this project.

The research reported below was undertaken to prepare and publish a diagrammatic key to assist with standardising assessment of powdery mildew in the vineyard, whilst acknowledging that visual assessment is subjective.

Materials and methods

The requirements and development of a key were discussed at successive meetings of the Project Steering Group.

Requirements and construction of diagrammatic keys

At the first meeting on 10 January 2013, Dr Emmett gave a presentation on assessment keys for powdery mildew and botrytis bunch rot. Keys based on severity categories are convenient for in-field assessment and categories should be readily distinguishable at the level of accuracy required. Keys should include a range of values that encompass variation in the desired “threshold severity”. Severe disease categories are also needed so that the overall severity on the block or vineyard can be calculated. Linear assessment keys (such as the bunch rot assessment key of Hill et al. 2010) are preferred over logarithmic keys. Diagrams coloured to represent grape bunches with powdery mildew are considered more useful than black and white diagrams. Steering Group members then discussed their experience of assessing powdery mildew on bunches in the vineyard.

Diagrammatic keys in use at three commercial operations in Australia had been submitted by members of the Steering Group for consideration; two of those keys were similar. Two different keys in commercial use and a research key prepared by Dr Emmett in 2003 (Figure 5.1.1) were used to assess bunches with various degrees of powdery mildew. Bunches of Chardonnay, Semillon and Grenache that had been sorted into disease severity (or infection) categories according to the three keys were presented in white trays. The 14 participants formed three groups, with industry representatives and researchers distributed across each, for hands-on assessment of powdery mildew. Participants familiarised themselves with the assessment of disease on the pre-sorted bunches using these keys, then examined unsorted bunches with various amounts of disease that had been supplied by Accolade Wines for this purpose and discussed assessment. Group reporters summarised key points from their small-group activity in a round-table discussion. It was agreed that the terms incidence and severity need to be distinguished and articulated clearly in contracts. Dispute resolution requires a uniform understanding, so the system must be standard and rigorous. Categories in keys must be fit for purpose (research or commercial vintage assessment). The 3-25% category in one of the keys was deemed too broad and intermediate categories are needed. Partially diseased berries present problems for assessment as some people count part-affected berries as fully-affected; it was agreed that images in keys should be based on surface area affected rather than number of berries affected. A modification of key A (Figure 5.1.1) to make it more like Dr Emmett’s research key (unpublished, 2003, Figure 5.1.1) was deemed most workable. The researchers undertook to prepare keys to assist with assessment of disease at the low end of the severity scale for consideration at the next Steering Group meeting.

Dr Emmett prepared diagrams of grape bunches with various areas shaded to represent powdery mildew. One standard bunch configuration comprising 50 green berries was used and areas were shaded grey empirically to represent powdery mildew. The diagrams were subjected to area assessment using the open-access image analysis software, ImageJ (Schneider et al. 2012, performed by Mr Zanker) and the Assess 2.0 (American Phytopathological Society Press, performed by Dr Evans). Briefly, screenshots of images were imported into the software, the hues in the image changed to increase contrast and the number of pixels of each hue calculated. "Disease severity" (%) was then calculated as the proportion of pixels coloured to simulate powdery mildew. Shading on diagrams of bunches was then adjusted so that the area was as close as possible to the percentage required. Six keys were prepared, having increments of 1, 2, 3, 4, 5 or 6% in the range 1-12% and standard categories of 25 and 50% thereafter. Three versions of each severity category diagram were prepared, with shading in different spots so that diagrams were not instantly recognisable as being in the key.

Testing of diagrammatic keys

Keys were tested for usefulness and bias at a meeting of the Steering Group on 9 January 2014. The group was augmented with additional professional assessors, researchers and research students to provide a panel of 19 assessors with various degrees of experience. Panellists were assigned a unique number and asked to indicate their degree of experience confidentially. Exercises were undertaken with and without diagrammatic keys to assess ability to discern small increments in disease severity at the lower end of the scale, the effect of keys on accuracy, repeatability and reproducibility. Exercises were designed by Dr Kravchuk with statistical rigour as Latinised rectangles (assessors and the order of assessments as random factors) to allow unbiased estimation of the effects of keys and of the variation within and amongst participants.

In Exercise 1, panellists were given two booklets of diagrams representing bunches of grapes with powdery mildew (13 diagrams, area shaded 0.5-18% in a randomised order, per booklet) and asked to write their estimate of the percentage of the surface area affected on each diagram without a key (unguided assessment). Diagrams were scaled to match the size of the berries to be assessed in Exercise 3. The exercise was timed to allow 2 minutes per booklet; each booklet was closed immediately after it was completed. After a break to decrease the influence of learning (familiarity with the diagrams), a similar exercise was undertaken but each participant used four diagrammatic keys to assess the percentage of each bunch diagram affected by powdery mildew (Exercise 2, guided assessment, Figure 5.1.2a). The keys consisted of diagrams with increments of 1, 2, 3 and 5% in powdery mildew severity. To assess repeatability (intra-participant performance), two configurations (A and B) of 7% of the diagram shaded were used. Each participant assessed diagram A twice with one key and diagram B twice with another key.

After another break, participants examined at three detached bunches with powdery mildew and other types of marks/scars to familiarise themselves with the symptoms to be assessed. Participants then used all six diagrammatic keys (guided assessment) and one blank key (unguided assessment) to assess severity of powdery mildew on seven sets of six bunches of grapes with similar ranges (0-25%) of the surface area covered with powdery mildew (Exercise 3). This was timed to allow a maximum of 4 minutes per set of bunches. Each bunch of grapes had been collected from the Waite Campus vineyard and assessed the previous afternoon by two trained persons then stored in a cool room overnight. Bunches were presented in white trays at seven workstations and were illuminated with desk lamps but could not be touched, to avoid disrupting the fungus on the berry surface, as each panellist assessed the same sets of bunches. After the workshop, each bunch was assessed using a magnifying lamp to provide a "gold standard" visual severity score for comparison with participants' scores in the analysis. Bunches were then photographed and frozen for subsequent objective analysis.

After another break, participants ranked the six keys in order of preference. It was agreed that the keys would be ranked separately for (i) industry assessment and (ii) research assessment, each according to a scale of 1 (most practical) to 6 (least practical).

During the workshop, Dr Kravchuk presented a statistical analysis of the data collected from Exercises 1 and 2, using one example (assessor) to explain the graphs. Each participant was given a confidential print-out of the analysis of his/her results for Exercise 2. There was insufficient time on the day to analyse data for Exercise 3. When all of the data, including the "gold standard" assessment, were analysed, each participant was sent the analysis of his/her own results for Exercise 3, along with the analysis of the combined data for all participants for each exercise. During the discussion, some panellists admitted to counting shaded berries (incidence) rather than assessing

area (severity); the researchers were aware of this possibility but to have asked the panel not to do this would have increased the likelihood that this would have happened unconsciously.

The key which proved most useful for improving the accuracy of assessment of area affected was tested in an exercise in the Coombe Vineyard, Waite Campus on 4 and 5 February 2014 (Exercise 4). Two groups of participants, six on each day, all experienced in working with powdery mildew, assessed 12 bunches each. On each day, three assessors worked on the sunny side of a row of Viognier vines and three on the shady side. The bunches were preselected in the range of 0.5-45% powdery mildew, as estimated by Dr Petrovic and Mr Zanker, tagged and each bunch assigned a unique code (indicating assessor, key or not, bunch number, see Figure 5.1.2b). A randomised stratified design was used to ensure that each participant had a unique but "representatively similar" set of bunches to assess without a key (six bunches) and using the key with 2% increments (six bunches). This design allowed examination of the effects of key, assessors and days on the outcome.

Data analysis

Exercise 1. A descriptive analysis only was conducted, as this exercise was partially a learning experience. The overall profile of the averages and standard deviations for each diagram (assuming each assessment to be independent) was calculated to illustrate the overall trend, biases and the uncertainty in the assessment as the % of area diseased changed. Individual profiles of the assessment were plotted as scatters of the assessment scores against the actual % area diseased to illustrate the variation among assessors. Summaries of the regression coefficients (slopes and intercepts for individual profiles within the range of 1-12%) were prepared.

Exercise 2. For each key, the regression slope and intercept were calculated for each assessor and the scatter of the assessment scores was generated for each regression. The Pearson correlation coefficient (measuring the "goodness of fit" of the assessment) and Lin's concordance coefficient (Lin 1989) (measuring closeness to the true assessment) were calculated for each set of scatter data. The effect of configuration for the 7% images was assessed in a generalised linear model, accounting for the effects of runs (fixed), versions of diagrams (fixed) and assessors (random).

Exercise 3. Profiles of averages and standard deviations amongst assessors were plotted for each bunch for each key at each desk. Scatters were plotted against the expert scores for each assessor for each key. The summaries of the slopes and intercept of the individual regression lines were tabulated and plotted on a histogram.

Exercise 4. The effect of key on the accuracy of the assessment was determined in a linear model, including the day of assessment and the participants within each day as random factors and the use of the key and the side of the row as fixed factors. Angular transformation was performed on the scores (asin(sqrt(score/100))). Scores by individual assessors were compared with the experts' scores using regression analysis.

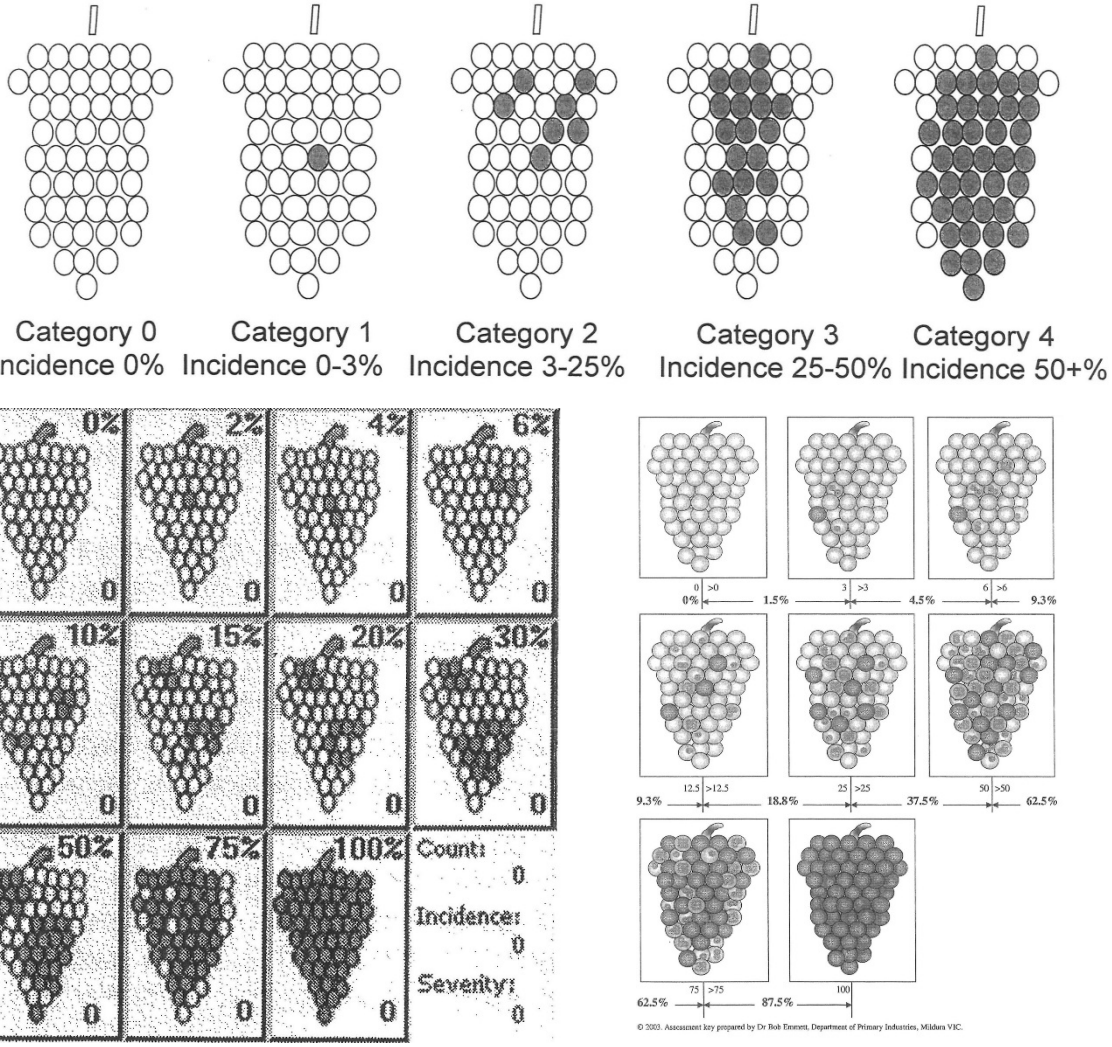
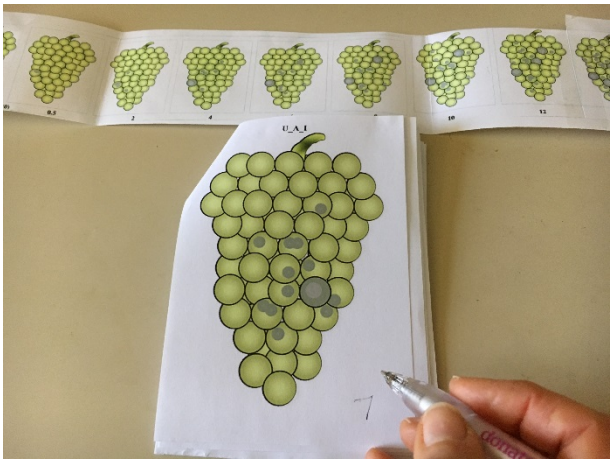


Figure 5.1.1. Two keys (A top, B left) in commercial use and a research key (C right, Emmett 2003) reviewed in first Project Steering Group meeting

a



b



Figure 5.1.2. Use of 2% increment key to assess (a) shading on diagrams and (b) powdery mildew on bunches

Results

Testing of diagrammatic keys

The results of the unguided assessment (Exercise 1) are presented in Figure 5.1.3, as assessment scores versus actual area. While the average assessment of diagrams was unbiased for the panel, there was substantial variation in the skills of the 19 assessors. The error of the assessment increased as the proportion of shading on diagrams increased towards 20%; this was valid only for the 1-18% range tested in the exercise. In spite of the variation in experience of the participants, the variation in assessment of diagrams among assessors and within assessors was very similar (variation among assessors was 3.39% for diagrams in the range 1-18%, and the variation within assessors was 3.58%). The smaller the percentage of the bunch shaded, the smaller the discrepancy among and within assessors in estimating that percentage.

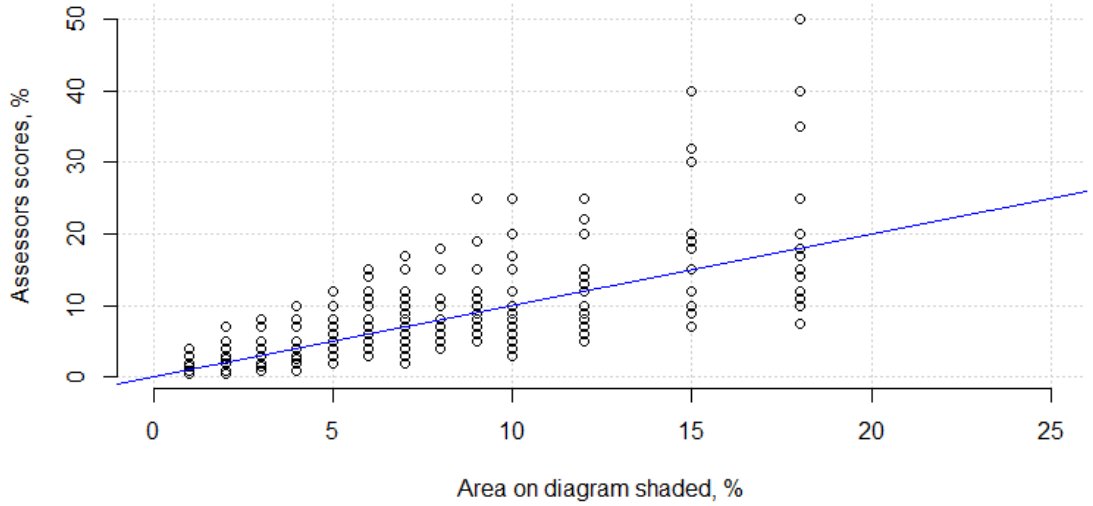


Figure 5.1.3. Assessment scores of 19 assessors versus actual area shaded on diagrams

The guided assessment of images, i.e. with keys (Exercise 2) was generally accurate and reproducible. Results, plotted as area assessed versus actual area, for a representative assessor are shown in Figure 5.1.4. The black line shows one to one correspondence, the blue line is the best fit of assessment. Values for Lin's concordance coefficient and Pearson's goodness of fit coefficient were above 0.9, indicating accurate assessment of diagrams. The two assessments of the same 7% diagram with one key were close, showing internal consistency, and close to the correspondence line, indicating accurate assessment.

Variation among assessors was comparable to variation within assessors, indicating that there was little segregation because of experience or other factors among the assessors in this panel. Keys with large increments led to a less consistent assessment amongst panellists than keys with smaller increments. The key with 1% increments produced a negatively biased assessment. There was a significant effect of the configuration of shading on the diagrams on the accuracy of the assessment (i.e. the same percentage area shaded grey, but shading distributed differently, was rated differently). The key with 2% increments resulted in least variation within assessors (Figure 5.1.5, Pearson's coefficient (Rsq) for 16 of the 19 assessors was R>0.9; for 11 of the assessors, R>0.95) and the best agreement between image assessment and true score for all 19 assessors (Lin's concordance coefficient >0.9). Using the 2% increment key, repeat assessment of 7% diagrams was consistent within 1% discrepancy and 16 assessors accurately assessed the 7% diagrams twice (Figure 5.1.6). In some cases, assessors tended to over- or under-estimate the areas larger than 9%, in which cases the best-fit line differs from the one-to-one correspondence line.

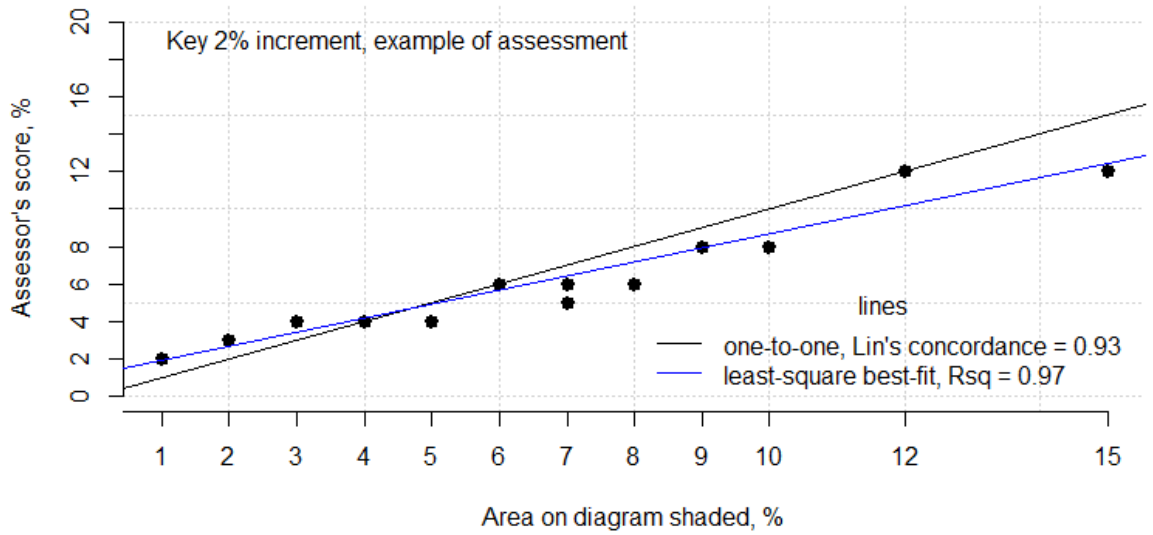


Figure 5.1.4. Area assessed against actual area on diagrams by a representative assessor using the 2% increment key

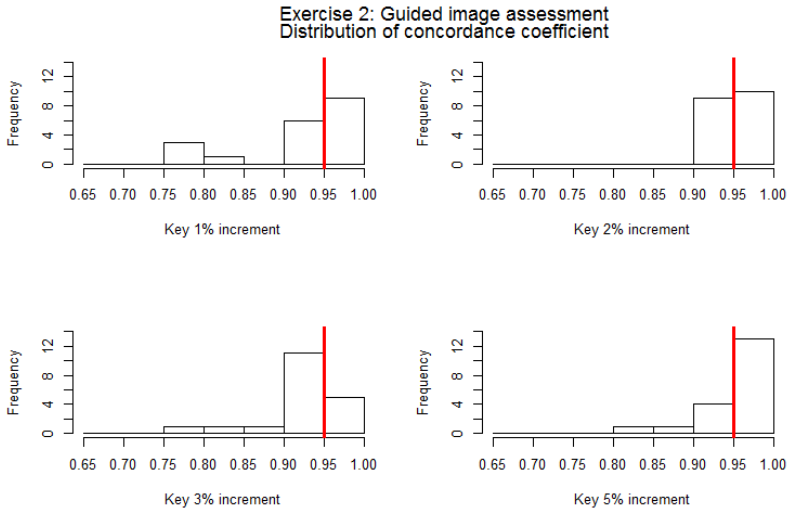


Figure 5.1.5. Distribution of Lin's concordance coefficient for various keys among the panel of 19 assessors

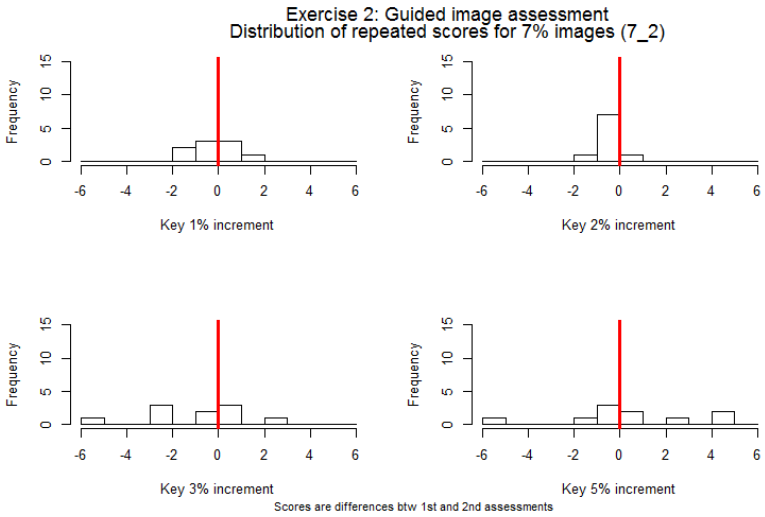


Figure 5.1.6. Distribution of the differences in repeated assessments of the same diagrams with 7% shading

Assessment of detached bunches in the laboratory (Exercise 3) showed there was no effect of using the keys to assist disease assessment (Figure 5.1.7). There was substantial variation among assessors when assessing bunches with the different keys as well as at the seven workstations. There was little effect of experience on agreement with the "gold standard", for example, one experienced assessor scored a bunch with 10% powdery mildew severity as 60%. The key with 2% increments gave the best results but still did not improve consistency of assessment (compared with the data without keys). Following discussion with the participants, it was concluded that visual assessment of severity of powdery mildew on bunches in the laboratory on 9 January was compromised, as the conditions were not representative of those in the field. In particular, people felt constrained by the inability to hold and rotate the bunch so that the fungus can be seen on the berry surface against the light. It was decided that an in-field assessment exercise was necessary (hence Exercise 4, below).

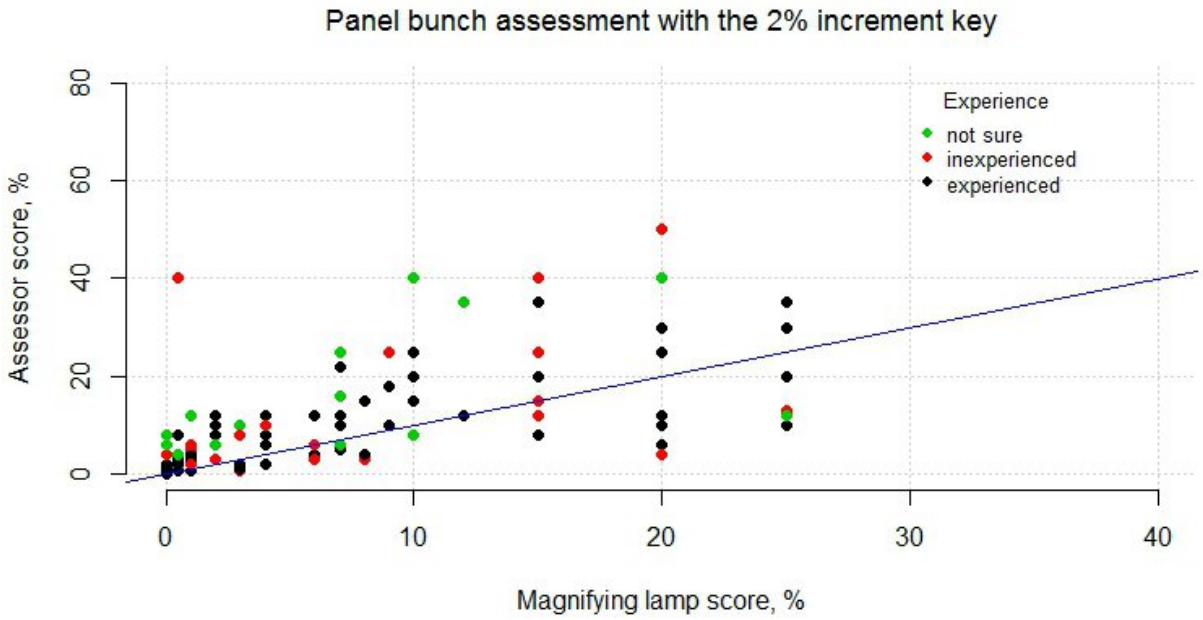


Figure 5.1.7. The distribution of scores assigned to detached bunches in the laboratory by a panel of assessors, of various self-declared degrees of experience, versus scores assigned by two experts with the aid of a magnifying lamp

Ranking of keys. The key with 1% increments was ranked as the least useful for commercial purposes, and there was no significant difference (P > 0.05) among the other five keys (Table 5.1). Keys with 1% and 2% increments were ranked as most useful for research purposes and keys with 5% and 6% increments least useful.

Table 5.1.1. Usefulness of the six keys for assessing area (1 = best to 6 = worst)

Increments in powdery mildew severity	1%	2%	3%	4%	5%	6%
Commercial setting (mean)	5.1	3.9	2.7	3.1	3.0	3.1
Research setting (mean)	2.1	2.0	3.0	3.8	4.7	5.3

Assessments of bunches on the sun-exposed and shaded sides of the vine row (Exercise 4) are presented separately, as the outcomes were different. However, for both sun-exposed and shaded bunches, there was a small but significant difference between the days of the assessment, which may be attributed to strong winds overnight between sessions. For assessments made on the sun-exposed side of the vine row, on each day, there was no difference between assessors (Figure 5.1.8 a). Only three of the assessors (1, 2, 3) detected the full range of severity (0.5-45%) but not consistently with and without the key. The average standard deviation across the assessment scores for the assessors was 10%. By the nature of the assessment task, the variation increased as the score increased towards 50%. Use of the 2% increment key did not affect the assessment. For assessments made on the shaded side of the vine row, on each day, there was a highly significant difference among the assessors (Figure 5.1.8 b). Only two of the assessors (3, 5) detected the full range of severity but not consistently with and without the key and two (1, 4) failed to recognise powdery mildew in the prevailing conditions. The average standard deviation across the assessment scores for assessors was 10%. Again, use of the 2% increment key did not affect the assessment.

Discussion

The exercises with the Steering Group provided useful information about the benefits of using diagrammatic keys and the challenges of visual assessment of powdery mildew on grape bunches, given that the symptoms and signs can be difficult to discern and distributed in a non-uniform manner. The keys developed here proved useful for training people to assess area affected. However, there was no compelling evidence that the use of diagrammatic keys improved the ability to assess powdery mildew on grape bunches in the laboratory or in the field in the conditions tested.

Results for the unguided assessment exercise showed that the panellists were able to estimate small areas of shading but that variation in ability increased with increasing area of shading. There appeared to be intuitive agreement about how to assess the areas shaded on diagrams, however, a protocol for training and quality control had the potential to improve accuracy, repeatability and reproducibility of the assessment. Assessment of diagrams using keys was accurate, repeatable and reproducible, with little evidence of segregating because of the experience of the assessor. The key with 2% increments resulted in least variation within assessors and the best agreement between diagram assessment and true score (accuracy) for all 19 assessors. It was concluded that the diagrammatic keys were a useful tool for training people to assess area affected. Likewise, Bock et al. (2010) reported improvements in the accuracy and reliability of assessments when diagrammatic keys were used. Hill et al. (2010) found that training eight assessors to recognise area on diagrams shaded to represent botrytis bunch rot resulted a small but statistically significant improvement in overall precision, whereas Nutter et al. (2006) reported that the assessment of 30 images representing

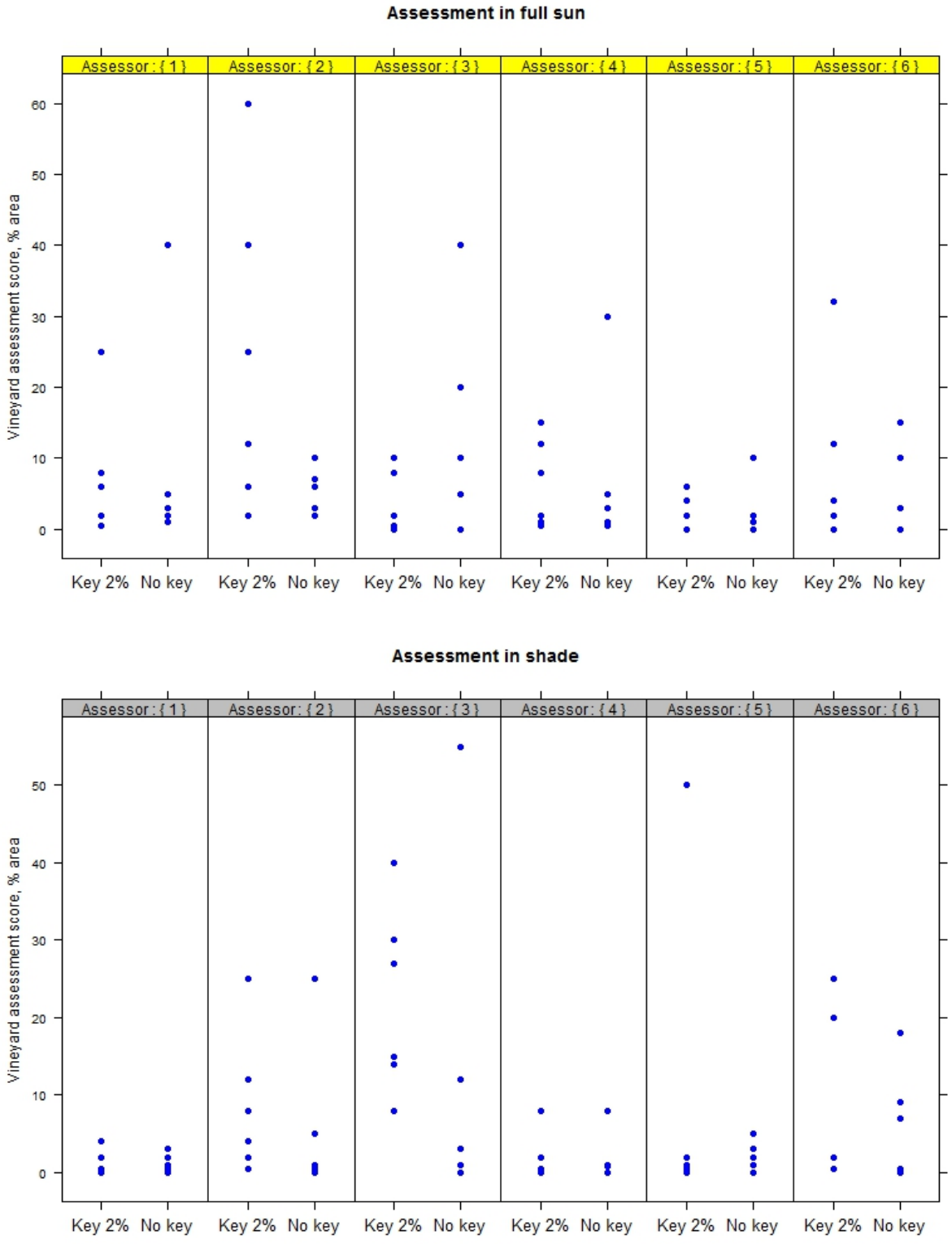


Figure 5.1.8. Assessment of powdery mildew on grape bunches in the vineyard with and without a diagrammatic key with 2% increments on the sun-exposed side (upper, a) and shaded side (lower, b) of the vine row

various severities of downy mildew on grape leaves by six assessors was greatly improved by the use of coloured SAD.

However, there was no compelling evidence that the use of diagrammatic keys improved the ability to assess powdery mildew signs and symptoms on grape bunches in the laboratory or in the field. While the conditions imposed during laboratory assessment were immediately recognised by the panellists as being atypical and inappropriate for the purpose, conditions in the vineyard were typical, being sunny mornings close to harvest. Assessments made on the sun-exposed side of the row were slightly more consistent with expectations than those in shade. One panellist working in the shade commented that she would like to have had the benefit of direct sunlight to view the bunches. However, irrespective of assessment in sun or shade, there was consistently large variation within assessors (i.e. individual assessors varied in assessments made for bunches with the same amount of powdery mildew) and use of the diagrammatic key did not improve the assessment. Discrepancies between assessors and conditions may reflect, at least in part, differences in the density of fungal mycelium and extent of sporulation on individual bunches. Nevertheless, some assessors find a diagrammatic key helpful for in-field assessment so the key with 2% increments was adapted for use in resources developed in this project. The flat, uniform images of bunches used in laboratory and vineyard tests described above were replaced with computer-generated images that incorporate highlights and shading to give a three-dimensional impression, and the key was published in the Australian and New Zealand Grapegrower and Winemaker (Emmett et al. 2015).

The variation within assessors and difficulty in assessing powdery mildew on the shady side of the vine suggested that more training is required for various conditions of assessment. Rather than deploying a stand-alone diagrammatic key for use in field assessment, the Steering Group proposed that the research team explore developing a training package comprising an area assessment training tool, analogous to the Bunch Rot Assessment Trainer (BRAT) (www.bunchrot.co.nz), and photographic images to facilitate recognition of powdery mildew. These resources should be available online and would include the key with 2% increments.

Overall, the research reported in this section reinforced the subjective nature of visual assessment, the potential for and limitations to improvement of visual assessment, and the need for objective measures.

5.2 Review of sampling strategies for in-field assessment of powdery mildew

Robert W. Emmett, Olena Kravchuk, Warren Birchmore, Katherine J. Evans, Eileen S. Scott

Introduction

Approaches for disease monitoring in the vineyard are well established (Viti-Notes 2005, 2010), however, assessment of severity on grape bunches is less well documented. Allan (2003) published a guide to winegrape assessment in the vineyard and at the winery, but interpretations of this guide appear to be variable among commercial operations and a standardised procedure for use in the vineyard is lacking.

The research team reviewed sampling strategies with a view to preparing guidelines for visual assessment of powdery mildew in the vineyard.

Materials and methods

Approaches for use in assessing vineyard patches or blocks for powdery mildew were collated, presented and reviewed at the Project Steering Group meeting in January 2013. The strategy prepared by Allan (2003) for the Cooperative Research Centre for Viticulture was discussed.

The approach to be used for assessment may be specified in contractual arrangements between the grower and the wine company, for example, the minimum number of bunches to be assessed and the pattern of sampling across the vineyard and patches within it. The conditions of light (time of day) and weather (e.g. rain or dew), which can influence the visibility of powdery mildew on berries, may also be specified. However, such agreements are not universal.

It was agreed that a standard means of assessment would be beneficial, comprising how and where and how many bunches to assess, whether to assess one disease at a time or all diseases/defects at once, what categories to use, and whether severity or incidence is recorded. Reproducibility was deemed important. It was agreed that a protocol to guide assessment of powdery mildew from scouting to assessment of severity would be devised and sent to participants for feedback.

Dr Emmett prepared a draft best practice guide for field assessment for consideration by the Steering Group in January 2015. This was intended to provide a generic approach to assessing powdery mildew in vineyards and guidance on how the disease assessment tools developed in this project might be applied in the field.

Results

The best practice guide drafted by Dr Emmett covered early season monitoring for management purposes through to mid- to late-season bunch assessments for quality of end-product. It also contained information relating to contractual arrangements, covering consultation between vineyard manager and buyer. The Steering Group provided feedback about the usefulness of the framework and the level of detail needed. It was agreed that the guide should focus on technical aspects of bunch assessment and leave matters such as contractual arrangements to the growers and wine-makers, and that any winery protocols already in place would take precedence. The guide was deemed most useful formatted as a simple flow chart or decision tree, with links to the detail underpinning each step. In keeping with the focus on bunch assessment, the material on early-season monitoring was placed in an appendix. The need to integrate the best practice guide with the Integrated Pest Management Viticulture Research to Practice Viti-notes and Wine Australia information sheets was acknowledged. The draft was adjusted in the light of feedback and the agreed document, Best Practice Guide for Vineyard Powdery Mildew Assessment, is attached to this report as Appendix 5.2, and incorporated into the online resource described in Section 5.4.

Discussion

It was agreed that a uniform, industry-wide sampling strategy for powdery mildew would be helpful, although winery protocols would take precedence where they exist. The vineyard powdery mildew

assessment guidelines developed through this project incorporate the recommendations of Allan (2003), who advised assessing 200 bunches. Despite numerous studies on sampling for disease assessment, the question remains as to how many samples and what sampling pattern should be used for accurate and reliable assessment of powdery mildew. Dr Kravchuk noted that assessment of 200 bunches in a patch should be sufficient for estimating incidence and severity when disease is moderate. The coefficient of variation should be calculated and, ideally, two assessors should assess the same plot independently and the confidence levels be examined. In general, the lower the disease incidence, the more samples are needed for accurate assessment. However, the distribution of disease is known to be influenced by the source of inoculum, whether from flag shoots or ascospores (Ovadia et al. 2006), and this should to be taken into account where possible. It is important that sampling and assessment of severity are robust, as findings or methodology may be challenged in court.

In-field visual assessment delivers an instant answer without the need for destructive sampling. Results for incidence of powdery mildew and visual assessment of severity, however crude, can be used in a process called “ranked set sampling” (McIntyre 1952, Patil 2002) to provide information on which to base sampling for objective measurement. Ranked set sampling, an approach being used increasingly to assess pastures, cereal crops, forestry and for environmental purposes, can provide greater precision using fewer samples than simple random sampling (Murray et al. 2000). It combines simple random sampling with the knowledge and judgement of an experienced assessor or field screening approaches to guide the selection of sampling sites (http://vsp.pnnl.gov/help/Vsample/Design_Ranked_Set_Sampling.htm). The use of PMapp would support and enhance the professional judgement of the vineyard assessor in the selection of locations at which to assess representative bunches and collect samples for objective measurement.

5.3 Development of PMapp, an app for in-field assessment of powdery mildew

Wade Perry, Warren Birchmore, Robert W. Emmett, Tijana Petrovic, Timothy Zanker, Katherine J. Evans, Olena Kravchuk and Eileen S. Scott

Introduction

In-field assessments of powdery mildew on bunches are usually recorded on paper and the data subsequently transcribed into spreadsheets in the office (Birchmore et al. 2015). Recording of results on the back of business cards is not unknown. Not only is this practice laborious and prone to error when data are handled twice or more, or are at risk of being misplaced, but the user also has to wait until the observations have been collated and analysed to have information about disease incidence and severity across the patch(es) being examined.

The widespread uptake of mobile devices such as smart-phones and tablets, as well as the ever-increasing number of applications (or apps) available for download, provided the opportunity to develop a new tool to facilitate in-field assessment of powdery mildew. At the outset of the project, the group was aware that an app was being developed for botrytis bunch rot and an app for assessing various fungal diseases on leaves, called Leaf Doctor, was released in 2015 (Pethybridge and Nelson 2015). Leaf doctor, a free app for Apple devices available in the USA (only), allows the user to photograph the specimen using a smart-phone and adjust the image such that diseased area has a blue hue and pixels can be counted. However, of the six diseases studied, powdery mildew on lilac leaves was the least amenable to this form of assessment and this was attributed to lack of contrast between diseased and healthy tissue. Similar challenges were also reported by Barbedo (2014). Given these concerns and the constraints described in Section 5.1, a photographic approach was not pursued.

The project team undertook to develop an app to facilitate assessment of powdery mildew in the field, while acknowledging that this was an interim measure until an objective measure is deployed.

Materials and methods

Development of the app, from the components to the name, was undertaken in close consultation with the Project Steering Group. A version for Apple devices was developed first, followed by a version for Android devices. Software developer, Wade Perry (Lemur Software), worked closely with the researchers and Steering Group members to develop the app. After preliminary consultation, Mr Perry prepared a prototype for consideration at the Steering Group meeting on 8 January 2015 and made it available to the research team via the platform TestFlight. The prototype app was installed on three iPhones and three iPads for use at the meeting.

The components of the prototype app were explained, then participants explored the features and undertook simple familiarisation exercises. Six volunteers were given two sets of five diagrams with shading to denote powdery mildew (selected from those used in 2014, as described in Section 5.1). They assessed the first set without a key (current experience) and the second set with a printed version of the diagrammatic key with 2% increments (experience plus key); they entered data into the app assessment screen as row 1 (no key) and row 2 (with key). They then compared their assessments with the actual severity for each diagram and the mean severity using information provided on the last page of their booklet (masked until completed). This allowed assessors to compare their results with the correct answer informally; results were not collected. This exercise was intended as preparation for assessing bunches in the vineyard, which has been assessed and coded by two experts the day before. Unfortunately, heavy rain fell during the morning and researchers and industry assessors agreed that it was not possible to discern powdery mildew on the wet bunches. The field exercise was abandoned. Steering Group members then discussed the features and usefulness of the prototype app and suggested improvements. By consensus, the app was named PMapp. A list of industry personnel to be invited to test the beta version of PMapp was compiled and provided to Mr Perry. As several Steering Group members were unable to attend the meeting on 8 January 2015, a second session was held on 16 February at which Dr Petrovic and Mr Birchmore demonstrated the prototype app and gained feedback from those present.

The second iteration of PMapp, which incorporated feedback provided on 8 January and 16 February 2015, was reviewed at the Steering Group's post-vintage meeting on 10 June 2015. Mr Perry had developed computer software to generate images of bunches to which could be added shading to

indicate powdery mildew, light blue was chosen to represent powdery mildew, and Dr Emmett used the software to generate a new set of images more representative of the range of bunch configurations encountered in the vineyard. The area shaded on each image was measured using ImageJ (Schneider et al. 2012) and a sub-set of images was measured using Assess 2.0 (American Phytopathological Society), as described in Section 5.1. The app with the computer-generated images had been made available to the Steering Group before the meeting. After discussion, improvements to PMapp were agreed and Mr Perry was asked to begin development of the Android version. Mr Timothy Spencer, Adelaide Research and Innovation, attended to give advice on intellectual property issues. Mr Birchmore and Dr Scott undertook to prepared detailed instructions for PMapp and Dr Scott and Mr Spencer to draft a disclaimer.

The third iteration of PMapp for Apple devices and the new Android version were presented, discussed and fine-tuned at the Steering Group meeting on 25 November 2015, which was timed to allow the app to be released for use in the Australian vintage 2016. PMapp was also presented at workshop 7, “Canopy management using grower-friendly digital tools”, during the Australian Wine Industry Technical Conference (AWITC) on 24 July 2016 and at the McLaren Vale Grape, Wine and Tourism Association Viticulture Conference on 13 September 2016. Feedback from these presentations was reviewed and amendments to PMapp prior to global release were discussed at the final Steering Group meeting on 14 September 2016.

Results

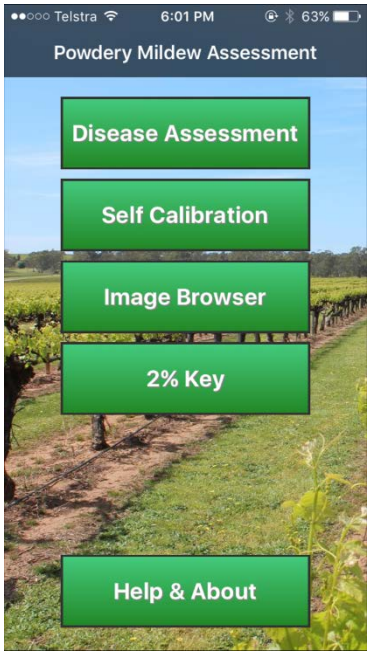
PMapp has four main components (Figure 5.3.1), the development of which is summarised below:

Disease severity assessment component. When a user begins a disease assessment, he/she is asked to enter the name and address of the assessment (which can be grower name and identification number, vineyard patch and variety). There is a notes page which can be used to capture other details, such as assessment pattern (number of bunches per vine, vines per row). Data are entered according to the best-fit category, for example, 1% could be anything from 0.6 to 1.5%, 2% anything from 1.6-2.5% etc. The decision to use categories rather than absolute values was based on common practice in industry and to minimise ambiguity. The first iteration of the assessment screen had a 5 x 6 matrix representing categories of 1% increments from 0 to 10%, then 12 and 15%, and 5% increments to 100%, with each value presented in a square. However, the Steering Group decided that the prototype assessment screen had too many squares, making it difficult to enter data in the field, particularly if the device was in a plastic bag to protect it from moisture and sticky fingers. It was agreed to reconfigure the screen with round buttons to show 0.5% (for trace), 1 to 10% in increments of 1%, then 12, 15, 20, 25, 30% and values in 10% increments thereafter, plus a button for 75%. The most recently entered value was to be shown in a different colour for emphasis. At the review in June, it was agreed that the heading on the disease assessment screen, which read “Scoring”, be changed to “Severity score (%)” for clarity.

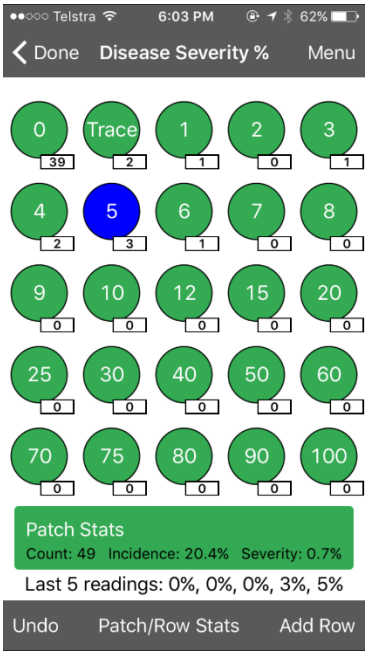
After assessing all rows in the patch, pressing the “Done” button gives the option of continuing scoring or emailing the data as a csv or xml file. The csv format converts readily to Excel, whereas the xml format is compatible with software used by some wine companies. Start and finish time and latitude and longitude coordinates, along with the contents of the notes page, are included in the email, and the data file name includes the title of the assessment (preferably vineyard and block name).

Image browser component. The image browser screen in the prototype displayed photographs of bunches of various shapes, sizes and disease severity and computer-generated images of a single bunch configuration with orange patches to represent area with powdery mildew. The photographs could be enlarged to magnify disease symptoms. It proved difficult to discern symptoms on the photographs on the screen of a phone, even when magnified, and the files proved too large for an app. The computer-generated bunches with orange shading were deemed unrealistic. The sample set of computer-generated bunch images Dr Emmett prepared for the meeting in June 2015 comprised six bunch configurations (several shapes, loose or compact) with blue spots applied to represent the agreed 25 severity categories, and six bunches per category. Checking the area shaded using ImageJ and Assess 2.0 revealed that the bunch generation tool tended to under-estimate the area shaded. An image could not be adjusted once exported from the tool, so a second set was generated and checked using ImageJ, then a third set. Images accurate to within 1% for 0-15%, and slightly larger margins of error for severity 20-90%, to within the appropriate category (e.g. 56-65% according to ImageJ, all of which would be scored 60%) were labelled with the actual ImageJ result as well as the category and used in the browser. The image browser, as released, contains 139 images.

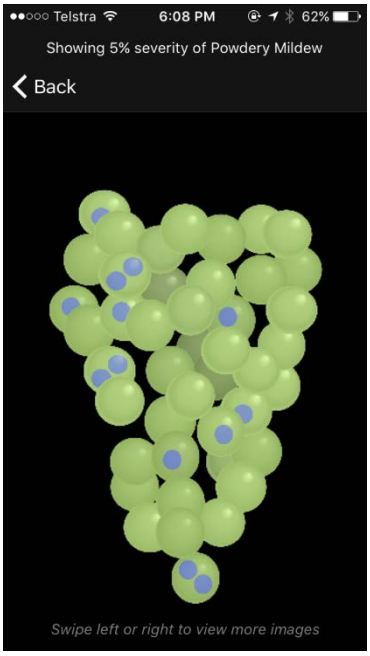
a


Telstra 6:01 PM 63%
Powdery Mildew Assessment
Disease Assessment
Self Calibration
Image Browser
2% Key
Help & About

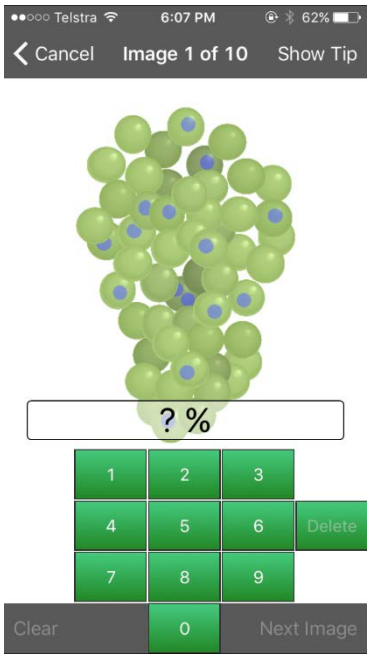
b


Telstra 6:03 PM 62%
Done
Disease Severity %
Menu
0 Trace 1 2 3
4 5 6 7 8
9 10 12 15 20
25 30 40 50 60
70 75 80 90 100
Patch Stats
Count: 49 Incidence: 20.4% Severity: 0.7%
Last 5 readings: 0%, 0%, 0%, 3%, 5%
Undo
Patch/Row Stats
Add Row

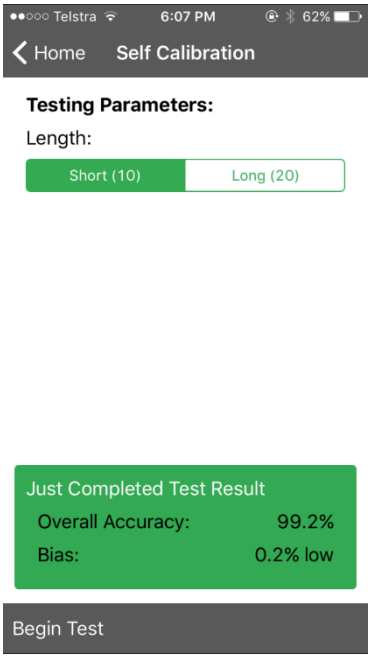
c


Telstra 6:08 PM 62%
Showing 5% severity of Powdery Mildew
Back
Swipe left or right to view more images

d


Telstra 6:07 PM 62%
Cancel
Image 1 of 10
Show Tip
? %
1 2 3
4 5 6 Delete
7 8 9
Clear
0
Next Image

e


Telstra 6:07 PM 62%
Home
Self Calibration
Testing Parameters:
Length:
Short (10)
Long (20)
Just Completed Test Result
Overall Accuracy: 99.2%
Bias: 0.2% low
Begin Test

f


Telstra 12:42 PM 90%
Home
Key
Grape powdery mildew severity assessment key (2% increments in low range)

Self calibration component. This was included to encourage users to check their area assessment skills before beginning a day of assessment, in accordance with best practice. The user can take a short (10 images) or long (20 images) exercise in which he or she assesses computer-generated images drawn at random from the image browser. The first iteration of PMapp contained a mixture of photographs of bunches with powdery mildew and computer-generated images with orange patches, but this was aligned with the image browser once the images were improved.

Key component. The key with 2% increments in the range 2-12% was revised to replace the original diagrams with equivalent images produced using the bunch generation software and annotated to provide the actual area measured using ImageJ in brackets after the category.

Release of PMapp. PMapp was released in Australia on 18 December 2015, and was free to download via the Apple App Store (https://appsto.re/au/qe-e5.i) and Google Play (https://play.google.com/store/apps/details?id=com.lemuresoftware.pmapp). Wine Australia approved release of PMapp globally in November 2016, to allow minor improvements suggested by users during Australian vintage 2016 and participants in the workshop at AWITC to be incorporated. The version released in November 2016 contains a link to the online resource (see section 5.4).

Discussion

Members of the Steering Group provided invaluable suggestions and feedback throughout development of PMapp. Personnel tended to vary from one meeting to the next, due to work and travel commitments; this occasionally led to different preferences about features of the app from one meeting to the next, but the group reached consensus on each occasion. PMapp was designed to be intuitive and easy to use by personnel ranging from experienced users of apps and information technology to novice users. As such, detailed instructions for use can be accessed via the Help and About button and printed to paper for the novice user, whereas headings on each screen guide confident users without the need to refer to the instructions. It must be emphasised that PMapp is not a decision support tool, rather it is a means of facilitating data collection. It was noted that the data file emailed at the conclusion of an assessment may constitute a legal document, so the data should be emailed to the user's account or company account and kept secure.

The research team and Mr Perry did their best to accommodate all suggestions but, with a finite budget, some were set aside for consideration for a future version of PMapp. For example, some of the Steering Group at the meeting on 10 June 2015 considered there were too many buttons and they had no use for values above 50%, while others wanted the full range. Accordingly, the next version of the app might allow the user to customise the assessment screen to show just the buttons for ≤50% severity, although with the caveat that when averaging severity, one bunch that is 50% diseased is not the same as one bunch that is 100% diseased. Alternatively, the user could have the option of changing the colour of frequently-used buttons so they stand out.

There was considerable interest in expanding the app to facilitate assessment of bunch rot as well, perhaps via an alternating screen so that a bunch could be assessed using one screen for powdery mildew and another for bunch rot. This suggestion was made again at the workshop at AWITC and the McLaren Vale Viticulture Conference. As bunch rot typically involves whole berries with symptoms, rather than part-berry surface as is the case for powdery mildew, this would be best supported by another set of images for the browser, key and self calibration components, as well as a parallel screen, spreadsheet and email for bunch rot data. As such, this suggestion has been added to the list of improvements that might be made in version 2.

Other suggestions made at the AWITC workshop were to include the ability to record whether powdery mildew was active or inactive and if active disease was present on the rachis and on unfertilised berries (micro-berries) in the bunch being assessed. These suggestions were discussed at the Steering Group meeting on 14 September 2016 but the consensus was that they would not be implemented at this stage.

Dr Kravchuk advised that the row and column grid data collected by the user could be used to determine if the sampling pattern is representative and to identify powdery mildew hot spots in the vineyard block. Such a grid might be linked to Google maps or some other format for local coordinates in future and could be used to produce "heat maps" of disease distribution and intensity.

Although it is possible to collect and analyse meta-data over time, it was agreed that there is little to be gained, as the assessment screen could be used to record the severity (or proportion of surface area affected) of any disease, disorder or damage of any crop, or any other task that collects data in categories as percentages.

Powdery mildew is less amenable than bunch rots to assessment using a camera and app in a smartphone or tablet due to the lack of contrast between healthy and diseased tissue (Barbedo 2014, Pethybridge and Nelson 2015), however such technology may be feasible in the future.

In view of the challenges involved in recognising and estimating powdery mildew severity on grape bunches (Section 5.1), and recognising that the accuracy and repeatability of assessments can be improved by training (Nutter et al. 2006, Bock et al. 2010), the Steering Group suggested, and researchers agreed, that a suite of online resources be developed to support PMapp. This work is reported in Section 5.4.

5.4 Development of online resources to support PMapp

Eileen S. Scott, Robert W. Emmett, Tijana Petrovic, Olena Kravchuk and Warren Birchmore

Introduction

Assessment of disease severity can be improved by training in disease recognition and area assessment to help identify and correct individual bias (Nutter et al. 2006, Bock et al. 2010), and various computer-based training packages are available to assist. For example, Forrest Nutter Jnr (Iowa State University, USA) developed the computer-based disease assessment training program, Disease.Pro, to simulate and provide training in assessment of four diseases of peanut leaves (Nutter and Schulz 1995, Nutter et al. 2015). The program gave rise to Severity.Pro, a more generic training program that allows the user to select a leaf shape and lesion type to simulate the desired foliar disease (Nutter et al. 2006). Nutter et al. (2000, 2006) reported that, following computer-based training, the accuracy and precision of five of six assessors estimating disease severity on 30 images representing downy mildew on grape leaves was improved. Training involved giving the trainee immediate feedback on the actual severity (area shaded) on each image.

Assessing disease severity on bunches is more challenging than assessing leaf diseases due to the three-dimensional nature of the bunch. The bunch rot assessment trainer (BRAT) tool was developed by Plant and Food Research New Zealand to improve skills in assessing severity of botrytis bunch rot (Hill et al. 2010). BRAT can be accessed at www.bunchrot.co.nz, where the user is permitted to undertake three attempts for free, after which he/she is required to pay for access. The Steering Group encouraged the research team to explore developing a simple “BRAT-like trainer” for powdery mildew to support the use of PMapp and assist new vintage field officers and other staff to develop and improve their skills in area assessment before beginning work in the vineyard.

Powdery mildew can be difficult to identify and assess because of the lack of contrast between diseased and healthy tissue and the typical pattern of scattered, multiple small colonies of mildew on the tissue. Recognition of powdery mildew on berries typically depends on seeing sporulation and being able to hold and rotate the bunch to see the spore-bearing structures against sunlight. Symptoms of powdery mildew are sometimes confused with those of other diseases, such as downy mildew, early stage botrytis rot, and sulfur deposits or dust; Dambergs et al. (2007) reported receiving from wine sector collaborators bunches infected by *Botrytis cinerea* when they sought powdery mildew samples for research on spectroscopy as a means of detecting powdery mildew.

The research team undertook to develop online resources for powdery mildew to support PMapp.

Materials and methods

Development of online resources to support PMapp was undertaken in close consultation with the Project Steering Group. The proposal to develop a training package arose from the Steering Group meeting on 9 January 2014. As a first step, Dr Petrovic and Mr Milos Novakovic (Technical Manager of software company, Data Revival) produced an Excel file with macros that contained diagrams described in Section 5.1 which allowed the user to enter their estimate and receive the correct answer. Dr Evans discussed the concept with Dr Gareth Hill (New Zealand Plant and Food Research) who was involved in developing BRAT, who advised that the work could possibly be undertaken by Plant and Food New Zealand. These developments were endorsed at the next Steering Group meeting and a plan for components of the resources was presented to the Steering Group on 10 June 2015. Those components were: (i) the vineyard powdery mildew assessment guide; (ii) a diagrammatic key; (iii) an area assessment training tool that uses the computer-generated images prepared for PMapp and (iv) a tool to assist recognition of powdery mildew, using high resolution photographs taken during the present and previous projects. Mr Novakovic attended this meeting to contribute advice on technical aspects of developing the area assessment training tool. He subsequently prepared a proof-of-concept version of an area assessment training tool for the research team, which provided valuable assistance in refining the features that might be included.

Four quotations were obtained for conducting this work and a project variation was approved subject to choosing the most cost-effective quotation. The research team provided the developers, GrapeBrain (formerly known as Seer Insights), with; the images used in PMapp, the Excel proof-of-

concept files prepared by Data Revival, detailed instructions for the requirements of the area assessment tool including a prototype for visualisation of assessment data and summary of outputs prepared by Dr Kravchuk, high-resolution photographs of bunches of white and black grapes with symptoms of powdery mildew and other diseases and disorders, photographs of vineyards for background to components, the best practice guide for vineyard powdery mildew assessment and an overview and instructions to preface each component of the resource. The prototype resource was reviewed by the research team and several members of the Steering Group at several points during development.

Hosting of the online resource was subsequently negotiated between Wine Australia and Arris Pty Ltd and the website made available for the AWITC workshop "Canopy management using grower-friendly digital tools" on 24 July 2016. Dr Scott presented the website and invited feedback from participants. She also presented the website at the McLaren Vale Grape Wine and Tourism Association Viticulture Conference on 13 September 2016 and sought feedback. The web address was also provided to members of the Steering Group. Feedback was discussed at the final Steering Group meeting on 14 September 2016 and it was agreed that the design be revised to make the functions and links between components more intuitive and the instructions more succinct. Revisions were undertaken by Dr Scott and Arris in consultation with the research team and Wine Australia.

Results

The grape powdery mildew assessment resource developed to support PMapp is available free at www.pmassessment.com.au. The user registers and logs in via his/her email address and a password. The welcome screen briefly explains the purpose of the resource and provides links to PMapp. The user can then click on images that link to the four component parts, as follows.

The **vineyard powdery mildew assessment guide** provides a step-wise procedure for assessing powdery mildew on grapes, with links to other components of the resource so that the user can address his/her training needs at the appropriate juncture (see Appendix 5.2). This can be downloaded as a pdf document and printed.

The **powdery mildew recognition exercise** begins with a familiarisation page comprising three photographs of bunches with powdery mildew and six showing diseases that may be confused with powdery mildew. The exercise proper comprises 28 high-resolution photographs of bunches of white and black grapes (5 taken at veraison) which appear at random except for the last one. These are presented as sets of three identical photographs with different areas of the surface outlined, and the user is asked to identify the bunch that has powdery mildew outlined most correctly (Figure 5.4.1). The photographs are randomised among and within sets of three and each can be enlarged by hovering the computer mouse over each image. The last set of three photographs features a severely diseased bunch and the user is asked to identify the photograph which shows the healthy grapes outlined most correctly. The last screen in this component provides a summary of the number of correct responses. Results are not retained and the exercise can be undertaken multiple times.

The **area assessment training tool** can be accessed as often as required and stores results for previous attempts, which are confidential to the individual user. The computer-generated images of bunches prepared for PMapp have been used except for those depicting 0 and 100% diseased, as these would skew results. The user is told that all values are whole numbers except 0.5%. He/she can choose between two sessions, one comprising 30 images spanning 0.5-90% of the bunch surface shaded ("Full range severity"), the other, 20 images spanning 0.5-15% ("Low range severity"), and set the timer to allow up to 10 or 20 seconds per image. There is also a pause button, to allow for interruptions, at which point the image disappears. Images appear semi-randomly although certain images are repeated to gauge internal repeatability. Once each set of images has been assessed, the user receives feedback to help improve his/her performance.

Feedback on performance at the end of each attempt comprises: a table listing the images assessed with the actual percentage of shading and the user's corresponding assessment; a chart of these results presented as a scatter-plot of circles proportional in diameter to the time the user took to assess that image, the one-to-one correspondence line and Lin's concordance coefficient (a measure of closeness of the assessment to the one-to-one correspondence line); the range of assessed surface (percentage) on the same image shown repeatedly (indicates repeatability of assessment) and the minimal and maximal time of image assessment (Figure 5.4.2). There is a link to an explanation of the outputs. The results can be printed.

The **diagrammatic key** with 2% increments in the range 2-12% is provided as a pdf document and can be downloaded and printed.

There is an option to provide feedback direct to Arris, the current hosts of the online resources. The online resource is linked to Wine Australia's Vinsights resources.

Discussion

The resources described above provide interactive tools to help personnel undertaking diagnosis and assessment of powdery mildew to improve their skills in advance of conducting in-field assessment. They also provide opportunities for students of viticulture and oenology to acquire these skills even when classes are not synchronised with the appearance of powdery mildew on grape bunches in the vineyard.

The stepwise format of the vineyard best practice assessment guide allows the user to identify her/his own training needs, if necessary under direction from a supervisor, and link directly to the component(s) that best addresses those needs.

The powdery mildew recognition component in this first version is limited to two-dimensional photographs and a simple multiple choice format. A subsequent version may incorporate more photographs and provide greater interactivity by allowing the user to draw around or shade the berry or bunch surface thought to have powdery mildew symptoms (active or inactive) and receive a score for accuracy on completion of the exercise. Advances in technology may allow three-dimensional photographs that the user can rotate, as an assessor would do in the vineyard to look for sporulation (conidiophores projecting from the berry surface) against sunlight.

A limitation of the area assessment training tool is the relatively small number of images used, such that a regular user may become familiar with the images over time. This may become important if an employer or a potential employee wishes to use outputs from the tool as evidence of capability. The resources are hosted by Arris Pty Ltd and were launched formally in November 2016. Whereas PMapp could be restricted to Australian users in the first instance, this proved impractical for the online resources and it is difficult to predict how widespread uptake will be. Hosting of the website in the future will need to include provision for updating in response to feedback and managing the site for an as yet unknown number and diversity of users. It is also possible that the website may be expanded in scope to include other diseases in future.

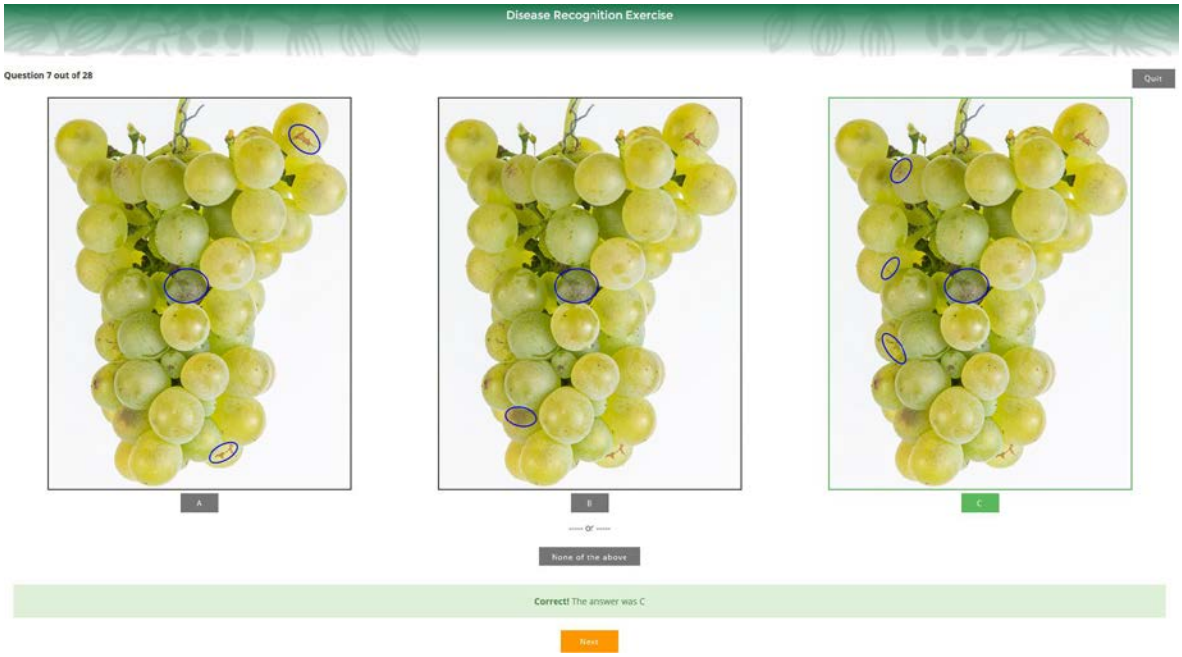
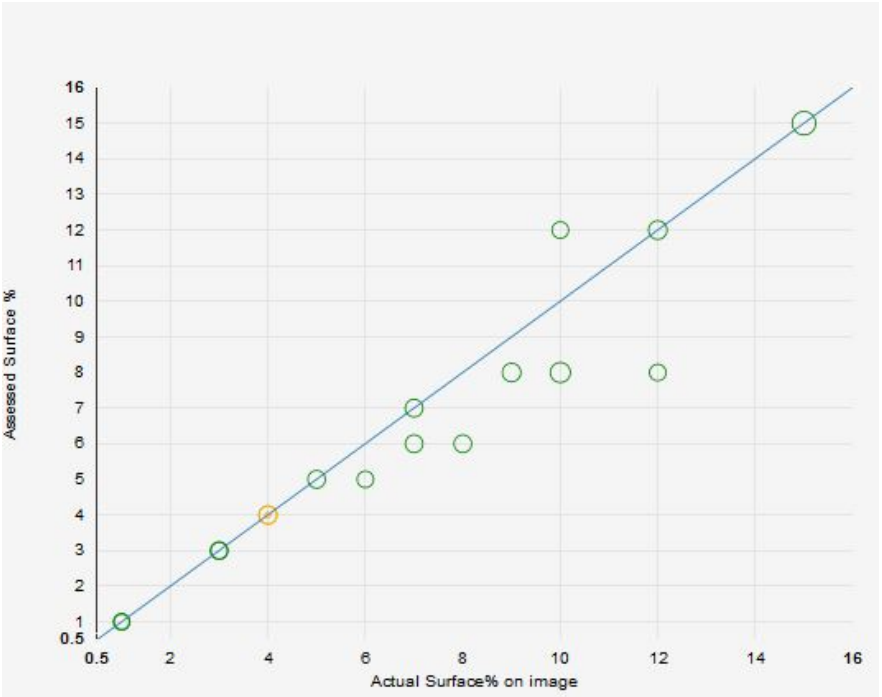


Figure 5.4.1. Disease recognition exercise: example showing correct answer



Assessment Diagnostics for Percentage Range Help?

Time of assessment (proportional to circle size)	min = **2** sec, max = **14 sec**
Very good agreement with actual %	(concordance R = **0.95**)
Almost perfect reproducibility	(3 repeats are less than 1%)

Figure 5.4.2. Area assessment tool: example chart from low range assessment test

References cited in this section

Allan W (2003) Winegrape assessment in the vineyard and at the winery. Winetitles, Adelaide SA, pp 7-8

Barbedo JGA (2014) An automatic method to detect and measure leaf disease symptoms using digital image processing. Plant Disease **98**, 1709-16

Birchmore W, Scott ES, Emmett RW, Perry W and Zanker T (2015). Update on smart-phone app for field assessment of powdery mildew. Australian and New Zealand Grapegrower and Winemaker **622**, 46-7

Bock CH, Parker PE, Cook AZ, Gottwald TR (2008) Characteristics of the perception of different severity measures of citrus canker and the relation between the various symptom types. Plant Disease **92**, 927-39

Bock CH, Poole GH, Parker PE and Gottwald TR (2010) Critical disease severity measured visually, by digital photography and image analysis, and by hyperspectral imaging. Critical Reviews in Plant Sciences **29**, 59-107

Braido R, Gonclaves-Zuliana AMH, Janeiro V, Carvalho SA, Belasque JJ, Bock CH, Nunes WMC (2014) Development and validation of standard area diagrams as assessment aids for estimating the severity of citrus canker on unripe oranges. Plant Disease **98**, 1543-50

Calonnec A, Cartolaro P, Poupot C, Dubourdieu D and Darriet, P (2004) Effects of *Uncinula necator* on the yield and quality of grapes (*Vitis Vinifera*) and wine. Plant Pathology **53**, 434-45

Dambergs, RG, Stummer B, Bevin C, Lim A, Cozzolino D, Gishen M and Scott ES (2007) Rapid analysis of powdery mildew in grapes: an industry trial. Proceedings of the 13th Australian Wine Industry Technical Conference, 28 July - 2 August, Adelaide, SA

Emmett R, Magarey P and Nutter F (1997) Assessing damage from grapevine diseases and pests. Australian Grapegrower and Winemaker **402a**, 49-52

Emmett R, Scott E, Petrovic T, Zanker T, Evans K, Kravchuk O, Perry W (2015) A diagrammatic key to assist assessment of powdery mildew severity on grape bunches. Australian and New Zealand Grapegrower and Winemaker **623**, 46-9

Gadoury DM, Seem RC, Wilcox WF, Henick-Kling T, Conterno L, Day A and Ficke A (2007) Effects of diffuse colonization of grape berries by *Uncinula necator* on bunch rots, berry microflora, and juice and wine quality, Phytopathology **97**, 1356-65.

Hill GN, Beresford RM and Evans KJ (2010) Tools for accurate assessment of botrytis bunch rot (*Botrytis cinerea*) on wine grapes. New Zealand Plant Protection **63**, 174-81

Hill GN, Evans KJ, Beresford RM and Dambergs RG (2013) Near and mid-infrared spectroscopy for the quantification of botrytis bunch rot in white wine grapes. Journal of Near Infrared Spectroscopy **21**, 467-75

Hill GN, Evans KJ, Beresford RM and Dambergs RG (2014) Comparison of methods for the quantification of botrytis bunch rot in white grapes. Australian Journal of Grape and Wine Research **20**, 432–41

Lin LI (1989) A concordance correlation coefficient to evaluate reproducibility. Biometrics **45**, 255-68

McIntyre GA (1952) A method for unbiased selective sampling, using ranked sets. Australian Journal of Agricultural Research **3**, 385-90

Murray RA, Ridout MS and Cross JV (2000) The use of ranked set sampling in spray deposit assessment. Aspect of Applied Biology **57**, 141-46

Nutter FW Jnr, Eggenberger SK and Streit AJ (2015) Disease severity assessment training using DiseasePro. In: Stevenson KL and Jeger MJ (eds) Exercises in Plant Disease Epidemiology, second edition, APS Press, MN, USA, pp.189-98

Nutter FW Jnr, Esker PD and Coelho Netto RA (2006) Disease assessment concepts and the advancements made in improving the accuracy and precision of plant disease data. European Journal of Pant Pathology **115**, 95-103

Nutter FW Jnr, Gleason ML, Jenco JH and Christians NC (1993) Assessing the accuracy, intra-rater repeatability, and inter-rater reliability of disease assessment systems. Phytopathology **83**, 806-12

Nutter FW Jnr and Schulz PM (1995) Improving the accuracy and precision of disease assessments: selection of methods and use of computer-aided training programs. Canadian Journal of Pant Pathology **17**, 174-84

Nutter FW Jnr, Teng PS and Shokes FM (1991) Disease assessment terms and concepts. Plant Disease **75**, 1187-88

Nutter FW Jnr, Wegulo SN, Litwiller D, Emmett RW and Magarey PA (2000) A computer training program to improve the accuracy and precision of disease severity assessments in grapevine. Proceedings of 3rd International Workshop on Grapevine Downy and Powdery Mildew Workshop

(Magarey PA, Thiele SA, Tschirpig KL, Emmett RW, Clarke K and Magarey RD, eds), Loxton, South Australia, 21-28 March 1998, SARDI Research Report Series No. 50, pp 64-9
Ovadia S, Shtienberg D, Dinoor A and Sztejnberg A (2006) Do flag shoots serve as the main source of primary inoculum in grape powdery mildew epidemics in Israel? In: Proceedings of 5th International Workshop on Grapevine Downy and Powdery Mildew Workshop (Gessler C, Pertot I, Gadoury DM, Gubler WD, Kassemeyer HH and Kast WK, eds), Trento, Italy, 17-24 June, pp. 35-6
Patil GP (2002) Ranked set sampling. In: Encyclopedia of Environmetrics, Volume 3, El-Shaarawi AH and Piergorsch WW (eds), Wiley, Chichester, UK, pp. 1684-90
Pethybridge SJ and Nelson SC (2015) Leaf doctor: a new portable application for quantifying plant disease severity. Plant Disease **99**, 1310-16
Schneider CA, Rasband WS and Eliceiri KW (2012) NIH Image to ImageJ: 25 years of image analysis. Nature Methods **9**, 671-67
Seem RC (1984) Disease incidence and severity relationships. Annual Review of Phytopathology **22**, 133-50
Sherwood RT, Berg CC, Hoover MR, Zeiders KE 1983 Illusions in visual assessment of Stagonospora leaf spot of orchard grass. Phytopathology **73**, 173-7
Stummer BE, Francis IL, Markides AJ and Scott ES (2003) The effect of powdery mildew infection of grape berries on juice and wine composition and on sensory properties of Chardonnay wines. Australian Journal of Grape and Wine Research **9**, 28-39
Stummer BE, Francis IL, Zanker T, Lattey KA and Scott ES (2005) Effects of powdery mildew on the sensory properties and composition of Chardonnay juice and wine when grape sugar ripeness is standardised. Australian Journal of Grape and Wine Research **11**, 66-78
Viti-Notes (2005) What wineries want …and why: winegrape assessment in the vineyard and at the winery. Grape purity 1. Diseases – powdery mildew, downy mildew, Botrytis and other moulds and rots. www.crcv.com.au/viticare/vitinotes
Viti-Notes (2010) Monitoring for powdery mildew. https://www.awri.com.au/wp-content/uploads/powdery_mildew_monitor.pdf

6. Development of objective measures for powdery mildew

Summary

A quantitative polymerase chain reaction (qPCR) assay sensitive enough to detect as little as 3 fg of DNA of *Erysiphe necator* was developed. Specificity testing revealed some cross-reactivity with the fungi which cause powdery mildew on pea and Swiss chard, neither of which is expected to occur on grape bunches, and with *Botrytis cinerea*, although at quantification cycle values (Ct) much larger than for *Erysiphe necator*. When applied to quantify powdery mildew on bunches of Chardonnay, Riesling, Grenache and Pinot Noir, the assay detected small amounts of *E. necator* biomass in homogenates prepared from grapes with no visible powdery mildew. While homogenates of grapes with visual powdery mildew severity of up to 2% were distinguished from other categories (healthy and > 2% severity), higher severity categories were not reliably distinguished, which reinforced the subjectivity of visual assessment of powdery mildew severity. The qPCR assay was used to calibrate mid-infrared spectroscopy (MIR). MIR proved insufficiently sensitive to distinguish small increments in visual powdery mildew severity when applied to homogenates of Chardonnay, Riesling, Grenache and Pinot Noir berries. While MIR spectroscopy resulted in a promising calibration model for Grenache grapes with powdery mildew, this was not the case for the other three varieties examined. NIR spectroscopy did not prove informative. Fatty acid analysis of conidia of *E. necator* using gas chromatography revealed that arachidic acid was the most abundant fatty acid. Arachidic acid also increased in abundance with increasing powdery mildew severity when individual grapes belonging to the categories healthy, half-infected and fully-infected were analysed. Arachidic acid has potential as a biomarker for powdery mildew on grapes.

6.1 Development and evaluation of a TaqMan duplex quantitative real-time PCR assay for quantifying *Erysiphe necator* (powdery mildew) on grape bunches

Tijana Petrovic, Timothy Zanker, Olena Kravchuk and Eileen S. Scott

Introduction

Objective and accurate measures of disease severity are needed to assess and grade fruit which can provide cost-effective and practical quantification of powdery mildew on bunches. Stummer et al. (2006) reported DNA-based tools (slot-blot assay, end-point PCR) that provided reliable means to detect and quantify *E. necator* biomass in grapes and resultant must and juice. When the concentration of *E. necator* DNA analysed by slot-blot hybridisation was used as reference data for visible to near-infrared spectroscopy (VNIR), a good prediction (R^2 = 0.85) of *E. necator* DNA concentration from a partial linear squares regression model was obtained, indicating that VNIR can measure and predict powdery mildew-affected grape samples (Scott et al. 2010). However, DNA slot blot technology involves radioactivity and is now rarely used. The end-point PCR was used to develop a qPCR assay by the Australian Genome Research Facility (AGRF) (J. Stephen, unpublished 2007).

In the last 10 years, several nucleic acid-based technologies (end-point PCR, quantitative real-time PCR and Loop Mediated Isothermal Amplification or LAMP) have been developed for detecting and quantifying airborne conidia of *E. necator* (Falacy et al. 2007, Mahaffee 2012, Carisse and Tremblay 2014, Huerga et al. 2014, Mahaffee 2014, Thiessen et al. 2016).

The accuracy, sensitivity and reliable quantification offered by qPCR make it a suitable “gold standard” for calibration of spectroscopic methods (NIR and MIR) in other pathosystems, such as botrytis bunch rot (Hill et al. 2014). Hill et al. (2014) demonstrated the accuracy of qPCR for predicting low visual bunch rot severities (0-10%). The need for accurate quantification of powdery mildew severity on bunches and berries and to use these data as a reference for calibration of spectroscopy led to development of real-time qPCR. The specific objectives of this research were to: (i) develop a sensitive and specific real-time qPCR assay suitable for discriminating healthy and slightly infected bunches (severity ≤ 5% based on visual assessment); (ii) test quantification of *E. necator* biomass in manufactured powdery mildew severities (weight by weight) and (iii) validate quantification of *E. necator* biomass in composite samples obtained by combining visually assessed bunches.

Materials and methods

Fungal collection. To test the specificity of the qPCR protocol, 31 microorganisms (10 obligate and 21 facultative) were collected from a range of host plants or obtained from fungal collections for use in this study. Obligately biotrophic powdery mildew fungi were collected from grapevine (5 strains) and 11 other host species (clover, cucumber, pea, petunia, plantago, pumpkin, rose, snake bean, Swiss chard, wheat and zucchini). *Plasmopara viticola* (grape downy mildew) and the majority of facultative organisms originated from grape bunches or canes.

Grape collection. Visually healthy and powdery mildew-affected grape bunches and berries were collected from vineyards at the University of Adelaide (Coombe and Alverstoke vineyards), the Riverland (Glossop) and Eden Valley in 2014-2016 (Table 6.1.1) for preparation of manufactured and composite samples. Manufactured samples were prepared by combining different proportions of homogenised visually healthy and fully-infected berries weight by weight. Composite samples were produced by combining all berries from destemmed bunches that were visually graded based on surface area with powdery mildew symptoms. Chardonnay and Riesling were collected at harvest from the Coombe vineyard in 2014 and 2015 to manufacture the desired powdery mildew severity categories and to prepare composite samples, respectively. In 2015, Grenache from the Coombe and Pinot Noir from the Lenswood vineyards were collected for manufactured and composite samples. Bunches were assessed in the laboratory on the day of harvest using a magnifying lamp; the surface area affected of each bunch was visually assessed on each side of bunch as the proportion of berry surface with powdery mildew symptoms and then averaged for the whole bunch. Assessed bunches for composite samples were placed individually into plastic bags and stored at -20 °C until required. When required, each frozen bunch was destemmed, peduncles were removed from berries and berries were combined to produce the desired visual severity category. Visually healthy and severely infected bunches collected to prepare manufactured samples were separated into small clusters, assessed for symptoms using a magnifying lamp, and individual healthy and fully-infected berries were detached, assigned either to healthy or fully-infected batches of berries for each cultivar and stored at -20 °C until required.

2014-2015

Manufacturing powdery mildew of known severity. For Chardonnay, Grenache and Pinot Noir, 1000 g of visually healthy and 290 g of fully-infected thawed berries were independently homogenised using a Grindomix GM200 (Retsch GmbH & Co) for 20 s at 8000 rpm. For Riesling, 1500 g of visually healthy and 300 g of fully-infected berries were homogenised. Nine severity categories (%, w/w) were manufactured by combining aliquots of homogenised visually healthy and fully-infected berries in a final weight of 90 g. Homogenates of visually healthy and fully-infected berries alone provided zero and 100% severity levels, respectively. Jars containing manufactured samples were mixed well by vortex and kept on ice during subsampling. Five subsamples per severity level were collected for DNA extraction (1 g/subsample) and an additional subsample was taken to measure total soluble solids (TSS).

Preparation of composite powdery mildew severities. Composite samples, approximately 8 to 13 kg per cultivar, were prepared by combining frozen berries from 10 (Chardonnay, Riesling), six (Grenache) or between six and 15 (Pinot Noir) destemmed bunches that belonged to the same visual severity category; the variation in number reflected the weight of bunches. In total, 10 (Chardonnay), nine (Riesling) and eight (Grenache, Pinot Noir) visual severity categories were prepared (Table 6.1.1). Seven (Grenache) and six (Chardonnay, Riesling, Pinot Noir) subsamples of berries (150-230 berries/subsample or 147-270 g/subsample depending on the variety) were collected from each designated powdery mildew severity category, thawed overnight at 4 °C, independently homogenised using the Grindomix GM200 (Retsch GmbH & Co) for 20 s at 8000 rpm and the homogenates kept on ice. From each subsample, four sub-subsamples were taken, for DNA extraction (1 g), TSS (1.5 mL), MIR (1.5 mL) and NIR scanning (5 mL).

Individual bunches. The sampling strategy was designed to obtain a representative range of individual Chardonnay bunches with 0-30% surface area affected likely to be present in the Coombe and Alverstoke vineyards on January 8, 2014 when TSS was from 5.6 to 19 °Brix, the majority of bunches having TSS 14-17 °Brix. In total, 42 bunches arranged in seven groups of six bunches were visually assessed by participants in the Project Steering Group workshop in January 2014 using the 2% increment key (Emmett et al. (2015), Section 5.1) and subsequently by experts using a magnifying lamp. Individual bunches were stored at -20 °C and later berries were detached from the surface side of bunches that had been assessed, homogenised and processed as described above.

2016

Preparation of composite powdery mildew severities. Chardonnay bunches (110) were collected from the Alverstoke vineyard when TSS reached 20.8 °Brix (January 18, 2016), visually assessed for powdery mildew and stored at -20 °C. Composite samples were prepared in a manner similar to vintage 2015. Nineteen healthy bunches, 8 to 12 bunches for each of eight visual severity categories (0.5-15%) and 19 bunches exhibiting 20-25% powdery mildew were combined within each severity category to obtain composite samples. The destemmed berries in each severity category were mixed, divided into six subsamples per category (150-360 g/category) and processed as for the Chardonnay samples from vintage 2015. Chardonnay bunches from the Glossop vineyard were visually assessed by an industry expert. Healthy (19) and powdery mildew-affected (153) (≥ 0.5-100% severity) bunches were placed into individual plastic bags after assessment and stored at -20 °C in the Accolade winery (Berri) until required. Composite samples were prepared by grouping 10 bunches from various visual severity categories to achieve each of 16 mean powdery mildew severities (200-272 g/category) (Table 6.1.1), then five subsamples of berries were taken from each for DNA extraction, spectroscopy and TSS. A similar approach was undertaken for Riesling collected from the vineyard in Eden Valley. Healthy (17) and powdery mildew-affected (132) (≥ 0.5-60%) bunches were collected and transported to the laboratory on the same day. After scoring, bunches were placed into individual plastic bags and stored at -20 °C. Composite samples were later prepared by grouping nine to 15 destemmed bunches that belonged to the same visual severity category (0, 0.5, 1-2, 2-4, 4-6, 6-8 and 12-15%). The remaining bunches from various visual severity categories were combined to achieve one of five mean powdery mildew severities (*i.e.* 3.9A, 3.9B, 8, 19 and 50%, Table 6.1.1). Five subsamples of berries (approx. 200 g/category) were collected from composite samples for each designated powdery mildew severity level. An additional 5 kg of bunches were collected at random as a “blind sample” to test the validity of the real-time PCR quantification. These bunches yielded a “blind sample” of 2 kg of destemmed berries, which was split into 10 subsamples and frozen.

Individual berries. The sampling strategy was designed to obtain a representative range of individual berries from healthy and infected bunches likely to be present in the Alverstoke vineyard on January 13, 2016 when TSS was 17-18 °Brix. In total, 61 berries (each with weight ≥ 250 mg) were selected for quantification of *E. necator* biomass. Balanced selection of healthy (n = 20), half- (n = 21) and fully-infected (n = 20) berries was matched whenever possible at the bunch level (see Section 6.4).

Extraction of genomic DNA. DNA of powdery mildew fungi (*Blumeria*, *Erysiphe* and *Podosphaera* spp.), *P. viticola* and 21 facultative microorganisms was extracted using a commercial NucleoSpin Plant II Kit (Macherey-Nagel GmbH & Co. KG, Düren, Germany) and cell lysis buffer containing CTAB (PL1 supplied with the kit). Frozen *E. necator* conidia (10-30 mg) that were collected from detached leaves of Cabernet Sauvignon were disrupted by mixing with glass beads on a vortex for 1 min. A range of leaves colonized by different powdery mildew fungi (100 mg) and facultative microorganisms harvested from yeast malt broth (100 mg) were disrupted by grinding in liquid nitrogen. The samples were processed according to the protocol supplied with the kit. The gDNA was finally eluted (2 x 50 µL) with low salt elution buffer PE (5mM Tris/HCl, pH 8.5). DNA purity was evaluated using a Nanodrop 2000 Spectrophotometer (Thermo Scientific) by comparing the absorbance ratio A260/A280. DNA was quantified (ng/µL) using a QuantiFluor dsDNA System with an 8-point standard curve.

DNA was also extracted from a known weight of four isolates of *E. necator* conidia stored at – 80 °C in the collection at the University of Adelaide, using a phenol:chloroform extraction method (Stummer et al. 2006). DNA was quantified, purified using a DNeasy Plant Mini Kit (Qiagen) and prepared for qPCR. DNA of these isolates was used to (a) determine the threshold of quantification, (b) relate number of *E. necator* fragment copies to amount of extracted *E. necator* genomic DNA (gDNA) and (c) test inhibition in the presence of background *V. vinifera* DNA.

V. vinifera gDNA was extracted from disease-free leaves of Cabernet Sauvignon (two leaves produced in tissue culture), and surface sterilised and homogenised Chardonnay berries (two replicates). One visually healthy bunch (20 °Brix) was separated into small clusters, powdery mildew-free berries were destemmed but with the peduncle in place and placed for 10 s in 70 % ethanol, then 2 min in 1% NaOCl, rinsed three times in sterile water and air-dried (Evans et al. 2013). The peduncle was removed, the berries were first homogenised for 30 s in a blender and two subsamples of 100 mg each were homogenised in liquid nitrogen. DNA was extracted using the Macherey-Nagel NucleoSpin Plant II Kit and used to determine the threshold of quantification and to test inhibition of qPCR amplification in the presence of *E. necator* DNA.

DNA was extracted from all manufactured and composite samples of Chardonnay, Riesling, Grenache and Pinot Noir (Table 6.1.1) as described above for extraction of DNA from leaves colonized by various powdery mildew fungi. Only the first elution of DNA was considered for duplex qPCR assay as the concentration was greater than the second elution. All the DNA solutions were normalised to 0.5 ng/µL or 1 ng/µL, depending on the variety.

Primer and probe development. Real-time PCR primers and probe were developed from the original pEnA1 fragment of *E. necator* (target) (Stummer et al. 2006) for quantification of fungal biomass in the presence of grape DNA and the *actin 1* gene of *V. vinifera* (endogenous control) (Hanania et al. 2004). In preliminary work by AGRF in 2007 (J. Stephen, unpublished), a duplex qPCR assay using TaqMan TAMRA probes amplified a 79 bp fragment of the original pEnA1 fragment of *E. necator* and a 71 bp fragment of the *actin 1* gene of *V. vinifera*. However, the mis-match of reaction efficiencies between the target (max 74%) and endogenous control (up to 90%) raised concerns about the accuracy of the assay. Consequently, new TaqMan MGB hybridisation probes were designed to be used with a contemporary ViiA 7 real-time PCR machine (Life Technologies, CA, USA); FAM (Ery-FAM: 5'-TAACTTCTCCCAATACGC-MGB-NFQ-3') and VIC (Vit-VIC: 5'-TAACTTGCTCCTTTGAC-MGB-NFQ-3') dye-labelled for target and endogenous control, respectively. The primers for target and endogenous control were also redesigned as follows; target (Enec-MGB-F: 5'-CCAATCTATAGCAGTGCCTATTCAGT-3'; Enec-MGB-R: 5'-CAACCTAATGTAACTAGCGACTGGAT) and endogenous control (Vvin-F: 5'-CTTTTCTATTGTTAGTGTTGCCTGAGTT-3'; Vvin-R: CATAAATTGGCACAGTGTGACTCA-3'), which produced amplicons of 74 and 100 bp, respectively.

Specificity of qPCR. Specificity of primer/probe was evaluated via *in silico* analyses using NCBI Primer Blast to ensure that primers were unique to *E. necator* and *V. vinifera*. Specificity of the primer sets was also evaluated using qPCR performed on 21 microbial species commonly associated with grape bunches and other grape tissues, as well as other powdery mildew fungi. Additionally, to address questions about possible cross-reactivity with *Botrytis cinerea*, a mixture of *E. necator* and *V. vinifera* DNA in two different proportions (5% and 66% weight/weight) was spiked with three concentrations of *B. cinerea* DNA to achieve final concentration of 3, 1.5 and 0.75 ng of *B. cinerea* per reaction along with a *B. cinerea*-free mixture as a control.

Sensitivity of qPCR. Sensitivity of the primer set was evaluated using monoplex and duplex qPCR performed on 10-fold serial dilutions of DNA extracted from four *E. necator* strains adjusted to a concentration of 1 ng/µL and 10-fold serial dilutions of *E. necator* DNA (5.8 ng) added to *V. vinifera* DNA (21.3 ng), respectively.

Effect of *V. vinifera* DNA on amplification of *E. necator* DNA and *vice versa.* Any possible influence of endogenous control DNA on amplification of target DNA was also tested using: (i) 10-fold serial dilutions of the mixture of *E. necator* and *V. vinifera* DNA, (ii) spiked homogenates of berries with *E. necator* conidia and (iii) spiked homogenates of visually healthy berries with fully-infected homogenised berries (see *Manufacturing powdery mildew of known severity*). Amplification of 10-fold serial dilutions of a mixture of *V. vinifera* DNA (1.6 ng) and *E. necator* DNA (3 ng) was evaluated in the duplex qPCR, expecting to have optimal efficiency of amplification of both DNAs.

Possible inhibition was evaluated using DNA extracted from homogenates of visually healthy Riesling berries and the homogenates spiked with 2.9 mg and 16.2 mg of *E. necator* conidia with addition of 10 µL of Tween20. Three visually healthy Riesling berries (total 3289 mg) were homogenised in liquid nitrogen and three samples of 800 mg were aliquoted into small mortars. Two samples were spiked with *E. necator* conidia, subjected to fine grinding in liquid nitrogen and then DNA was extracted according to the protocol supplied with the NucleoSpin Plant II MN kit, as above. DNA concentration was normalized to 0.5 ng/µL. All qPCR reactions were performed with 3 µL of DNA template and 10-fold dilution series of *E. necator* and *V. vinifera* plasmid DNA standards.

Table 6.1.1. Grape bunch and berry samples collected for quantification of *Erysiphe necator* biomass

Sample type	Cultivar	Vineyard	Collection date			Powdery mildew severity (%)	Number of subsamples	TSS, TA, pH
			2014	2015	2016			
Manufactured	Chardonnay	Coombe	13 Jan			11 (w/w)	5	17.5 °Brix, 14.4%, 3.03
	Riesling	Coombe	16 Jan			11	5	14 °Brix, 1.6%, 2.9
	Grenache	Coombe		12-13 Feb		11	5	22 °Brix
	Pinot Noir	Coombe		23 Feb		11	5	
Composite	Chardonnay	Coombe		15-16 Jan		0, 0.5, 1, 2, 3-4, 5-6, 7-9, 10-12, 15-18, 20-25	6	18.6 °Brix
		Alverstoke			18 Jan	0, 0.5, 1-2, 2-3, 3-4, 5-6, 6-8, 8-10, 10-15, 20-25	6	21.1 °Brix
		Glossop			19 Jan	0, 3.1, 3.5, 3.8, 4.1, 4.7, 5.5, 5.6, 6.3A, 6.3B, 7.7, 15.2, 28, 57, 65.5, 68	5	16.8 °Brix
	Riesling	Coombe		28-29 Jan		0, 0.5, 1-2, 3-4, 5-6, 6-8, 10-12, 15-20, 20-25	6	19.5 °Brix
		Eden Valley			11 Feb	0, 0.5, 1-2, 2-4, 4-6, 6-8, 12-15, 3.9A, 3.9B, 8, 19, 50 & 10 unknowns	5	20.9 °Brix
	Grenache	Coombe		12-13 Feb		0, 0.5, 1-2, 3-5, 6-8, 10-15, 18-20, 20-25	7	22 °Brix
	Pinot Noir	Lenswood		23 Feb		0, 0.5, 2-4, 4-6, 8-10, 10-12, 15-20, 20-25	6	22 °Brix
Individual bunches	Chardonnay	Alverstoke Coombe	8 Jan					5.6-19 °Brix
Individual berries	Chardonnay	Alverstoke			13 Jan			17-18 °Brix

Preparation of the calibration standards. Synthetic oligo DNA standards for quantification of target and endogenous control were designed for use in the new TaqMan MGB assay. Ordering of the HPLC-purified primers for target (Enec-MGB-F/-R) and endogenous control (Vvin-F-MGB-F/-R), and the synthetic oligo standard for target at the same time from the supplier resulted in a problem with quality control during synthesis such that both sets of primers were contaminated with synthetic oligo standard for target. Painstaking, step-wise testing for the source of contamination in the end-point and qPCR assays, and waiting time for primers that were eventually ordered from another suppler (Invitrogen), caused a delay of 2 months. Consequently, plasmid DNA standards for target and endogenous control were chosen for further work to prevent possible contamination. Plasmids containing the *E. necator*-specific 450 bp DNA fragment pEnA1 (Stummer et al. 2006) and cloned 100 bp DNA fragment of *Vitis actin 1* (Hanania et al. 2004) were used to create standards for the target (*E. necator*) and endogenous control (*V. vinifera*), respectively. Purified and linearised plasmid DNA solutions were calibrated and 10-fold serial dilutions thereof were prepared and stored at -20 °C until use. Standards contained from $3x10^7$ to 3 copies of the target plasmid DNA per 3 µL. qPCR reaction efficiency was assessed by generating standard curves for a dilution series of *E. necator* and *V. vinifera* plasmid DNA templates.

Real-time PCR. A duplex qPCR assay was optimized experimentally using DNA of *E. necator*, *V. vinifera* and mixture of *E. necator* and *V. vinifera*. Amplification and quantification of the *E. necator* fragment pEnA1 was achieved using 0.666 µM Enec-MGB-F/-R primers, 0.233 µM Ery-FAM probe, 0.466 µM Vvin-F/-R primers, 133 µM Vit-VIC probe, 1x iTaq Universal Probes Supermix and 3 µL of template DNA in a 15 µL reaction. All reactions were carried out in MicroAmp optical 96-well plates (Applied Biosystems) in a ViiA 7 real-time PCR machine. Reactions were performed in triplicate for optimization and in duplicate for manufactured and composite grape samples. All qPCR plates contained *E. necator* reference sample 193 3s "B" and non-template controls, and most of the plates contained a *V. vinifera* sample (Vvin3) also. The cycle for this duplex assay comprised an initial denaturation step at 95 °C for 8 min followed by 40 cycles of denaturation at 95 °C for 15 sec, annealing at 60 °C for 30 sec and elongation at 72 °C for 35 sec.

Data handling and analysis. Results for each individual duplex amplification were examined and quantification cycles (Cts) were linearly interpolated between the two readings closest to the threshold line at 0.04 and 0.07 for *V. vinifera* and *E. necator*, respectively. Reproducibility of the qPCR assay was evaluated by comparing the results of the same DNA tested in at least 10 separate runs. Change in the logarithm of *E. necator* Ct or *V. vinifera* Ct/*E. necator* Ct were modelled with a nonlinear least squares regression in R (nls statistical package). Results are presented as a change in the logarithm of *E. necator* Ct against either severity weight/weight (%) or surface area (%) in manufactured and composite samples, respectively.

Results

Specificity of the qPCR assay

No homology to primer pairs Enec-MGB-F/-R and Vvit-F/-R was observed during *in silico* NCBI Primer Blast analysis (Reference Sequence Database) apart from the homology to GenBank sequences of the original pEnA1 fragment of *E. necator* (Stummer et al. 2006) and *actin 1* gene of *V. vinifera* (Hanania et al. 2004), respectively. Additionally, no homology to the 74 bp sequence of pEnA1 fragment or 100 bp sequence of *actin 1* was observed during GenBank searches apart from homology to the original sequences and the whole-genome sequences of both organisms. However, a fragment of the appropriate length was amplified from DNA of *Erysiphe pisi* (Ct 21.78 ± 0.03) and *E. betae* (Ct 24.09 ± 0.11) from powdery mildew on pea and Swiss chard, respectively (Figure 6.1.1). Amplification products resulted from loading 3 ng of pure *B. cinerea* DNA at Ct ≥ 29.8 ± 1.02. Amplification of a mixture of *E. necator* and *V. vinifera* DNA spiked with *B. cinerea* DNA resulted in no change of *E. necator* Ct in comparison to the control (non-spiked) (Table 6.1.2).

Primer set Enec-MGB-F/-R did not cross react with *V. vinifera* and amplifications of fungal DNA at Ct > 32 (31.60 ± 0.46) were considered non-specific (false positive). Random amplification of fungal DNA with primer set Vvit-F/-R occurred at Ct > 35 and was considered as negative.

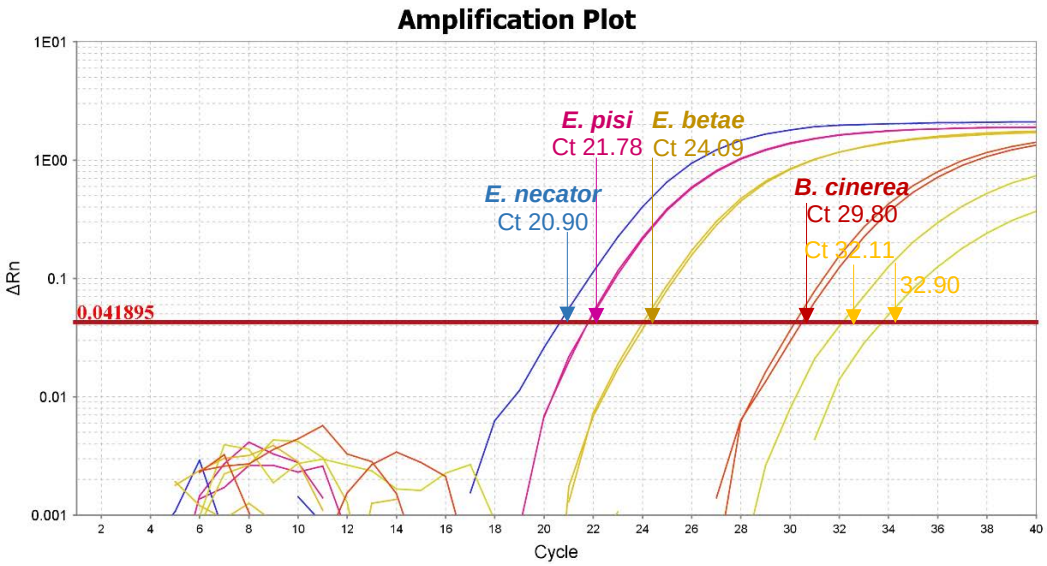


Figure 6.1.1. Specificity of the TaqMan MGB qPCR. Raw fluorescence curves showing quantification cycles (Ct) for *E. necator* (0.001 ng/reaction), and *E. pisi, E. betae* and *B. cinerea* (3 ng/reaction).

Table 6.1.2. Amplification of *B. cinerea* DNA in a mixture of *E. necator* and *V. vinifera* DNA

***E. necator* & *V. vinifera* (w/w)†**	***B. cinerea* ng/reaction**	**Ct**	***E. necator* & *V. vinifera* (w/w)†**	***B. cinerea* ng/reaction**	**Ct**
5%	0	19.92	66%	0	17.34
5%	0.25	19.92	66%	0.25	17.31
5%	0.5	19.90	66%	0.5	17.25
5%	1	20.05	66%	1	17.30

† Mixture of *E. necator* and *V. vinifera* DNA was spiked with *B. cinerea* DNA to achieve the concentrations of *B. cinerea* in column 2 and 5.

Sensitivity of the qPCR assay

Sensitivity of the *E. necator* qPCR assay was assessed using a 10-fold dilution series of four *E. necator* strains in water (monoplex qPCR) (Figure 6.1.2a) and 10-fold diluted series of *E. necator* DNA in a background of *V. vinifera* DNA (duplex qPCR) (Figure 6.1.2b). The standard curves obtained using *E. necator* genomic DNA diluted in water and the *E. necator* plasmid DNA gave an efficiency of ≥ 97 % (Figure 6.1.2a). *E. necator* DNA from conidia of four isolates was detected to a limit of detection (LOD) of 3 fg *E. necator* (Ct 31.99 ± 0.65) which is close to few as 30 *E. necator* copies of plasmid DNA standard (Ct 31.60 ± 0.46).

Diluting the *E. necator* genomic DNA in a background of *V. vinifera* DNA from leaves affected the standard curve obtained (Figure 6.1.2b). In duplex qPCR, Ct values for reactions where the largest *E. necator* DNA concentration (6 orders of magnitude) was used were higher when *V. vinifera* DNA was added to the reaction than when sterile water was added. However, when the smallest *E. necator* DNA concentration was used, Ct values for reactions were lower when *V. vinifera* DNA was added. As a result, a difference was observed in the slope of the monoplex and duplex qPCR reactions, giving efficiency values of 91% and 107%, respectively. The amount of *V. vinifera* DNA amplified was within two Ct values for different concentrations of *E. necator* DNA in the duplex qPCR (Figure 6.1.2b; grey triangle).

The effect of grape DNA on amplification of *E. necator* was also tested in 10-fold serial dilutions of the mixture of *E. necator* and *V. vinifera* DNA from berries. Diluting the mixture of DNAs for duplex qPCR did not affect the standard curve of *E. necator* DNA, but slightly affected the standard curve of *V. vinifera* DNA, suggesting the presence of inhibitors in the DNA template.

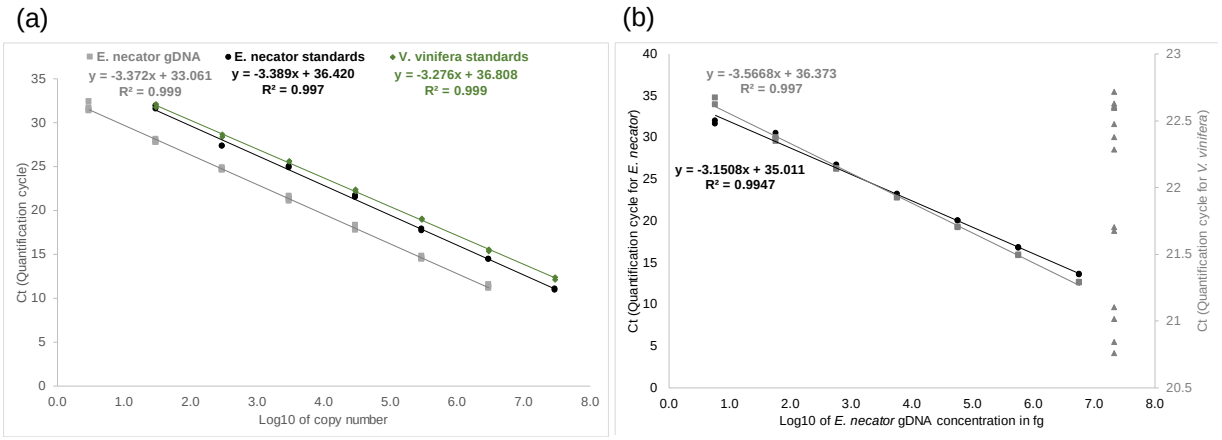


Figure 6.1.2. Sensitivity of the monoplex (a) and duplex (b) qPCRs. Standard curve assessed with a 10-fold serial dilution of *Erysiphe necator* DNA from conidia diluted in water (grey line) and plasmid DNA standard (black line) in monoplex qPCR (a). Standard curve of *Erysiphe necator* DNA from conidia diluted in a background of *V. vinifera* DNA (black line) and water (grey line) in duplex qPCR (b). Ct for *V. vinifera* DNA in duplex qPCR is also shown (grey triangles, b). Quantification cycle (Ct) is plotted against logarithm of the concentration (fg) of *E. necator* DNA samples or copy number of plasmid DNA standard.

Sensitivity of qPCR using spiked and manufactured homogenates. Amplification of *E. necator* DNA in the duplex qPCR was consistent among homogenates of Riesling berries spiked with conidia, with mean Ct 16.54 (± 0.28) in samples with 2.9 mg of conidia and Ct 13.70 (± 0.16) in samples with 16.2 mg of conidia. Trace amounts of *E. necator* DNA were detected in non-spiked samples that were used as the negative control (Ct 27.40 ± 0.20). The efficiency of amplification based on the standards was 101%. However, amplification of *V. vinifera* DNA was inhibited in three of 10 samples by the presence of *E. necator* DNA.

In manufactured powdery mildew severities (w/w) of Chardonnay, the amount of *E. necator* DNA in duplex qPCR showed a logarithmic increase with the increase of severity. Trace amounts of *E. necator* DNA were detected in homogenised samples of Chardonnay obtained from berries that appeared free from powdery mildew and were used for manufacturing powdery mildew of known severity (Ct 28.11 ± 0.27). The amount of *V. vinifera* DNA amplified was within 1.5 Ct values for the various powdery mildew severity categories; this gave 5% error relative to the mean *V. vinifera* Ct value (Ct 27.38 ± 0.49), indicating possible but negligible inhibition of the endogenous control. A similar effect was observed when the logarithmic ratio of *V. vinifera* and *E. necator* quantification cycles (Ct) were plotted against increasing powdery mildew severity. Consequently, further analyses of quantification of powdery mildew in manufactured and composite samples considered only quantification thresholds of *E. necator*.

Quantification of powdery mildew in manufactured and composite samples

Chardonnay and Riesling

Quantification of *E. necator* in manufactured Chardonnay and Riesling samples by qPCR showed that visually healthy samples used for manufacturing were well separated from the remaining 10 severities (weight/weight), and severity of 1% was well separated from the remaining severities (Figure 6.1.3a, b). Quantified biomass in the Chardonnay manufactured samples was indistinguishable in the following severities (w/w): (i) 3% and 5%; (ii) 7% and 9%; (iii) 14% and 17%, and (iv) 33%, 66% and 100% (Figure 6.1.3a). In the Riesling manufactured samples, the following powdery mildew severities (w/w) could not be separated: (i) 3% and 5%; (ii) from 7% to 17%, and (iii) from 33% to 100% (Figure 6.1.3b).

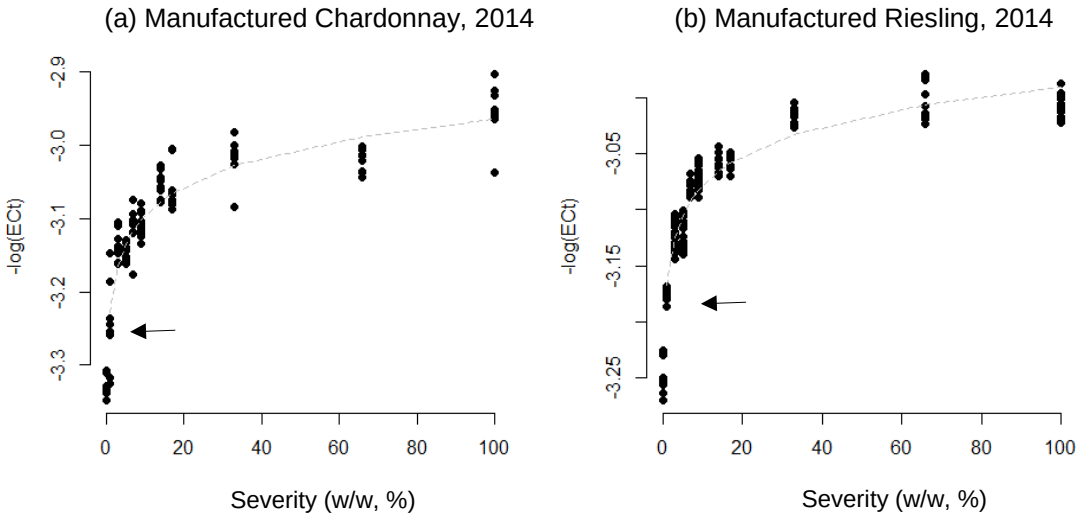


Figure 6.1.3. Regressions of the *E. necator* quantification cycle (Ct) resulting from duplex qPCR versus manufactured powdery mildew severity (w/w) in percentage (%). Visually healthy samples used for manufacturing are defined with negative Log Ct values < 3.3 (Chardonnay) (a) and ≤ 3.25 (Riesling) (b). Manufactured samples of 1% severity w/w for both varieties are separated from the remaining samples (arrow).

In the composite preparations of Chardonnay from the Coombe vineyard (2015), samples that were visually healthy or below 2% severity based on visual assessment were considered unaffected based on the qPCR and the threshold of 3.4 (Log *E. necator* Ct) or Ct 31 (Figure 6.1.4a). *E. necator* biomass (qPCR) separated samples with visual severity 2% and 4% from samples considered ≥ 7% (Figure 6.1.4a). In the composite Chardonnay samples from the Alverstoke vineyard (2016), visually healthy samples were well discriminated from the remaining samples based on the qPCR (Figure 6.1.4b). *E. necator* biomass separated samples visually assigned to 0.5% and 2% from those with ≥ 4% (Figure 6.1.4b). *E. necator* biomass clearly separated severely infected samples (20-25% visual severity) from all other samples.

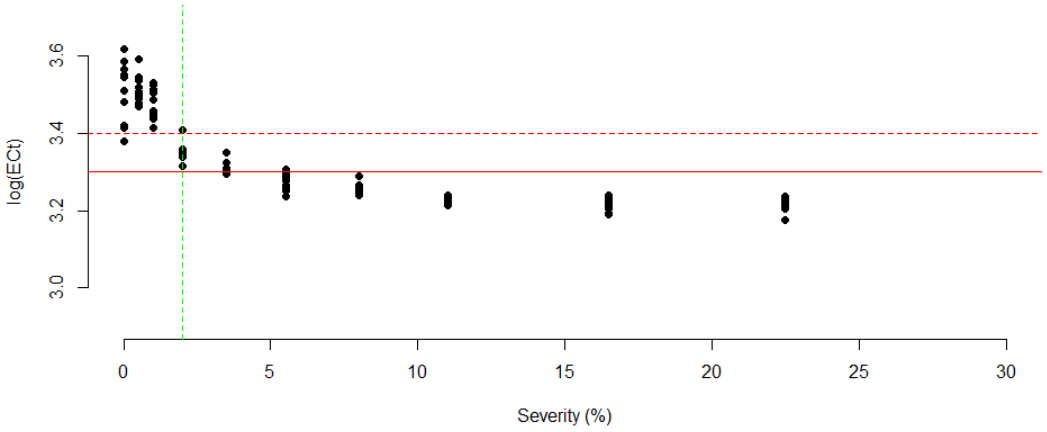
In the composite Chardonnay samples from the Glossop vineyard (2016), no samples were unaffected by powdery mildew as determined by the qPCR (Figure 6.1.4c). *E. necator* biomass distinguished samples with mean visual severity ≤ 5.5% from samples with ≥ 7.7%.

Individual Chardonnay bunches (2014) (Figure 6.1.5a) and berries (2016) (Figure 6.1.5b) showed a trend in fungal biomass similar to the trend observed in the composite Chardonnay samples. Unaffected individual bunches and berries were above the threshold of 3.4 (Log *E. necator* Ct), and traces of *E. necator* were quantified in the samples with the threshold above 3.3 (Log *E. necator* Ct). Increase of *E. necator* biomass, as measured by decrease of Log (*E. necator* Ct), was observed in bunches (Figure 6.1.5a) and berries (Figure 6.1.5b) with increasing visual severity.

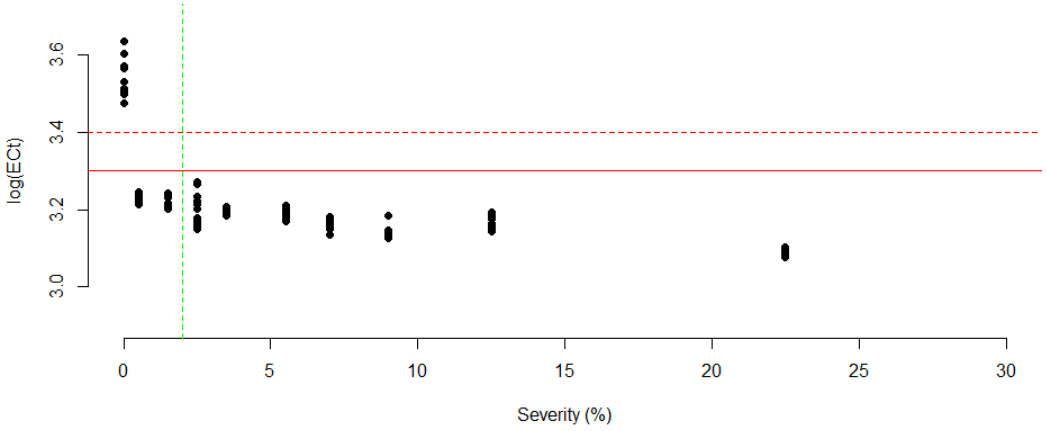
In the composite preparations of Riesling from the Coombe vineyard (2015), qPCR detected *E. necator* in all samples, including visually healthy samples. Visually healthy and samples with severity ≤ 2% were classified as having traces of powdery mildew due to the threshold above Log (*E. necator* Ct) 3.3 for most of the samples (Figure 6.1.6a), and they were well separated from the remaining visual severities ≥ 3-4%. *E. necator* biomass was similar in the visual categories from ≥ 3-4% to ≤ 20-25% (Figure 6.1.6b).

Composite Riesling samples from the Eden Valley vineyard (2016) showed a trend in fungal biomass similar to that for Riesling samples from the Coombe vineyard (2015). The qPCR did not detect bunches unaffected by powdery mildew. Visually healthy bunches had traces of powdery mildew, as the Log *E. necator* Ct was above 3.3 (Figure 6.1.6b). *E. necator* biomass in samples having traces of powdery mildew based on the visual assessment (0.5%) were separated from the rest of the samples (Figure 6.1.6b). There was no clear separation of the remaining samples based on *E. necator* biomass.

(a) Composite Chardonnay Coombe vineyard, 2015



(b) Composite Chardonnay Alverstoke vineyard, 2016



(c) Composite Chardonnay Glossop vineyard, 2016

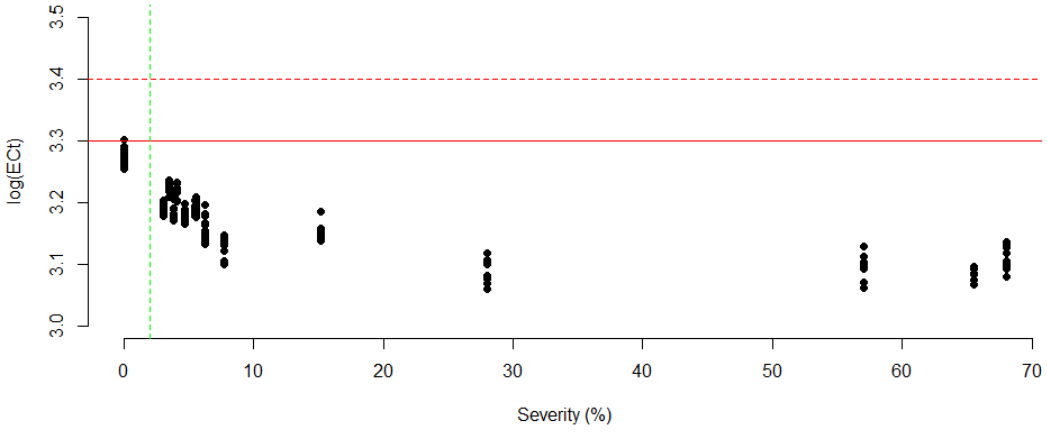
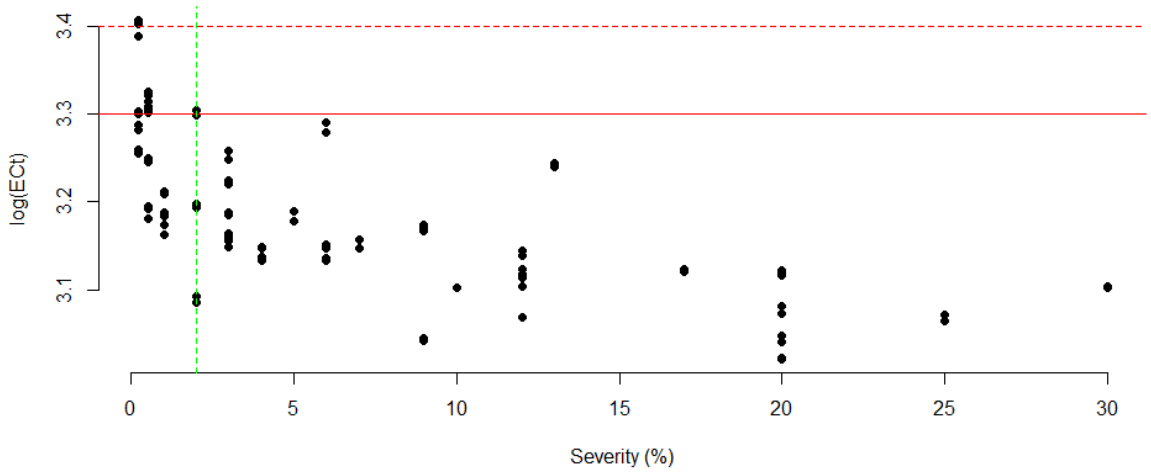


Figure 6.1.4. Regressions of the *E. necator* quantification cycle (Ct) resulting from duplex qPCR versus visual surface area powdery mildew severity in percentage (%). *E. necator*-free samples and samples with traces are separated from the diseased samples by green dashed and red continuous lines based on qPCR, respectively. The threshold for *E. necator*-free samples is set at Log (*E. necator* Ct) 3.4 which is equivalent to the Ct 31 (red dashed line). Chardonnay bunches for composite samples originated from the following vineyards: Coombe (a), Alverstoke (b) and Glossop (c).

(a) Chardonnay individual bunches Steering Group Workshop 2014



(b) Chardonnay individual berries, 2016

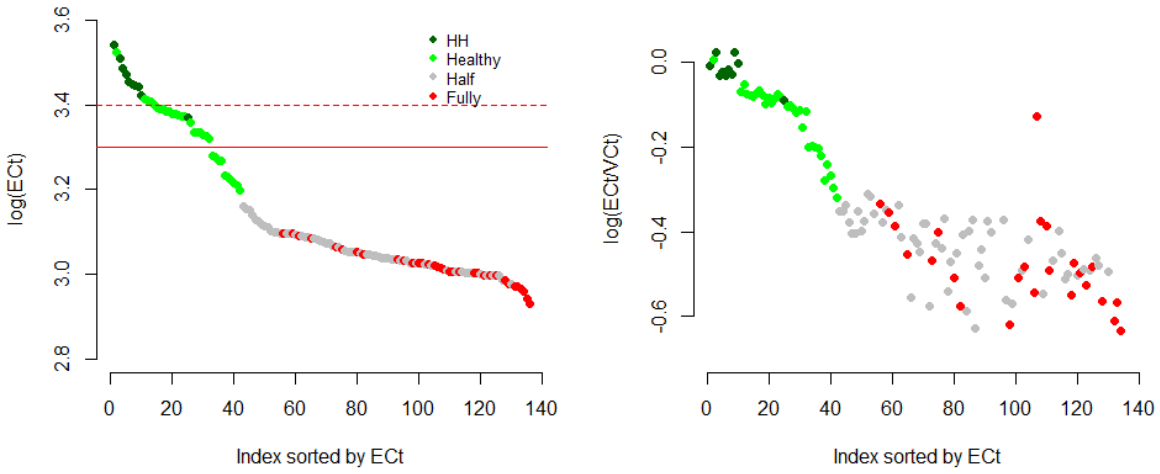
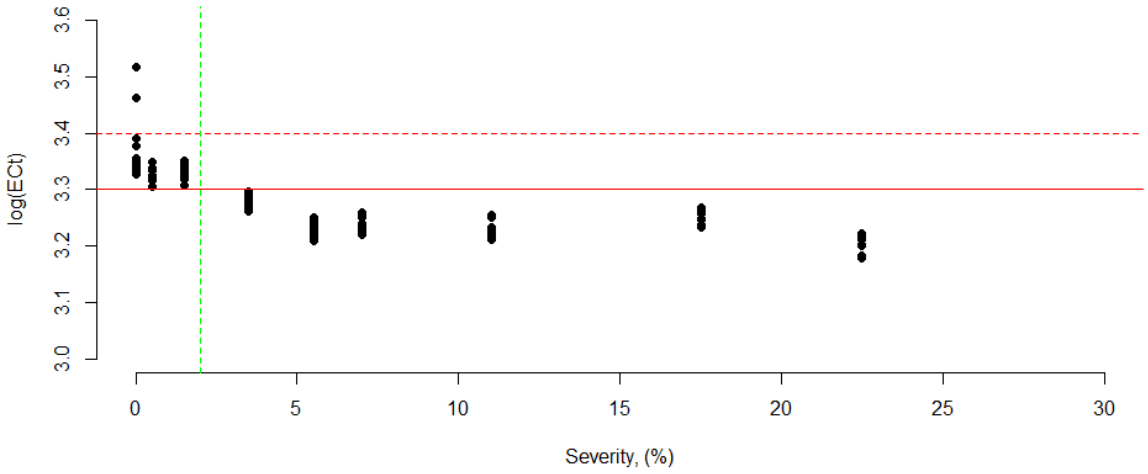


Figure 6.1.5. Regression of the *E. necator* quantification cycle (Ct) resulting from duplex qPCR versus powdery mildew severity in percentage (%). Surface area affected was visually assessed on individual bunches (a) and berries (b) of Chardonnay in 2014 and 2016, respectively. *E. necator*-free bunches (a), berries (b) and those with traces are separated from the diseased bunches (a) and berries (b) by green dashed and red continuous lines based on qPCR, respectively. Berries with traces are separated from diseased berries by red continuous line. Each berry is colour-coded based on visual assessment. Berries denoted HH originated from visually healthy bunches and berries denoted healthy, half- and fully-infected originated from bunches with some berries infected. The threshold for *E. necator*-free bunches and berries is set at Log (*E. necator* Ct) 3.4 (red dashed line).

(a) Composite Riesling Coombe vineyard, 2015



(b) Composite Riesling Eden Valley vineyard, 2016

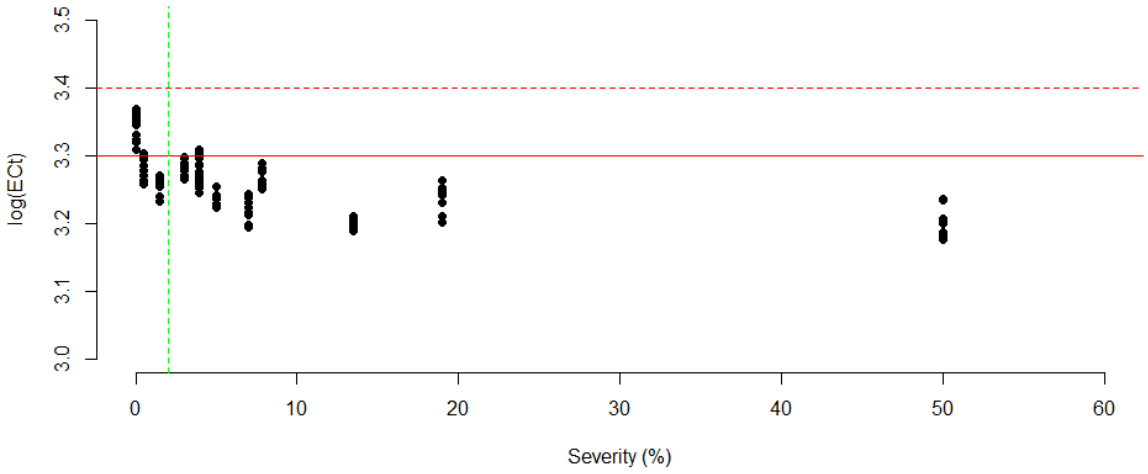


Figure 6.1.6. Regressions of the *E. necator* quantification cycle (Ct) resulting from duplex qPCR versus visual surface area powdery mildew severity in percentage (%). Samples with traces of *E. necator* are separated from the diseased samples based on qPCR (red continuous line). The threshold for samples with traces is set at Log (*E. necator* Ct) 3.3. *E. necator* biomass separates Riesling samples visually assessed as ≤ 2% from the rest of the samples (green dashed line). No clear separation based on *E. necator* biomass detected in the samples collected in the Eden Valley vineyard (b). Riesling bunches for composite samples originated from the Coombe (a) and Eden Valley (b) vineyards.

Grenache and Pinot Noir

In manufactured samples of Grenache and Pinot Noir, quantification of *E. necator* by qPCR showed that visually healthy grapes used for manufacturing were well separated from the remaining 10 severities (weight/weight) (Figure 6.1.7a, b). The manufactured severity of 1% was not well separated from 3% severity for Grenache (Figure 6.1.7a), but it was well distinguished for Pinot Noir (Figure 6.1.7b). Quantified biomass in manufactured samples of both Grenache and Pinot Noir was similar for the following severities (w/w): (i) 5%, 7% and 9%, and (ii) 14% and 17%. Higher severities for both varieties were well separated.

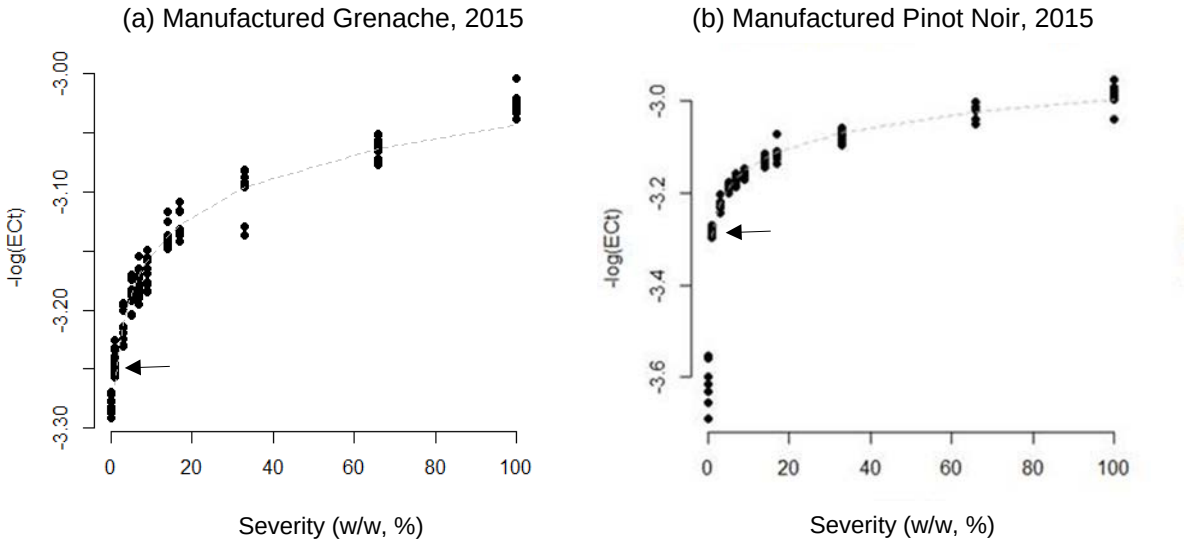


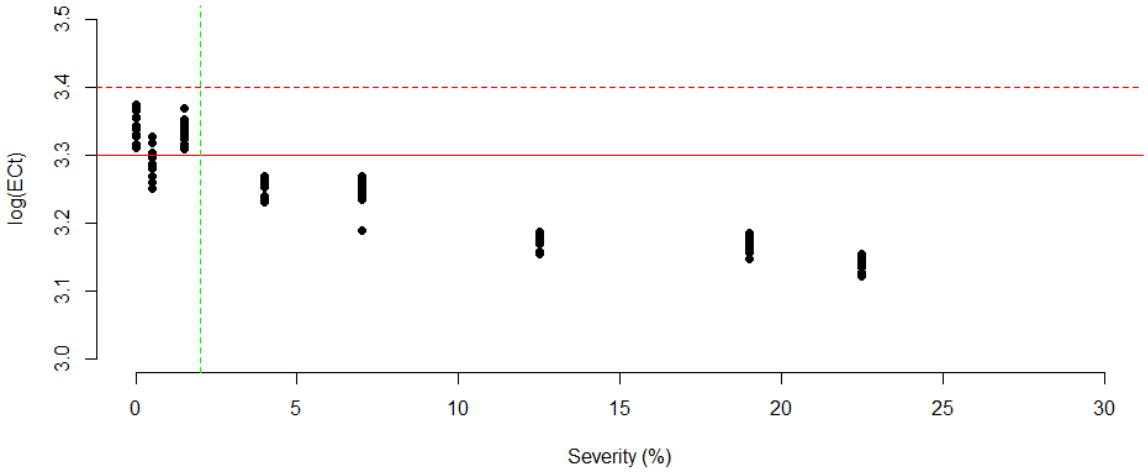
Figure 6.1.7. Regressions of the *E. necator* quantification cycle (Ct) resulting from duplex qPCR versus manufactured powdery mildew (w/w) severity in percentage (%). Visually healthy samples used for manufacturing are defined with negative Log Ct values < 3.3 (Grenache; 7a) and < 3.6 (Pinot Noir; 7b). Manufactured Grenache samples of 1% severity (w/w) overlapped with 3% severity (a) but in Pinot Noir they are separated (b) (arrow).

In the composite preparations of Grenache from the Coombe vineyard (2015), qPCR did not detect samples with no powdery mildew symptoms. *E. necator* biomass was quantified in the visually healthy and ≤ 2% samples and therefore these samples were classified as samples with traces (Figure 6.1.8a). The threshold for these was above Log Ct 3.3. These samples were also separated from the remaining samples. Quantified *E. necator* biomass was similar in the samples with mean visual severity of 4% and 7%, but different from the biomass quantified in the samples with mean severity ≥ 13% (Figure 6.1.8a). In the composite Pinot Noir samples from the Lenswood vineyard (2015), qPCR either did not detect or detected traces of powdery mildew in samples visually assessed to be 0% and 0.5% severity (Figure 6.1.8b). No clear separation of samples based on *E. necator* biomass was observed.

Discussion

The qPCR was sensitive enough to quantify 3 fg of pure fungus, which corresponded to a few as 30 copies of *E. necator* plasmid standard, and a limit of quantification at Ct 31.99 ± 0.65 (standard deviation) was set for pure fungus. The assay was sufficiently sensitive to quantify traces of *E. necator* on individual berries and bunches and in manufactured (w/w) and composite (surface area) samples designated as healthy based on visual assessment (0% severity). In those samples, the average *E. necator* Log Ct of 3.4 ± 0.01 (standard deviation) was estimated across varieties and conditions. A conservative estimate of Log Ct of 3.3 ± 0.01 (standard error) for the threshold of *E. necator* DNA in visually healthy material was established as the lower 10% population percentile. Therefore, to discount spurious results that may arise from airborne conidia on the surface of berries (Mahaffee and Stoll 2016), values at or below this threshold were designated “traces of *E. necator*”. Likewise, taking into account results for homogenised samples and the requirements of a good qPCR in terms of efficiency of reaction, a threshold for healthy (unaffected) samples of Ct 31 (Log *E. necator* Ct 3.4) was applied. These thresholds need to be related to organoleptic qualities of winegrapes or the resulting wines in future research.

(a) Composite Grenache Coombe vineyard, 2015



(b) Composite Pinot Noir Lenswood vineyard, 2015

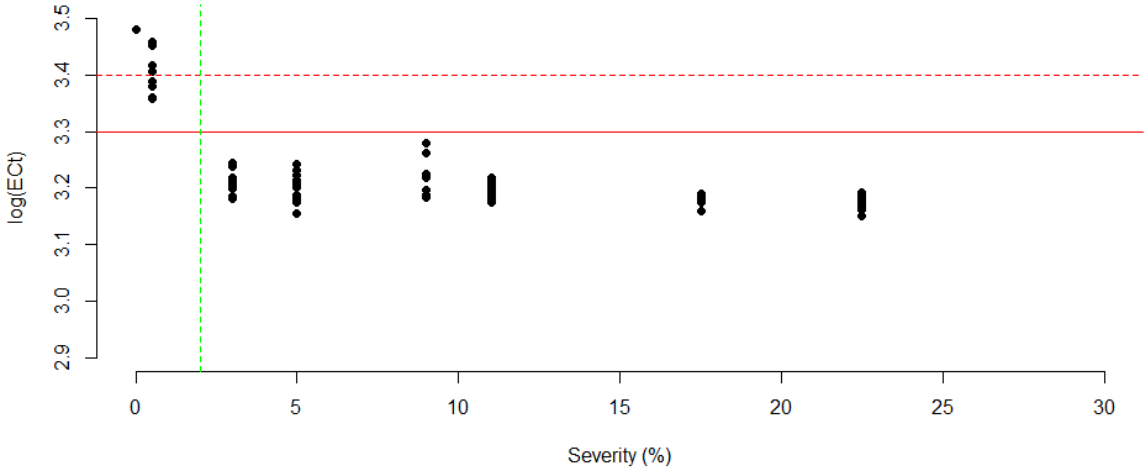


Figure 6.1.8. Regressions of the *E. necator* quantification cycle (Ct) resulting from duplex qPCR versus visual surface area powdery mildew severity in percentage (%). Visually healthy and samples with traces (≤ 2%) are separated from the diseased samples based on qPCR (red continuous line) (a, b). The threshold for samples with traces of *E. necator* is set at Log (*E. necator* Ct) 3.3. *E. necator* biomass separates samples of Grenache visually assessed as ≤ 2% from the rest of the samples (a). No clear separation based on *E. necator* biomass in Pinot Noir samples collected in the Lenswood vineyard (b). Grenache bunches for composite samples originated from the Coombe (a) and Lenswood (b) vineyards.

This qPCR assay targets a moderately repetitive DNA sequence present at between 60-80 copies per genome based on the whole genome sequences assembled for five *E. necator* isolates in GenBank (Jones et al. 2014). Results indicated that these repetitive sequences are conserved among isolates as amplification of DNA from four isolates of *E. necator* gave very similar Ct values (Figure 6.1.2a). However, the primer-probe combination cross-reacted with DNA from non-target organisms namely, two powdery mildew fungi of vegetables (*E. pisi* and *E. betae*) and *B. cinerea*, which may be encountered on grape berries. Sequence analysis using NCBI Blast search (*in silico* approach) showed that the 74 bp *E. necator*

fragment of the original pEnA1 fragment does not share any identity with whole genome sequences assembled for four *B. cinerea* isolates. Although a specificity test with 3 ng DNA/reaction gave amplification of *B. cinerea* at Ct 29.8, an experiment in which a mixture of *E. necator* and *V. vinifera* DNA was spiked with *B. cinerea* DNA showed no change in the quantification cycle of *E. necator* in comparison to the control (non-spiked) (Table 6.1.2). Limited cross-reactivity with *B. cinerea* does not affect the ability to quantify *E. necator*. Cross-reactivity with *E. pisi* and *E. betae* is not considered important as those species do not infect grapevine and their vegetable hosts are not grown in proximity to vineyards. Specificity testing confirmed that the *in silico* approach significantly reduced the development time for the new assay, but extensive quality control throughout the assay design process and during its use is still necessary (Mahaffee and Stoll 2016).

The sensitivity of a qPCR assay relies on the quality of the DNA and the efficiency of the reaction itself. Despite the slight increase in the efficiency of the duplex qPCR (Figure 6.1.2b), the difference between duplex and monoplex reactions was not statistically significant. The efficiency of both duplex and monoplex reactions was in the range of 90-110%, which meets the requirements of a good reaction (www.thermofisher.com/content/dam/LifeTech/global/Forms/PDF/real-time-pcr-handbook.pdf). The qPCR described here yielded highly repeatable results with as little as 3 fg of *E. necator* DNA from pure fungus per reaction, which corresponded to as few as 30 copies of the *E. necator* plasmid standard and this, therefore, was designated the limit of quantification. The qPCR was more sensitive (detected 3 fg) than the end-point PCR assay (detected 1000 fg) using primers designed based on the clone pEnA1 (Stummer et al. 2006) and is more sensitive than the qPCR assays reported for quantification of other pathogens associated with grape bunches [e.g. *B. cinerea* – 10 fg (Sanzani et al. 2012) and 1000 fg (Saito et al. 2013); *Greeneria uvicola* and *Colletotrichum acutatum* – 20 fg (Samuelian et al. 2011)].

Inhibitors of amplification can affect accuracy and sensitivity of qPCR assays and, consequently, quantification of target organism. The sensitivity of the duplex qPCR in the 10-fold dilution series of mixed *E. necator* and *V. vinifera* DNA was not compromised when amplification of *E. necator* DNA was considered. However, a high concentration of *E. necator* DNA appeared to inhibit the amplification of the highest concentration of *V. vinifera* DNA. As reported for other pathogens (e.g. *Pseudoperonospora humuli*) (Gent et al. 2009), 10-fold dilution of DNA template eliminates the inhibition without reducing sensitivity, as occurred here when DNA of *V. vinifera* was amplified in the duplex qPCR when compared to amplification in the monoplex reaction. Negligible inhibition of amplification of *V. vinifera* DNA was observed for berry homogenates spiked with *E. necator* conidia and for manufactured homogenates. Inhibition of amplification of *V. vinifera* DNA (endogenous control) in manufactured Chardonnay samples was estimated to be 1.5 Ct values and was comparable to the inhibition of *V. vinifera* DNA in the duplex qPCR (Figure 6.1.2b), 2 Ct values. Mahaffee and Stoll (2016) found that inhibitors affecting the qPCR quantification of trapped spores of *E. necator* may include pollen, pesticide residues, spider webs and insects, factors which might be applicable to the grape bunches used in our experiments. Furthermore, organic compounds, such as polyphenols and polysaccharides, present within plant tissue can inhibit or enhance PCR amplification (Saito et al. 2013), which might also explain the range of Ct values in the endogenous control.

This duplex qPCR assay was able to detect E. necator when visual assessment did not. This was evident for visually healthy berries used to manufacture homogenates representing various powdery mildew severities (2014-2015), and for individual berries that were analysed in 2016 and had been examined carefully using a magnifying lamp. When duplex qPCR was performed on homogenates of visually healthy berries (0% powdery mildew) used to manufacture powdery mildew severities for Chardonnay, Riesling and Grenache, more *E. necator* DNA was quantified than in the composite samples prepared from berries detached from bunches of these three varieties. While reasons for this discrepancy are not obvious, it may be related to water content, variation in bunch ripeness and/or environmental factors. A discrepancy in fungal biomass between manufactured and composite samples of visually healthy Grenache and Pinot Noir was not unexpected because powdery mildew was difficult to discern on the skin of Pinot Noir berries close to harvest. The biomass of *E. necator* in homogenates manufactured from fully-infected berries (100% severity) of all four grape varieties was similar, i.e. Log Ct 3.02 (or Ct 20.6) to Log Ct 2.95 (or Ct 19.2).

The duplex qPCR was sufficiently sensitive to distinguish three groups of samples that corresponded to the following visual severity categories: (i) healthy (Log Ct 3.4) Chardonnay individual bunches 2014, composite samples 2015 (Coombe vineyard), 2016 (Alverstoke vineyard) and Pinot Noir 2015; (ii) up to 2% severity (Log Ct 3.3) Chardonnay individual bunches 2014, composite samples 2015 (Coombe

vineyard), Riesling 2015 (Coombe vineyard), 2016 (Eden Valley), Grenache 2015 and Pinot Noir 2015 and (iii) > 2% severity on all four varieties but severity categories could not be distinguished reliably. *E. necator* DNA was amplified in homogenates of the four grape varieties that differ in biochemical composition and anatomical traits (white and red), in various type of samples (i.e. individual berries, bunches, manufactured severities and composite samples) and from vineyards with different management practices. In these samples, visual traces of powdery mildew (up to 2%) could be readily distinguished from the remaining samples.

While the TaqMan qPCR assay used to quantify E. necator in these experiments was fit for purpose, additional work was undertaken to refine the qPCR to remove the risk of cross-reactivity. Additional primers and single-locked nucleic acid (LNA) probes for detection and quantification of *E. necator* DNA in the presence of *V. vinifera* DNA were designed using the Beacon Designer™ software (PREMIER Biosoft, CA, USA). The specificity and sensitivity of LNA probes make qPCR assays useful for molecular differentiation and quantification of other obligately biotrophic pathogens such as *Pseudoperonospora* (downy mildew pathogens) and *Puccinia* (rust fungi) of various hosts (Glynn et al. 2010, Summers et al. 2015). Accordingly, sequences of the internal transcribed space (ITS) region and 9-cis-epoxycarotenoid dioxygenase 2 (NCED 2) were used to detect sequence regions specific for *E. necator* and *V. vinifera*, respectively. These sequences were suitable for the design of primers flanking the probe binding sites. Specific *E. necator* primers amplifying 136 bp of the ITS region and specific *V. vinifera* primers amplifying a short fragment of NCED 2 were designed. Two very specific LNA probes that contain FAM as reporter dye at the 5' end and a non-fluorescent dark quencher at the 3' end were also designed. Primers and LNA probe targeting the NCED 2 of *V. vinifera* DNA did not perform well in the qPCR tests and, therefore, were replaced with primers and LNA probe targeting *actin 1* of *V. vinifera* DNA. The primers and probe showed high specificity for *E. necator* and no cross-reactivity with any of the suite of microorganisms tested here. However, this assay was developed after grape homogenates had been tested and it was not validated nor used to quantify powdery mildew on grapes because of time constraints.

Quantitative PCR provides an absolute measure of the amount of *E. necator*, based on the amount of DNA (and therefore copies of the target sequence) of the fungus present. However, this study showed that the biomass of *E. necator* on grape bunches and berries as determined by qPCR did not reliably reflect visual severity of powdery mildew. Biomass of the fungus on bunches and berries varied considerably less than might be inferred from differences in surface area affected by *E. necator* (e.g. Figures 6.1.4a,c; 6.1.6a,b). The degree of colonisation, density of mycelium and of sporulation, and viability of the fungus are likely to contribute to the discrepancy between qPCR and visual assessment.

While the qPCR assay was sufficiently sensitive to quantify traces of the fungus not detectable to the human eye, the consequences of such small amounts of contamination are not known. The amount of biomass of *E. necator* that influences the organoleptic qualities of winegrapes or the resulting wines has yet to be determined. While such research might be undertaken for academic purposes, a qPCR assay would take several days to provide a result for *E. necator* biomass and therefore would not be a practical measure of contamination in the vineyard or winery.

References cited in this section

Carisse O and Tremblay DM (2014) Quantitative analysis of grape multi-diseases development: the groundwork for improved management. In: 7th International Workshop on Grapevine Downy and Powdery Mildew, Díez-Navajas AM, Ortiz-Barredo A, Menendez C, Emmett R, Gadoury DM, Gubler WD, Kassemeyer H-H, Magarey P and Seem R (eds), Vitoria Gasteiz, Spain, 30 June - 4 July (Arabako Foru Aldundia), pp. 20-1

Emmett B, Scott ES, Petrovic T, Zanker T, Evans KJ, Kravchuk O and Perry W (2015) A diagrammatic key to assist assessment of powdery mildew severity on grape bunches. Australian & New Zealand Grapegrower & Winemaker **623**, 46-9

Evans KJ, Palmer AK and Metcalf DA (2013) Effect of aerated compost tea on grapevine powdery mildew, botrytis bunch rot and microbial abundance on leaves. European Journal of Plant Pathology **135**, 661-73

Falacy JS, Grove GG, Mahaffee WF, Galloway H, Glawe DA, Larsen RC and Vandemark GJ (2007) Detection of *Erysiphe necator* in air samples using the polymerase chain reaction and species-specific primers. Phytopathology **97**, 1290-7

Gent DH, Nelson MN, Farnsworth JL and Grove GG (2009) PCR detection of *Pseudoperonospora humuli* in air samples from hop yards. Plant Pathology **58**, 1081-91
Hanania U, Velcheva M and Perl A (2004) *Vitis vinifera* actin 1 (act1) gene, partial cds. (National Center for Biotechnology Information), Vol. 2016
Huerga V, Salas B, Ortíz Barredo A and Díez-Navajas AM (2014) Inhibitor-free multiplex PCR for the simultaneous detection of *Plasmopara viticola* and *Erysiphe necator* spores in environmental samples. In: 7th International Workshop on Grapevine Downy and Powdery Mildew, Díez-Navajas AM, Ortiz-Barredo A, Menendez C, Emmett R, Gadoury DM, Gubler WD, Kassemeyer H-H, Magarey P and Seem R (eds), Vitoria Gasteiz, Spain, 30 June - 4 July (Arabako Foru Aldundia), pp. 85-86
Hill GN, Evans KJ, Beresford RM and Dambergs RG (2014) Comparison of methods for the quantification of botrytis bunch rot in white wine grapes. Australian Journal of Grape and Wine Research **20**, 432-41
Jones L, Riaz S, Morales-Cruz A, Amrine KCH, McGuire B, Gubler WD, Walker MA and Cantu D (2014) Adaptive genomic structural variation in the grape powdery mildew pathogen, *Erysiphe necator*. BMC Genomics **15**, 1081
Mahaffee WF (2014) Use of airborne inoculum detection for disease management decisions. In: Detection and diagnostics of plant pathogens, Ludovica Gullino M and Bonants PJM (eds), Springer: Dordrecht, The Netherlands, pp. 39-54
Mahaffee WF and Stoll R (2016) The ebb and flow of airborne pathogens: monitoring and use in disease management decisions. Phytopathology **106**, 420-31
Saito S, Dunne KJ, Evans KJ, Barry K, Cadle-Davidson L and Wilcox WF (2013) Optimisation of techniques for quantification of *Botrytis cinerea* in grape berries and receptacles by quantitative polymerase chain reaction. Australian Journal of Grape and Wine Research **19**, 68-73
Samuelian SK, Greer LA, Savocchia S and Steel CC (2011) Detection and monitoring of *Greeneria uvicola* and *Colletotrichum acutatum* development on grapevines by real-time PCR. Plant Disease **95**, 298-303
Sanzani SM, Schena L, Cicco Vd and Ippolito A (2012) Early detection of *Botrytis cinerea* latent infections as a tool to improve postharvest quality of table grapes. Postharvest Biology and Technology **68**, 64-71
Scott ES, Dambergs RG and Stummer BE (2010) Fungal contaminants in the vineyard and wine quality. In: Reynolds AG (ed) Managing Wine Quality: Viticulture and Wine Quality (Volume 1), Woodhead Publishing Ltd, Cambridge, UK, pp. 481-514
Stummer BE, Zanker T, Harvey PR and Scott ES (2006) Detection and quantification of *Erysiphe necator* DNA in wine grapes and resultant must and juice. Mycological Research **110**, 1184-92
Thiessen LD, Keune JA, Neill TM, Turechek WW, Grove GG and Mahaffee WF (2016) Development of a grower-conducted inoculum detection assay for management of grape powdery mildew. Plant Pathology **65**, 238-49

6.2 Mid-infrared spectroscopy for discrimination of powdery mildew-affected grapes

Tijana Petrovic, Daniel Cozzolino, Olena Kravchuk and Eileen S. Scott

Introduction

Mid-infrared spectroscopy (MIR) is a rapid method known for simplicity of sample preparation and ease of operation, and is widely used for assessment and classification of fungal contamination and mycotoxins in agricultural products (McMullin et al. 2015). In the wine sector, MIR is used for measuring juice composition, assessment of wine fermentation processes and classification of wine styles and cultivars (Bevin et al. 2008, Cozzolino and Dambergs 2010). MIR spectroscopy offers indirect assessment of quality by examining fingerprint regions of MIR spectra for alterations in fundamental crop characteristics. For example, Fourier Transform Infrared spectroscopy in the MIR (4000-926 cm^{-1}) and a section of the near-infrared (NIR, 5012-4000 cm^{-1}) range in combination with partial least squares (PLS) regression showed that sour, rotten grapes were responsible for changes in chemical composition of grape must and wine (Barata et al. 2011). Recently, the potential of MIR spectroscopy for the quantification of Botrytis bunch rot in homogenised grape berries was demonstrated by producing a PLS model with high predictive ability based on the spectral range 1141-1050 cm^{-1} (Hill et al. 2013). Hill et al. (2013) showed that MIR spectroscopy separated visually assessed botrytis bunch rot within lower and higher severity categories to some degree, but that additional calibration was necessary. However, to our knowledge, MIR has not yet been applied to quantify powdery mildew severity on grapes.

The objectives of this research were to: (i) develop predictive MIR calibration models for white and red grape varieties using qPCR data as a reference for calibration; (ii) validate the MIR models for Chardonnay and Riesling using independent test samples of these varieties.

Materials and methods

Collection and preparation of grapes. The collection of visually healthy and powdery mildew-affected grape bunches and berries from vineyards at the University of Adelaide (Coombe and Alverstoke vineyards), in the Riverland (Glossop) and Eden Valley in 2014-2016 and preparation of composite samples were described in Section 6.1 (see Table 6.2.1) and re-stated here for convenience. Berries from destemmed bunches (approx. 8 to 13 kg per cultivar) that had been visually graded were used to prepare visual severity categories of Chardonnay (10), Riesling (9) and Grenache (8) and Pinot Noir (8). Subsamples of Chardonnay (6), Riesling (6), Pinot Noir (6) and Grenache (7) berries (150-230 berries/subsample or 147-270 g/subsample depending on the variety) were collected from each designated powdery mildew severity category, thawed overnight at 4 °C, independently homogenised and an aliquot of 1 mL was taken from each subsample for MIR spectroscopy.

Attenuated Total Reflectance (ATR)-MIR spectroscopy. The entire 1-mL sample was pipetted into and scanned using a platinum diamond ATR sampling module cell mounted in a Bruker Alpha instrument (Bruker Optics GmbH, Ettlingen, Germany). All samples were at room temperature and spectra were collected in the range 4000-400 cm^{-1}. Thirty-two co-added scans with spectral resolution 4 cm^{-1} were collected at each measurement without temperature equilibration. The sample cell was cleaned with distilled water between samples.

Analysis of ATR-MIR spectra. Raw spectra were exported from OPUS to The Unscrambler X (version 10.4, CAMO ASA, Oslo, Norway) and pre-processed using the second derivative transformation, Savitzky-Golay derivation and smoothing (11 points on both sides and second order polynomial) (Baker et al. 2014). Spectra were truncated in the main fingerprint region (1800-800 cm^{-1}), which included most of the biochemical information, and then further truncated to avoid polysaccharide, ribose, glycogen and nucleic acid regions (1185-900 cm^{-1}) (Naumann 2009). Principal component analysis (PCA) was applied to reduce the dimensions of the spectral data (435 wavenumbers), followed by PLS regressions. Up to 15 PCs explaining 80-85% of the total variation among samples were used for the PLS regressions. The PCA with singular value decomposition (SVD) algorithm and PLS regressions using kernel PLS algorithm with a maximum of seven components were performed. The performance of the PLS regression models

developed for each variety were tested by applying the full cross validation method in which each calibration standard was quantified as the validation standard.

Calibration of MIR spectroscopy. Samples subjected to MIR were also subjected to duplex qPCR (see Section 6.1) as the reference method for calibration of MIR. The quantification cycle (Ct) determined for *E. necator* (target) and *V. vinifera* (endogenous control) in each sample included in qPCR was used to calculate the pathogen coefficient as the ratio of logarithmic transformation of Ct for *V. vinifera* divided by that for *E. necator* (Saito et al. 2013). Pathogen coefficient was used as the reference value to build PLS regression models for each variety.

Results

Chardonnay and Riesling

PCA for Chardonnay samples was performed on profiles of the second derivative of smoothed ATR-MIR spectra of 195 composite samples from Coombe, Alverstoke and Glossop vineyards, including 435 wavenumbers in the main fingerprint region (1800-1185 cm^{-1}) that is indicative of a mixture of lipid moieties, amide I and II, protein carboxyls, nucleic acids and fatty acid esters. The score plot of the first two components explained 61% of the variation, and separated samples from the Alverstoke and Glossop vineyards sampled (a day apart) in 2016 from samples collected from the Coombe vineyard in 2015. In the PC3-PC4 scores plot (Figure 6.2.1a) (PC3 explained 3% of the variation, PC4 explained 2%), the majority of Chardonnay samples from the Alverstoke and Glossop vineyards were separated (Figure 6.2.1a), which may be attributed to amides/proteins (1650-1655 cm^{-1}/1790 cm^{-1}) and phosphate compounds (1270 cm^{-1}), based on the loading variables for PC3 (Figure 6.2.1b).

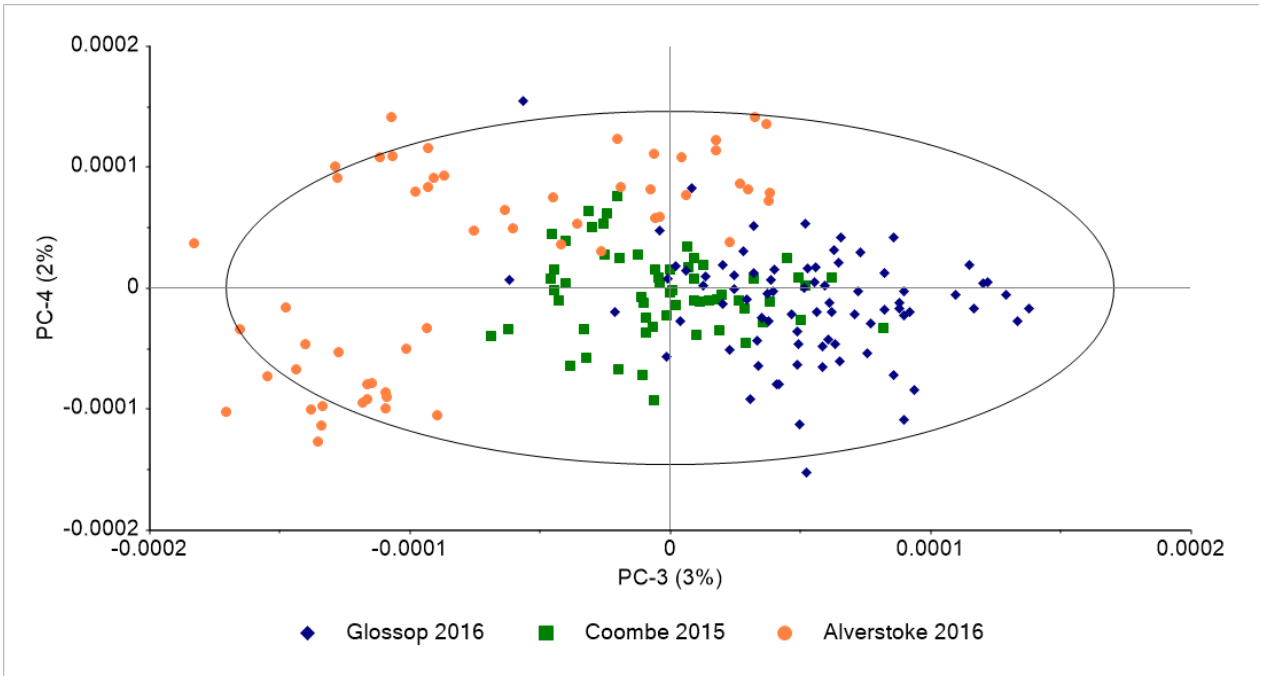
Calibration. PLS showed that the chosen spectral region had limited potential to predict the pathogen coefficient as a measure of powdery mildew severity in Chardonnay from the Coombe, Alverstoke and Glossop vineyards. The R^2 value of the PLS regression was 0.66, and the root mean square error of cross validation (RMSECV) was 0.059 for Chardonnay from Coombe (Figure 6.2.1c) and $R^2 \geq 0.52$ and RMSECV = 0.042 for samples from Alverstoke (Figure 6.2.1d) and Glossop (Figure 6.2.1e) vineyards. (RMSECV measures the dispersion of the validation samples around the regression line when cross validation is used).

There was considerable and expected discrepancy in the prediction of powdery mildew (log pathogen coefficient in calibration samples that initially were derived from the same pool of berries (or visual severity category). This was indicative of variation in biomass of *E. necator* among the berries included in each sample.

The calibration model developed based on Chardonnay samples from the Coombe and Alverstoke vineyards could not predict powdery mildew in the Chardonnay samples collected from the Glossop vineyard (*data not presented*).

For individual Chardonnay bunches (2014), slight spectral differences did not separate bunches with different fungal biomass measured by qPCR (Figure 6.2.2a). Calibration models could not be obtained using either pathogen coefficient or logarithmic transformation of Ct for *E. necator* with a few PLS factors that would be optimal and without overfitting or underfitting. However, for individual berries, spectral differences among berries with different fungal biomass were noticeable in the region with high positive (1383 cm^{-1}, 1310 cm^{-1}) and negative loadings (1690 cm^{-1}, 1650 cm^{-1} and 1480 cm^{-1}), contributing to the separation of unaffected from severely affected berries (Figure 6.2.2b). Given that individual berries were treated differently from composite samples and individual bunches (i.e. seeds were removed from each berry in the first group), log of Ct for *E. necator* was used as reference data to construct the PLS regression model. Parameters of the model (R^2 = 0.72; RMSEC = 0.088) indicated that a calibration model can be developed to determine *E. necator* biomass on individual berries (Figure 6.2.2c).

(a)



(b)

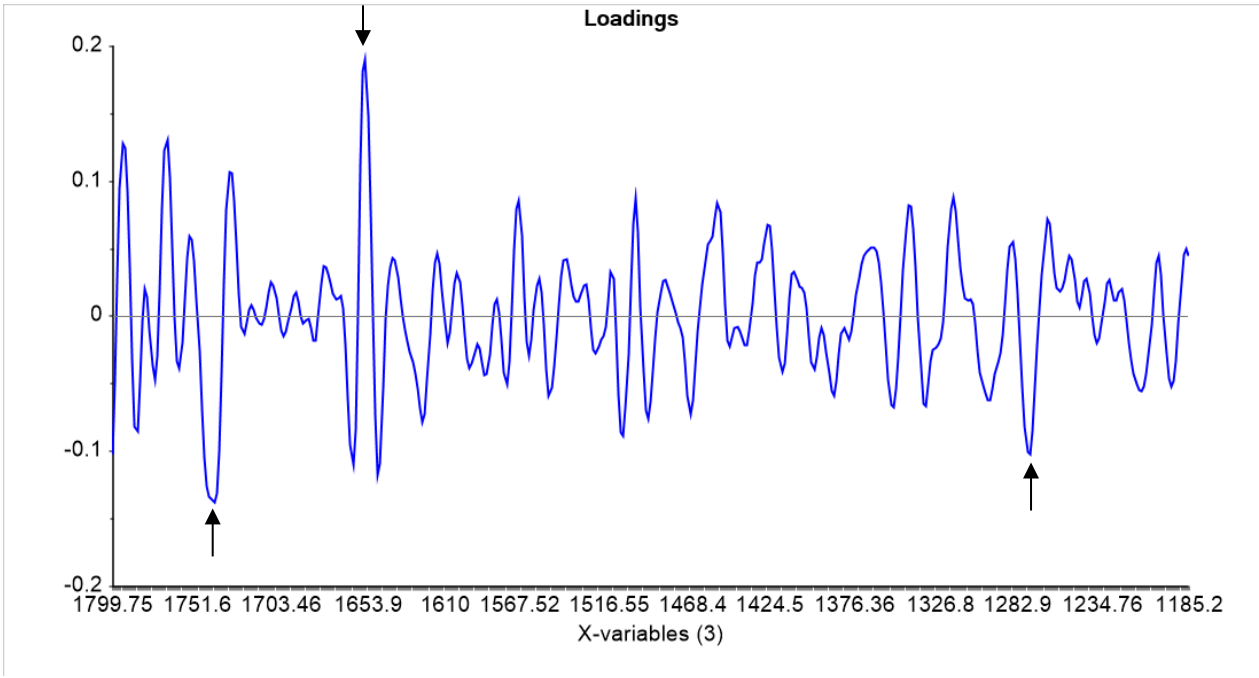
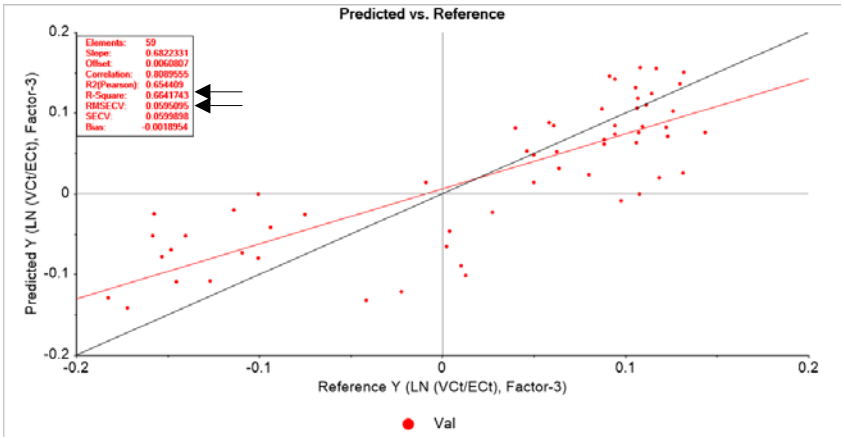
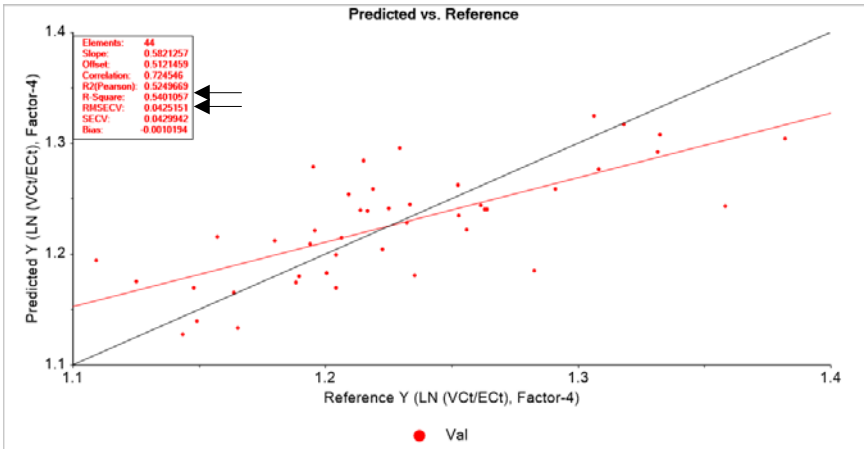


Figure 6.2.1. (continued on next page)

(c)



(d)



(e)

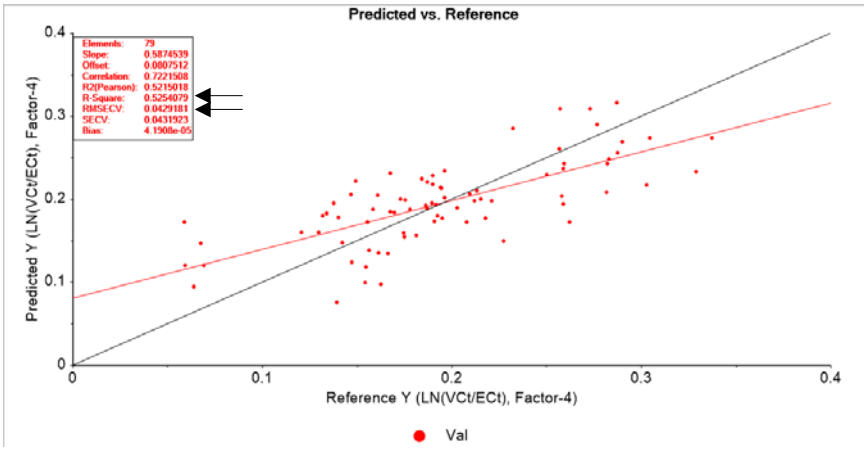
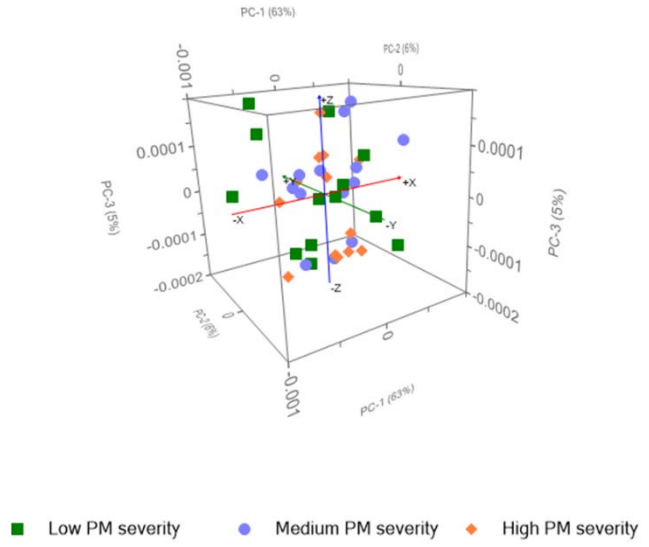
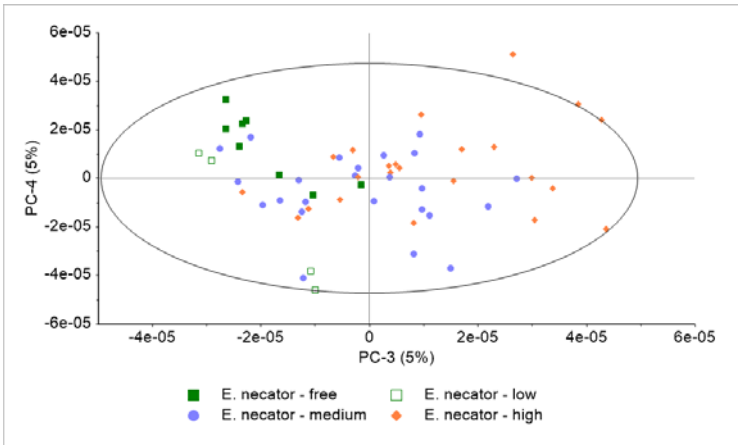


Figure 6.2.1. Mid-infrared spectroscopic analysis of Chardonnay composite samples from the Coombe, Alverstoke and Glossop vineyards. (a) PCA plot with 95% confidence ellipse showing the distribution of 195 samples and separation of the majority of samples from Glossop (blue diamond) from some samples from Coombe (green square) and the majority of samples from Alverstoke (orange dot) along PC3; (b) the PC3 loadings with arrows indicating the main peaks that contributed most to separation of the majority of samples from Glossop; (c-e) Validation plots for cross validation using log of pathogen coefficient from qPCR as reference data (x-axis) against log pathogen coefficient predicted (y-axis) by MIR spectroscopy of samples from Coombe (c), Alverstoke (d) and Glossop (e) vineyards. Black line represents the one-to-one line (y = x), red line is the best-fit regression line.

(a)



(b)



(c)

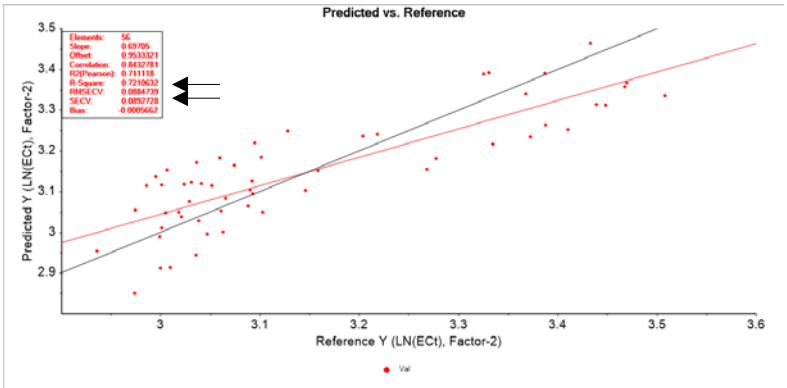


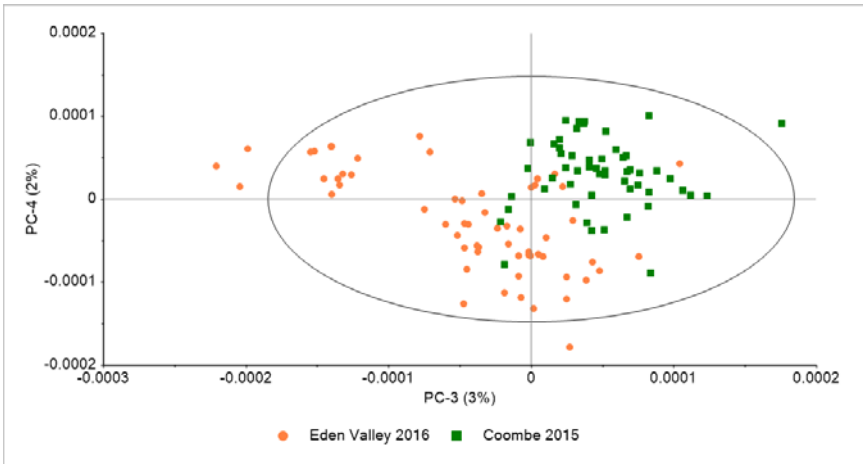
Figure 6.2.2. Mid-infrared spectroscopic analysis of Chardonnay individual bunches (a) and berries (b-d). (a) 3D PCA plot showing the distribution of 40 bunches and lack of separation of bunches with different *E. necator* biomass measured by qPCR; (b) PCA plot with 95% confidence ellipse showing the distribution of 59 berries and separation of *E. necator*-free (green) from highly affected berries (orange) measured by qPCR; (c) regression of log of Ct for *E. necator* in berries estimated by qPCR against log of Ct for *E. necator* predicted by MIR. Black line represents the one-to-one line (y = x), red line is the best-fit regression line.

PCA for Riesling samples was performed on profiles of the second derivative of smoothed ATR-MIR spectra of 114 composite samples from the Coombe and Eden Valley vineyards. The score plot of the first two components explained 73% of the variation; samples from Eden Valley were more diverse than those from the Coombe vineyard. In the PC3-PC4 scores plot (PC3 explained 3% of the variation, PC4 2%), Riesling samples from the Eden Valley vineyard were slightly separated from samples from the Coombe vineyard (Figure 6.2.3a) in the direction of PC3, which may be attributed to water with soluble proteins (1603 cm^{-1}), amide II (1520 cm^{-1}) and aldehydes (1740 cm^{-1}), based on the loading variables for PC3 (Figure 6.2.3b). Ten "blind samples" (originating from the pool of randomly collected bunches), and detached and mixed berries that were used for validation of qPCR, showed some segregation from the remaining samples (Figure 6.2.3c), mainly driven by a high loading for PC4 at 1350 cm^{-1}.

Calibration. PLS showed that the chosen region had limited potential to predict the pathogen coefficient as a measure of powdery mildew severity in Riesling from the Coombe vineyard based on R^2 value of PLS being 0.61 and RMSECV of 0.028 (Figure 6.2.3d). The prediction of pathogen coefficient for Riesling from Eden Valley (R^2 =0.54; RMSECV = 0.028) (Figure 6.2.3e) was similar to that for Riesling from the Coombe vineyard.

The calibration model developed based on Riesling samples from the Coombe vineyard could not predict *E. necator* biomass in the Riesling samples collected from the Eden Valley vineyard (data not presented).

(a)



(b)

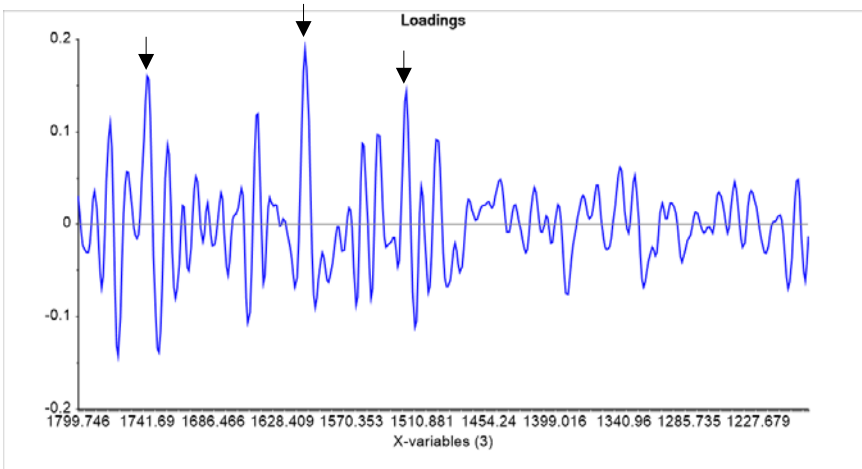
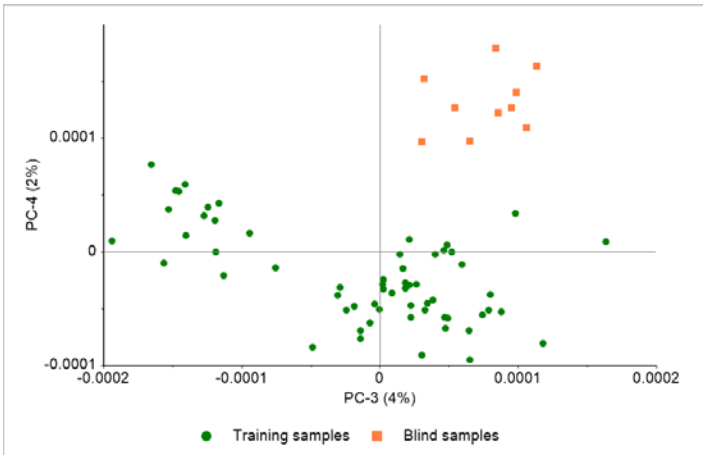
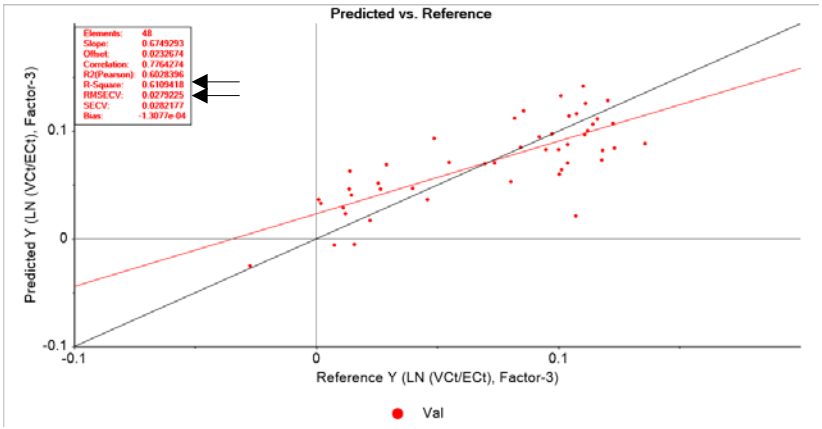


Figure 6.2.3. (continued on next page)

(c)



(d)



(e)

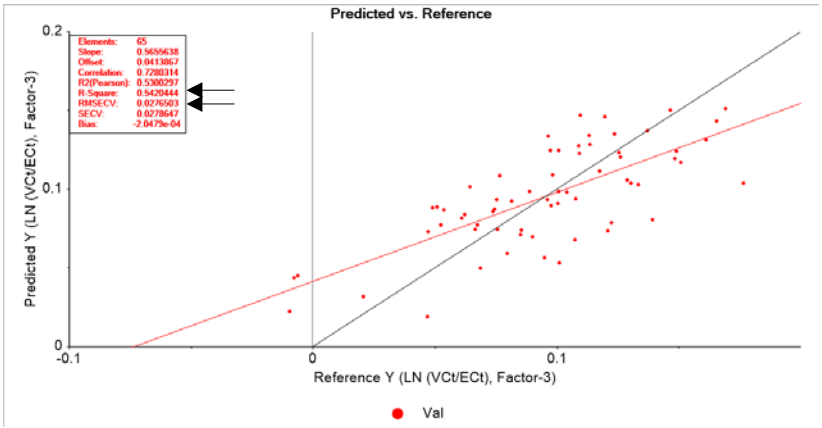


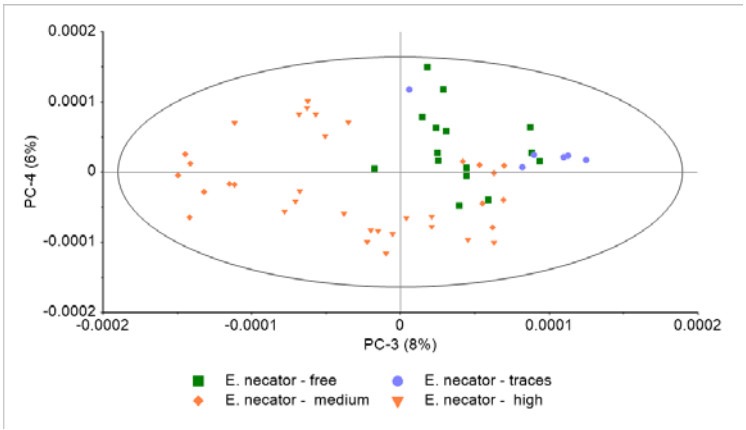
Figure 6.2.3. Mid-infrared spectroscopic analysis of Riesling composite samples from the Coombe and Eden Valley vineyards. (a) PCA plot with 95% confidence ellipse showing the distribution of 114 samples and separation of the majority of samples from Eden Valley (orange square) from samples from Coombe (green dot) along PC3; (b) the PC3 loadings showing main peaks that contributed most to separation of the majority of samples from Eden Valley from the remaining samples from Coombe along PC3; (c) segregation of 10 “blind samples” derived from the pool of randomly collected bunches, from which berries were detached and mixed. (d-e) Validation plots for cross validation using log of pathogen coefficient from qPCR as reference data (x-axis) against pathogen coefficient predicted (y-axis) by MIR spectroscopy of samples from Coombe (d) and Eden Valley vineyards (e). Black line represents the one-to-one line (y = x), red line is the best-fit regression line.

Grenache and Pinot Noir

PCA for Grenache samples performed on 56 profiles of the second derivative of the chosen spectral region (1800-1185 cm^{-1}) showed no clear separation of samples based on *E. necator* biomass in the score plot of the first two PCs that explained 31% of the variation. In the PC3-PC4 score plot, *E. necator*-free samples and samples with traces of *E. necator*, based on the qPCR and pathogen coefficient, appeared in the same quadrant (upper right-hand) but were not clearly separated from the medium-infected samples (Figure 6.2.4a). PC3 and PC4 explained 8% and 6% of the variation, respectively.

Calibration. PLS determined strong correlations in the multivariate space using spectral variables. The analysis yielded strong positive relationships for the powdery mildew-affected samples (55) when one outlier was excluded (R^2 = 0.83; RMSECV = 0.028) (Figure 6.2.4b). This showed that the spectral region 1800-1185 cm^{-1} provided very good prediction of the pathogen coefficient as a measure of *E. necator* biomass in Grenache.

(a)



(b)

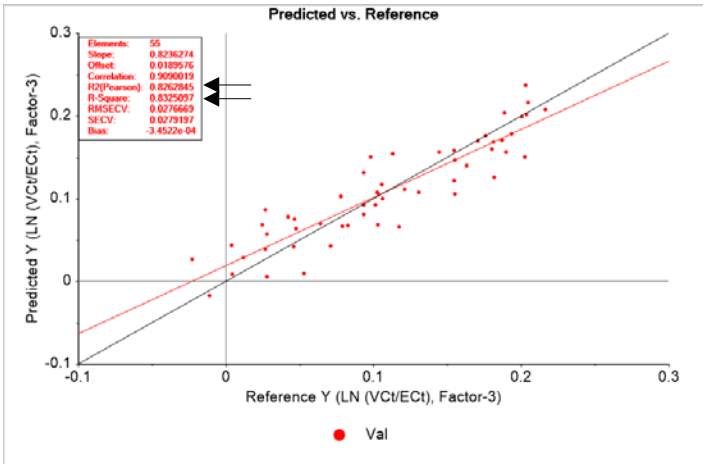
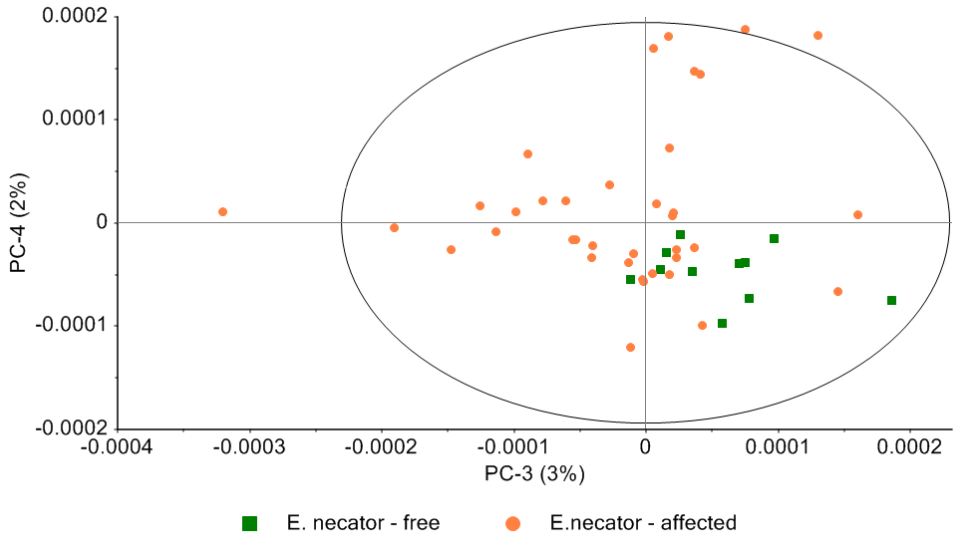


Figure 6.2.4. Mid-infrared spectroscopic analysis of Grenache composite samples from the Coombe vineyard. (a) PCA plot with 95% confidence ellipse showing the distribution of 56 samples and lack of clear separation of the *E. necator*-free samples (green) and with traces of *E. necator* (blue) from the remaining samples; (b) regression of log pathogen coefficient in grapes estimated by qPCR against log pathogen coefficient predicted by MIR. Black line represents the one-to-one line (y = x), red line is the best-fit regression line.

PCA for Pinot Noir samples performed on 48 profiles of the second derivative of spectra showed no clear separation of samples based on *E. necator* biomass in the score plot of the first two PCs that explained 82% of the variation. In the PC3-PC4 score plot *E. necator*-free samples and samples with pathogen, based on the qPCR and pathogen coefficient, appeared in the same quadrant (lower right-hand) (Figure 6.2.5a). PC3 and PC4 explained 3% and 2% of the variation, respectively.

Calibration. PLS showed that even with an R^2 value of 0.74, dispersion of calibration samples around the regression line was large (RMSECV = 0.071) indicating that the regression model would not help much in predicting a pathogen coefficient as a measure of powdery mildew severity (Figure 6.2.5b).

(a)



(b)

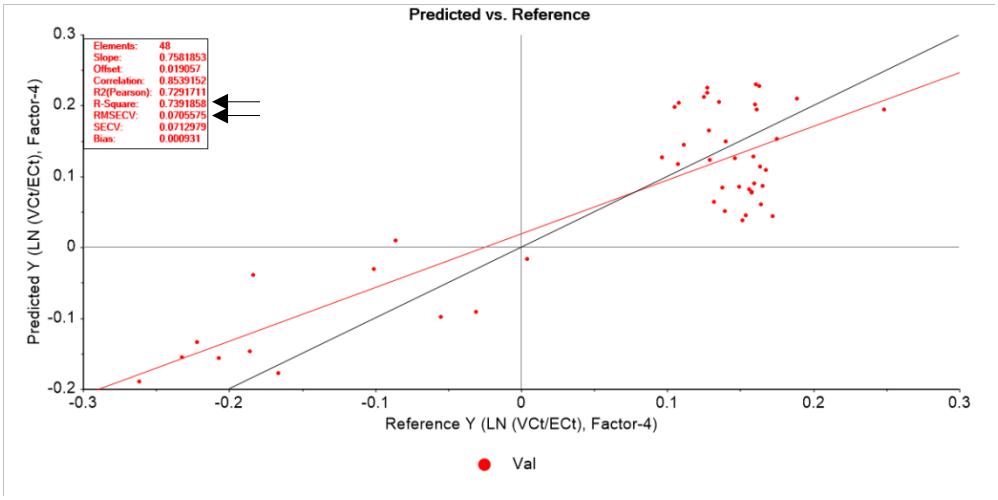


Figure 6.2.5. Mid-infrared spectroscopic analysis of Pinot Noir composite samples from the Coombe vineyard. (a) PCA plot with 95% confidence ellipse showing the distribution of 48 samples and lack of separation of the *E. necator*-free samples (green) from the affected samples based on the qPCR; (b) regression of log pathogen coefficient in grapes estimated by qPCR against log pathogen coefficient predicted by MIR. Black line represents the one-to-one line (y = x), red line is the best-fit regression line.

Discussion

In this study, qPCR was used as an analytical and objective method to calibrate MIR spectroscopy. However, the results showed that MIR did not provide a sufficiently sensitive means of quantifying powdery mildew on grape bunches, as indicated by pathogen biomass. Statistical PLS models based on MIR spectroscopy for Chardonnay and Riesling grapes calibrated using the logarithm of the pathogen coefficient from qPCR assays as reference values did not demonstrate potential to predict powdery mildew severity in independent test samples. The calibration model obtained for Grenache (R^2 = 0.83) using 55 samples demonstrated that MIR has good potential as a tool to predict *E. necator* -free and affected grapes of this variety but needs to be validated using independent test samples in the future. The calibration model for Pinot Noir was informative only for samples from healthy grapes whereas the biomass of *E. necator* as measured by qPCR was similar in the remaining samples. For example, the pathogen coefficient for 16 bunches was 0.15-0.17 (reference data) but spectrally these bunches were diverse, which was reflected in a broad range of predicted pathogen coefficients (Figure 6.2.5b). Consequently, either bunches with more diverse fungal biomass or methodological improvement in measuring fungal biomass by qPCR are required, so that a better calibration model can be obtained (as for Grenache).

The use of qPCR for calibrating MIR demonstrated a lack of strong correlation between *E. necator* biomass and the critical degree of compositional changes that are measured by MIR. A broad spectral range indicative of a mixture of lipid moieties, amide I and II, protein carboxyls, nucleic acids and fatty acid esters was used for calibration. Two regions within the spectra, indicative of amide I (1695-1625 cm^{-1}) and amide II (1560-1525 cm^{-1}) components of proteins (Lecellier et al. 2014), were identified as regions with good potential to quantify powdery mildew (*E. necator* biomass) in composite samples (Figures 6.2.1b, 6.2.3b) and individual berries based on PCA and PLS loadings. However, when these spectral wavenumbers, individually or combined, were used in calibration, it was not possible to obtain calibration models with R^2 higher than 0.4 and low RMSECV. RMSECV describes total error for samples within the calibration data set and a lower RMSECV value indicates better robustness of the calibration model (Porep et al. 2015). It might be that the protein content of infected grapes is not well correlated with the biomass of *E. necator*. Pathogenesis-related (PR) proteins increase in grapes affected by powdery mildew compared with healthy grapes (Jacobs 1999, Tian et al. 2015), although Girbau et al. (2004) showed that the concentration of total PR proteins differed little in free run juice from Chardonnay bunches with 0 to 30% powdery mildew severity, then increased markedly in juice from grapes with 30-100% severity. Therefore, it seems that the concentration of PR proteins is not directly proportional to the severity of powdery mildew, which is in agreement with the results presented here. In other pathosystems, the amount of protein, protease activity or free amino acids may differ significantly among fungal species grown on the same hosts. For example, some *Aspergillus* species first metabolise peanut proteins and then fungal proteins begin to be spectrally observable after a certain amount of fungal growth (Kaya-Celiker et al. 2016). Consequently, PLS regressions for powdery mildew when the protein spectral region and *E. necator* biomass were used in analyses showed that MIR had little or no potential as a method for quantitative analysis of *E. necator* on berries in this conditions used in this research. Hill et al. (2014), likewise, found that MIR failed to distinguish homogenates prepared from bunches of Riesling grapes with 5, 10 and 25% botrytis bunch rot severity.

The potential of pathogen coefficient values derived from qPCR assays to provide reference values for powdery mildew severity was demonstrated, as was previously reported for botrytis bunch rot (Hill et al. 2014). Given that calibration models for Chardonnay and Riesling based on MIR were unsuitable for predicting powdery mildew severity in the independent test samples, the pathogen coefficient from qPCR might instead be applied to provide information relating to sensory attributes of the resulting wine, as was suggested by Hill et al. (2014) for botrytis bunch rot.

In summary, while MIR spectroscopy resulted in a promising calibration model for Grenache grapes affected by powdery mildew, this approach was not sufficiently informative for the other three varieties examined. While it is possible that further research might help to identify the biochemical changes that are detected in powdery mildew-affected grapes using MIR, there is no certainty that such changes would be directly proportional to disease severity or to the biomass of the powdery mildew fungus.

References cited in this section

Baker MJ, Trevisan J, Bassan P, Bhargava R, Butler HJ, Dorling KM, Fielden PR, Fogarty SW, Fullwood NJ, Heys KA, Hughes C, Lasch P, Martin-Hirsch PL, Obinaju B, Sockalingum GD, Sule-Suso J, Strong RJ, Walsh MJ, Wood BR, Gardner P and Martin FL (2014) Using Fourier transform IR spectroscopy to analyze biological materials. Nature Protocols **9**, 1771-91

Barata A, Pais A, Malfeito-Ferreira M and Loureiro V (2011) Influence of sour rotten grapes on chemical composition and quality of grape must and wine. European Food Research and Technology **233**, 183-94

Bevin CJ, Dambergs RG, Fergusson AJ and Cozzolino D (2008) Varietal discrimination of Australian wines by means of mid-infrared spectroscopy and multivariate analysis. Analytica Chimica Acta **621**, 19-23

Cozzolino D and Dambergs RG (2010) Instrumental analysis of grape, must and wine. I In: Reynolds AG (ed) Managing Wine Quality: Viticulture and Wine Quality (Volume 1), Woodhead Publishing Ltd, Cambridge, UK, pp. 134-88

Girbau T, Stummer BE, Pocock KF, Baldock GA, Scott ES and Waters EJ (2004) The effect of *Uncinula necator* (powdery mildew) and *Botrytis cinerea* infection of grapes on the levels of haze-forming pathogenesis-related proteins in grape juice and wine. Australian Journal of Grape and Wine Research **10**, 125-33

Hill GN, Evans KJ, Beresford RM and Dambergs RG (2013) Near and mid-infrared spectroscopy for the quantification of botrytis bunch rot in white wine grapes. Journal of Near Infrared Spectroscopy **21**, 467-75

Hill GN, Evans KJ, Beresford RM and Dambergs RG (2014) Comparison of methods for the quantification of botrytis bunch rot in white wine grapes. Australian Journal of Grape and Wine Research **20**, 432-41

Jacobs D (1999) Induction of different pathogenesis-related cDNAs in grapevine infected with powdery mildew and treated with ethephon. Plant Pathology **48**, 325-36

Kaya-Celiker H, Mallikarjunan PK and Kaaya A (2016) Characterization of invasion of genus *Aspergillus* on peanut seeds using FTIR-PAS. Food Analytical Methods **9**, 105-13

Lecellier A, Mounier J, Gaydou V, Castrec L, Barbier G, Ablain W, Manfait M, Toubas D and Sockalingum GD (2014) Differentiation and identification of filamentous fungi by high-throughput FTIR spectroscopic analysis of mycelia. International Journal of Food Microbiology **168-169**, 32-41

McMullin D, Mizaikoff B and Krska R (2015) Advancements in IR spectroscopic approaches for the determination of fungal derived contaminations in food crops. Analytical and Bioanalytical Chemistry **407**, 653-60

Naumann A (2009) A novel procedure for strain classification of fungal mycelium by cluster and artificial neural network analysis of Fourier transform infrared (FTIR) spectra. Analyst **134**, 1215–23

Porep JU, Kammerer DR and Reinhold C (2015) On-line application of near infrared (NIR) spectroscopy in food production. Trends in Food Science & Technology **46**, 211-30

Saito S, Dunne KJ, Evans KJ, Barry K, Cadle-Davidson L and Wilcox WF (2013) Optimisation of techniques for quantification of *Botrytis cinerea* in grape berries and receptacles by quantitative polymerase chain reaction. Australian Journal of Grape and Wine Research **19**, 68-73

Tian B, Harrison R, Jaspers M and Morton J (2015) Influence of ultraviolet exclusion and of powdery mildew infection on Sauvignon Blanc grape composition and on extraction of pathogenesis-related proteins into juice. Australian Journal of Grape and Wine Research **21**, 417-24

6.3. Discrimination of powdery mildew-affected grape berries at harvest using near-infrared spectroscopy

Tijana Petrovic, Timothy Zanker and Eileen S. Scott

Introduction

Previous research in the CRC for Viticulture and GWRDC project UA08/05 suggested that near infra-red (NIR) spectroscopy may have potential for quantifying powdery mildew in homogenates prepared from Chardonnay grapes. Following principal component analysis (PCA), NIR spectral data were clustered according to visual severity category as confirmed by DNA analysis. Linear discriminant analysis of the first three PCA scores correctly classified 37 of the 38 samples (Scott et al. 2010). However, the severity categories used in that research were relatively broad (<1%, 1-10%, 11-30%, 31-60% and >60%) and there was a need for finer-scale research.

The most informative region that had strong correlation with *E. necator* DNA in previous research was around 900 nm (or 11111 cm^{-1}, Scott et al. 2006), which corresponds to short-wave NIR. This was achieved by using a FOSS NIRSystems 6500 machine. Unfortunately, this machine was no longer available and a direct replacement could not be found.

Materials and methods

NIR spectrometric measurements. All composite severity categories and subsamples listed in Table 6.1.1 were analysed in reflectance mode with a "gold standard" reference shortly after homogenisation. Homogenates were placed in the glass vials (38) that were closed with lids and covered with aluminium foil to prevent light scattering. Vials were placed on the autosampler of the Antaris II FT-NIR Analyzer at the Australian Wine Research Institute. Acquisition of spectra was performed in the range 11998-3799 cm^{-1}. Twenty-four co-added scans with spectral resolution 4 cm^{-1} were collected at each measurement.

Samples were also analysed by spectroscopy in transmission mode and for this purpose 50% ethanol extracts of the total homogenates were obtained following the AWRI methodology for extraction of total anthocyanins in grapes (https://www.awri.com.au/wp-content/uploads/anthocyanins_fact_sheet.pdf). Each extract was placed in the cuvette with path-length of 1 mm and acquisition of spectra was performed in the range 10000-3999 cm^{-1}.

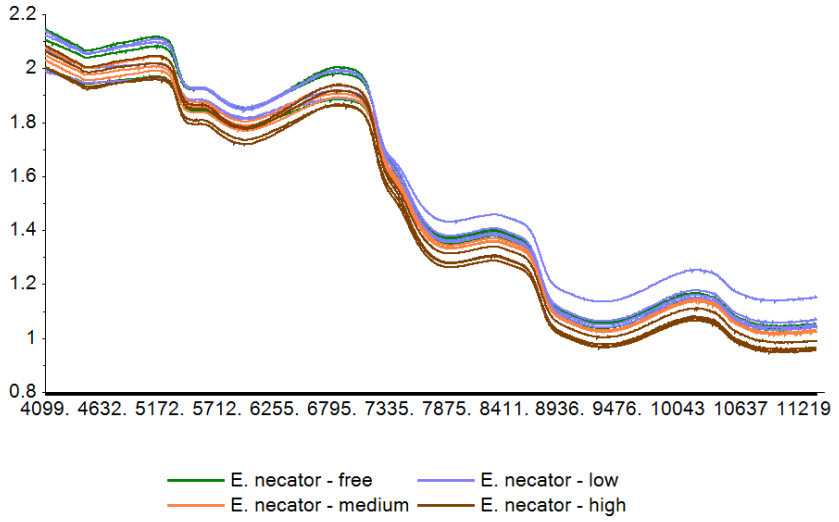
Analysis of NIR spectra. Raw spectra were exported from GRAMS to The Unscrambler X (version 10.4, CAMO ASA, Oslo, Norway) and pre-processed using the first derivative transformation, Savitzky-Golay derivation and smoothing (11 points on both sides and second order polynomial) (Baker et al. 2014). To avoid the usage of noisy edge regions, the NIR region was limited to 11362 - 4099 cm^{-1} (spectra measured by reflection) or entire the NIR region was used for spectra measured by transmission. PCA was applied to reduce the dimensions of the spectral data (1884 wavenumbers), followed by PLS regressions. Seven to 10 PCs explaining up to 95% of the total variation among samples were used for the PLS regressions. The PCA with singular value decomposition (SVD) algorithm and PLS regressions using kernel PLS algorithm with a maximum of seven components were performed. The performance of the PLS regression models developed for each variety were tested by applying the full cross validation method in which each calibration standard was quantified as the validation standard.

Results

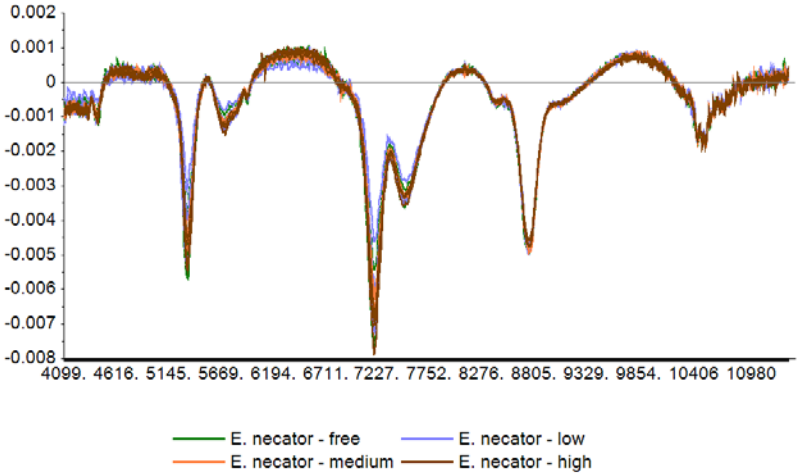
Calibrations for discriminating *E. necator*-free samples, samples with traces and the remaining infected samples could not be obtained for Chardonnay, Riesling and Pinot Noir when the pathogen coefficient was used as reference data and reflectance spectra used for prediction. Consequently, only NIR results for Grenache are presented in this report.

The raw and the first derivative of reflectance spectra changed with severity of powdery mildew over a wide range of wavenumbers (Figure 6.3.1a, b). The PLS analysis identified PC4 as the most important factor (Figure 6.3.1c) for the prediction of pathogen coefficient as a measure of powdery mildew severity (R^2 = 0.77 and RMSECV = 0.032).

(a)



(b)



(c)

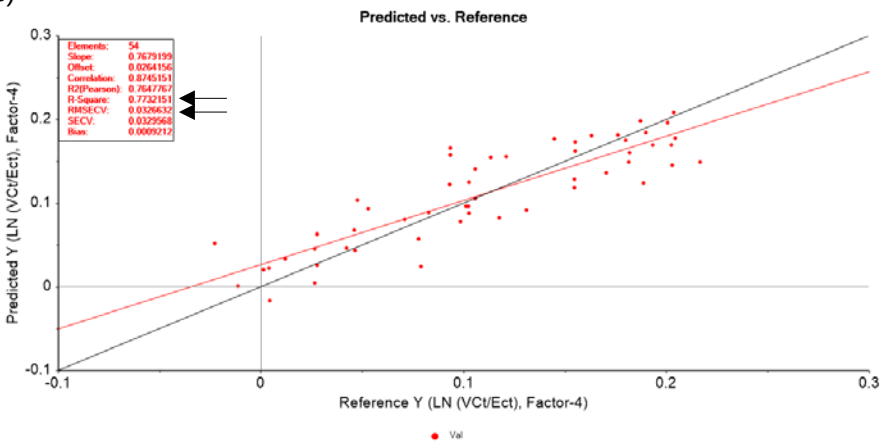
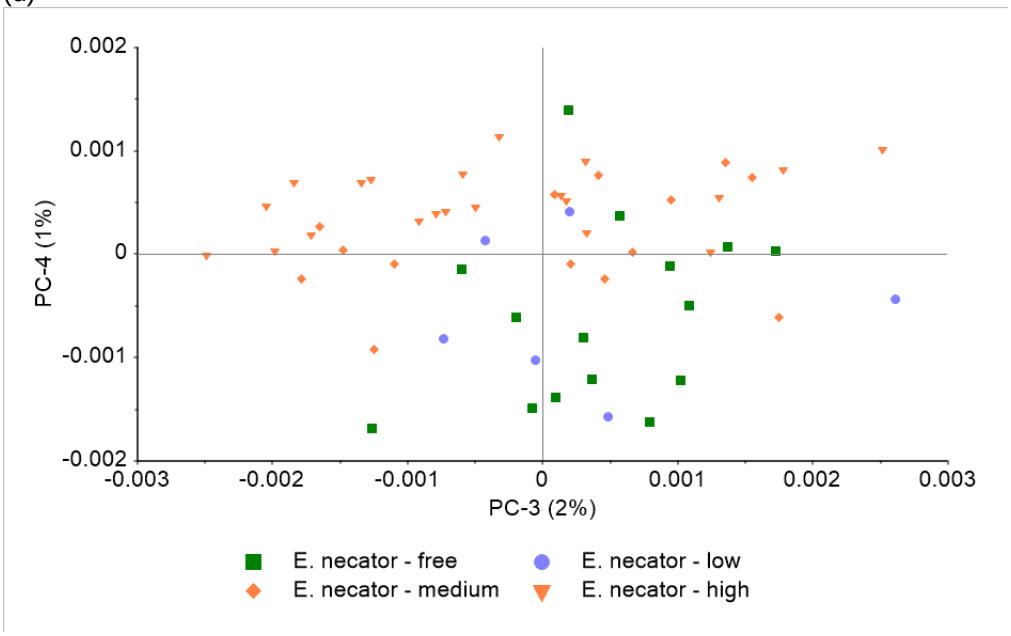


Figure 6.3.1. (continued on next page)

(d)



(e)

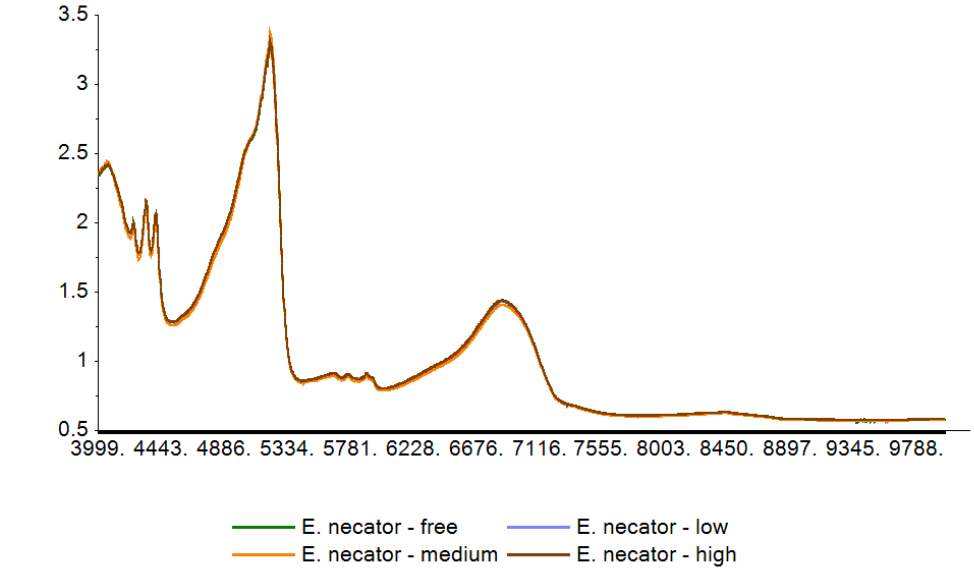


Figure 6.3.1. Near-infrared spectroscopic analysis of Grenache composite samples from the Coombe vineyard. Raw (a) and first derivative (b) of reflectance spectra showing change in the absorption of spectra in composite samples that are *E. necator*-free or -affected based on qPCR; (c) regression of log pathogen coefficient in grapes estimated by qPCR against log pathogen coefficient predicted by NIR [black line represents the one-to-one line (y = x), red line is the best-fit regression line]; (d) PCA plot with 95% confidence ellipse showing the distribution of 56 samples and slight separation of the powdery mildew-free samples (green) from the affected samples based on the qPCR in the direction of PC4; (e) raw transmission spectra with reduced noise.

PCA for Grenache samples performed on 56 profiles of the first derivative of the spectral region (11362-4099 cm^{-1}) showed no clear separation of samples based on powdery mildew severity in the score plot of the first two PCs that explained 88% of the variation. However, in the PC3-PC4 score plot, PC4 contributed to slight separation of powdery mildew-unaffected samples from the remaining samples (Figure 6.3.1d) which is congruent with a PLS selection of the most important factor for calibration.

The raw (Figure 6.3.1e) and the first derivative of transmission spectra was less noisy than reflectance spectra, but PLS calibration using first 7 PCs that explained 99% of the variation could not be obtained.

Discussion

In the research reported here, an Antaris II FT-NIR Analyzer was used instead of the FOSS NIRSystems 6500. While the Antaris machine does acquire spectra at 900 nm (or 11111 cm^{-1}), the region of particular interest, the spectra contained a lot of noise. The poor quality of NIR spectra in the required range collected on the Antaris II FT-NIR Analyser hindered attempts at calibration. A subsequent attempt to scan homogenates of Chardonnay and Riesling grapes collected in vintage 2015 in an industry setting using an InfraXact machine with scanning range 570-1850nm (Vis-NIR, which is informative for powdery mildew, Dambergs 2016 pers. com.) at Accolade Wines, Berri, was unsuccessful.

The inability to obtain meaningful data from NIR spectroscopy, considered alongside the failure of MIR to discriminate small differences in powdery mildew severity and similar findings reported for both MIR and NIR by Hill et al. (2014), led us to discontinue this aspect of the research.

References cited in this section

Baker MJ, Trevison J, Bassan P, Bhargava R, Butler HJ, Dorling KM, Fielden PR, Fogarty SW, Fullwood NJ, Heys KA, Hughes C, Lasch P, Martin-Hirsch PL, Obinaju B, Sockalingum GD, Sule-Sos J, Strong RJ, Walsh MJ, Wood BR, Gardner P and Martin FL (2014) Using Fourier transform IR spectra to analyse biological materials. Nature Protocols **9**, 1771-91

Hill GN, Evans KJ, Beresford RM and Dambergs RG (2014) Comparison of methods for the quantification of botrytis bunch rot in white grapes. Australian Journal of Grape and Wine Research **20**, 432–41

Scott ES, Dambergs RG, Stummer BE (2010) Fungal contaminants in the vineyard and wine quality. In: Reynolds AG (ed) Managing Wine Quality: Viticulture and Wine Quality (Volume 1), Woodhead Publishing Ltd, Cambridge, UK, pp 481-514

Scott ES, Stummer BE and Leong SL (2006) Fungal contaminants and their impact on wine quality GWRDC project CRV 99/23 (http://research.wineaustralia.com/completed_projects/fungal-contaminants-and-their-impact-on-wine-quality-1-5-2/)

6.4. Discrimination of powdery mildew-affected grape berries at harvest using mid-infrared attenuated total reflection spectroscopy and fatty acid profiling

Tijana Petrovic, Dilhani Perera, Daniel Cozzolino, Olena Kravchuk, Timothy Zanker, Jessamy Bennett and Eileen S. Scott

As submitted to the Australian Journal of Grape and Wine Research, October 2016, AJGWR-16-122, with the editor's permission

Abstract

Background and Aims: Powdery mildew (*Erysiphe necator*) reduces the quality of winegrapes and objective methods for assessment are required. Mid-infrared (MIR) spectroscopy and fatty acid analysis were investigated for rapid diagnosis of affected berries.
Methods and Results: Colonization by *E. necator* reduced berry diameter, weight and seed number. MIR spectra (1800–1185 cm^{-1}) contained information on *E. necator* and compounds related to infection but spectral similarity of visually healthy and half-infected berries confounded differentiation between these groups. Fatty acids in *E. necator* and berries were identified and quantified by gas chromatography. Six saturated even-chain fatty acids were prevalent in *E. necator*, arachidic acid being most abundant. Following stepwise linear discriminant analysis, four saturated fatty acids distinguished 97% of healthy berries and assigned approx. 75% of half- and fully-infected berries to their original groups. Arachidic acid, which changed amongst healthy, half- and fully-infected berries ($p = 0.001$), correctly classified 90% of healthy berries.
Conclusions: Analysis of fatty acids allowed discrimination of healthy and infected berries whereas MIR spectroscopy proved less informative. Arachidic acid content increased with disease severity.
Significance of the Study: Fatty acid analysis offers a new approach for objective measurement of powdery mildew. Arachidic acid is proposed as a biomarker for powdery mildew on grapes.

Introduction

Grape berries (*Vitis vinifera* L.) are infected by many pathogens, of which the obligately biotrophic fungus *Erysiphe necator* is the most devastating in vineyards worldwide (Gadoury et al. 2012). *E. necator* causes powdery mildew on all green tissues. On young berries, the fungus grows superficially and haustoria (specialized feeding structures) arise from appressoria (infection cells) that penetrate the cuticle and epidermal cell wall. The degree of susceptibility, measured as successful penetration by the fungus, decreases with phenological development of the berry (Ficke et al. 2003). On berries infected early in development (E-L 23–26) (Coombe 1995), when highly susceptible, the pathogen grows rapidly and colonizes the whole berry and rachis. As berries develop, ontogenetic or age-related resistance is expressed and the incidence of successful penetration and development of haustoria is nil or trace (Ficke et al. 2003, Gee et al. 2008). Diffuse, nonsporulating colonies, formed on berries in transition from susceptible to resistant, die as berries age, leaving a netting of necrotic epidermal cells (Gadoury et al. 2007). Guilpart et al. (2014) identified bunch closure (E-L 33) as a relevant threshold for susceptibility to powdery mildew.

Powdery mildew may lead to compositional and sensory changes in wine made from bunches with as little as 1–5% of the surface area affected (Stummer et al. 2005). Many Australian wineries reject or downgrade harvests that have more than 3 to 5% of the bunch surface area affected (Iland et al. 2011). Visual assessment is commonly used but is subjective, prone to error in field conditions and requires training in recognition and area assessment (Birchmore et al. 2015). Visual assessment at the winery may be compromised when grapes are machine-harvested and delivered partially or completely covered in juice. These constraints, as well as time and cost considerations, create a demand for more reliable and rapid methods of identification and quantification of powdery mildew on grape berries.

Mid-infrared spectroscopy (MIR) is widely used for assessment and classification of fungal contamination and mycotoxins in agricultural products, and assessment of wine fermentation processes (McMullin et al. 2015, Moore et al. 2015). It offers indirect assessment of quality by examining fingerprint regions of MIR spectra for alterations in fundamental crop characteristics. Recently, the potential of MIR spectroscopy for quantifying Botrytis bunch rot in homogenised grape berries was demonstrated by producing a partial

least squares model with high predictive ability based on the spectral range 1141–1050 cm^{-1} (Hill et al. 2013). To our knowledge MIR has not yet been applied to powdery mildew on grapes.

Biochemical changes in the composition of infected grapes also offer potential markers for powdery mildew. Grape skin contains diverse constitutive or induced compounds that may influence infection by and pathogenesis of *E. necator* (Ficke et al. 2004). These compounds include lipids, which are important in the structure, organization and processes of plant cells. The most abundant lipids in grape cells are those derived from fatty acid and glycerolipid biosynthetic pathways. Unsaturated and saturated fatty acids are present in the skin, pericarp (flesh) and seeds (Millan et al. 1992, Corte et al. 2015). Fatty acids in skin and flesh are important for vinification as some increase yeast populations, accelerate fermentation under anaerobiosis and affect wine organoleptic properties (Corte et al. 2015, Waterhouse et al. 2016).

Lipid profiles of grape berries depend on berry maturity, grape variety and environment. Similarly, lipid profiles of fungi are influenced by environmental conditions, substrate nutrients, age and developmental stage of the fungus (Losel 1991, Muchembled et al. 2000, 2005). Commonly identified and quantified lipids are those present in fungal cell membranes, *i.e.* fatty acid moieties of phospholipids and glycolipids, and sterols. Cellular fatty acid profiles can be used to differentiate fungal phyla and even to discriminate among species grown in standard conditions (Stahl and Klug 1996). Ergosterol, for example, a lipid specific for fungi, is prevalent in moulds associated with bunch rots of grapes but absent from *E. necator* and other powdery mildew species (Loeffler et al. 1992, Debieu et al. 1995, Porep et al. 2014b). Consequently, lipids provide selective markers for fungal diseases of grapes (Porep et al. 2014a,b, Agudelo-Romero et al. 2015) but have not yet been studied in depth for powdery mildew.

The present study was undertaken to investigate (i) feasibility of Attenuated Total Reflectance (ATR) MIR for diagnosis of powdery mildew-affected berries with minimal sample preparation, (ii) discriminatory potential of MIR spectral analysis to distinguish powdery mildew-affected berries from healthy berries, (iii) suitability of medium chain fatty acids as objective biochemical indicators of powdery mildew on berries and (iv) potential of fatty acid(s) to distinguish powdery mildew-affected berries from healthy berries.

Materials and methods

Grapevines

Chardonnay grapes (*V. vinifera*, clone I10V1) from the Alverstoke research vineyard (Waite Campus, University of Adelaide) (E 138° 38′ 15.97″, S 34 ° 58′ 6.95″), South Australia were used (Figure 1a). The spray program comprised application of Microthiol Disperss (sulfur) (Nufarm, Melbourne, Vic., Australia) with Enhance paraffinic oil (E-L 3) (SACOA, Osborne Park, WA, Australia), Microthiol Disperss alone (E-L 4, E-L 23; E-L 28, E-L 31), ecocarb (potassium bicarbonate) (OCP, Turrella, NSW, Australia) with Enhance (E-L 16, E-L 30, E-L 33), and Uni-Shield (sulfur) (UPL, Sydney, NSW, Australia) (E-L 33; E-L 34). The last treatments with paraffinic oil (December 4, 2015) and sulfur (December 21, 2015) were applied 5 and 3 weeks prior to sampling, respectively.

Sampling protocol

Grape bunches and berries. The sampling strategy was designed to obtain a representative range of individual berries (diam. > 7 mm) from healthy and infected bunches likely to be present in the vineyard. It considered the probable time of bunch infection (E-L 23–26 and shortly before E-L 33), and spatial stratification of disease severity. Fifty three grapevines were inspected for powdery mildew symptoms on bunches. Five vines in four panels were identified as 'hot spots' (Figure 1a) due to the number of severely diseased bunches. Some of the clusters were deemed likely to have become infected at or a few days after bloom (E-L 23–26) when highly susceptible. The remaining 48 vines carried visually healthy bunches and bunches deemed to have become infected shortly before bunch closure (E-L 33) when ontogenic resistance is acquired.

Thirty bunches (25 designated powdery mildew-affected and 5 visually healthy) with no signs of other abiotic/biotic damage were selected from the 53 vines (Figure 1b,c) when total soluble solids (TSS) reached 17–18 °Brix (January 13, 2016). Five bunches deemed infected at E-L 23–26 were randomly selected from five 'hot spot' vines. Twenty bunches deemed to have become infected after E-L 26 and before E-L 33 were selected in the following manner: a random sample of 10 bunches, and a purposive sample of 10 bunches from ‘non-hot spot’ vines, in which each bunch had to have at least one fully-infected berry (diam. > 7 mm).

Each bunch was separated into small clusters, assessed for symptoms using a magnifying lamp, and individual berries (diam. > 7 mm) were randomly chosen to represent three categories of surface area affected by powdery mildew, *viz.*; visually healthy, half-infected and fully-infected (Figure 1b). To prevent oxidation, berries were removed with pedicel attached and assessed using a stereomicroscope (Wild Heerbrugg, ×18 magnification). All analyses were conducted using individual berries. In total, 138 berries from 30 bunches were retained for analysis of phenotypic characters and MIR (Figure 1c); two berries, one healthy and one fully-infected from bunches in the 'hot spot' (E-L 23–26) and 'non-hot spot' (E-L 33), respectively, were unripe based on low TSS content and MIR analysis, and these outliers were subsequently excluded from data analyses.

From the 138 berries used for MIR analysis, a subsample of 61 (each with weight ≥ 250 mg) was selected for subsequent fatty acid analysis. Balanced selection of healthy (n = 20), half- (n = 21) and fully-infected (n = 20) berries was matched whenever possible at the bunch level (Figure 1c). When the weight of a homogenised berry was < 250 mg after MIR scanning, replacements (one healthy, five half-infected and four fully-infected) were selected from the remaining bunches (Figure 1c). Five healthy berries from each of three healthy bunches were also selected.

Fungal conidia. Fully-infected berries collected from 'hot spot' and 'non-hot spot' bunches were used as a source of *E. necator* conidia. Conidia from 'hot spot' (three samples) and 'non-hot spot' (four samples) bunches, 2.5–10 mg/sample, were harvested using a cyclone separator device (Evans et al. 1996), stored at –20 °C and freeze-dried (Dynavac, Hingham, MA, USA) for fatty acid analysis. Those samples were independent collections of conidia from several berries. For comparison, healthy Chardonnay (17–18 °Brix) and Cabernet Sauvignon (23–24 °Brix) grapes were inoculated with a suspension of conidia of *Botrytis cinerea* (FRR6173, CBS140599, GenBank accession KX710078) grown on V8 medium. Following surface-sterilization, six (Chardonnay) or eight (Cabernet Sauvignon) berries in each of four containers were inoculated with *B. cinerea* and controls were treated with sterile water (two containers) (Evans et al. 2013). Conidia and conidiophores were collected after 7 days using sterile needles, stored at –20 °C and freeze-dried. Six collections (2–3 mg), two from Chardonnay and four from Cabernet Sauvignon, were subjected to fatty acid analysis.

Phenotypic characteristics and TSS of berries

Berry diameter, weight, and number and weight of seeds per berry were measured. Width and length of each berry were measured using digital calipers (Vernier ROK, Guangdong, China). Pedicels were removed and each berry was weighed, dissected in a mortar to prevent loss of juice, and seeds were removed, counted and weighed. TSS were measured in 30 µL of juice per berry using a digital refractometer (Hanna Instruments, Keysborough, Vic. Australia). Each berry was homogenised in liquid nitrogen and the homogenate stored at –20 °C. The small volume of single berries precluded measurement of titratable acidity.

ATR–MIR spectroscopy

Conidia collected from several berries and pooled (n = 1), and individual homogenised deseeded grape berries (n = 138) were scanned using a platinum diamond ATR sampling module cell mounted in a Bruker Alpha instrument (Bruker Optics GmbH, Ettlingen, Germany). Approximately 60 µg of homogenate was placed on the ATR accessory and spectra were collected in the range 4000–400 cm^{-1}. Thirty-two co-added scans with spectral resolution 4 cm^{-1} were collected in each measurement without temperature equilibration. The sample cell was cleaned with distilled water between samples.

Analysis of ATR-MIR spectra

Raw spectra were exported from OPUS to The Unscrambler X (version 10.4, CAMO ASA, Oslo, Norway) and pre-processed using the second derivative transformation, Savitzky-Golay derivation and smoothing (10 points on both sides and second order polynomial) (Baker et al. 2014). Spectra were truncated in the main fingerprint region (1800–800 cm^{-1}) which included most of the biochemical information, then divided into six ranges and further truncated to avoid polysaccharide, ribose, glycogen and nucleic acid regions (1185–900 cm^{-1}) (Naumann 2009, Lecellier et al. 2014). A total of 435 wavenumbers were analysed. Principal component analysis (PCA) was applied to reduce the dimensions of the spectral data, followed by linear discriminant analysis (LDA).

A forward selection stepwise linear discriminant analysis (SLDA) on up to 15 PCs for 136 berries and 7 PCs for the subset of 61 berries used for fatty acid analysis was performed, with the aim of separating

healthy and powdery mildew severity groups. The analysis was conducted using Genstat *for Windows*, 18th edition (VSN International Ltd, UK) and was based on Wilk's lambda selection criteria to build an optimal model; bootstrapping was the error rate method.

Fatty acid analysis

Total lipids were extracted from freeze-dried conidia of *E. necator, B. cinerea* and from homogenised deseeded individual grape berries (250–700 mg/berry sample). Lipid extraction, methylation and gas chromatographic (GC) analysis of fatty acid methyl esters were conducted according to standard methodology of the Waite Lipid Analysis Services (University of Adelaide) (Tu et al. 2013). The identity of individual fatty acids (C14-C24) was verified by calculation of Estimated Chain Lengths (ECL) based on retention times of the authentic standard mixture (GLC-463, Nu-Chek Prep Inc., MN, USA) used to calibrate of the instrument (Stransky et al. 1997). Individual fatty acids were quantified using external calibrations prepared from authentic standards for total lipids [cholesteryl heptadecanoate 99% (Nu-Chek CH-816) and heptadecanoic acid 99% (Nu-Chek N-17-A)]. Results were reported as mg total fatty acid/100 g dry weight of freeze-dried conidia or fresh weight of deseeded berry.

Quantile data summaries (minimum, median and maximum) of concentrations of individual fatty acids were tabulated. Statistical inferential and discriminatory analyses were performed on log–transformed concentrations. Concentrations for the infection groups were estimated using mixed-model ANOVA (analysis of variance) corresponding to the sampling design and compared. Probability values of tests are reported in the text. Multivariate SLDA was performed on significant fatty acids with the aim of optimal separation of the 61 berries into the infection groups (Wilk's criteria, bootstrap error rate method). Analyses were performed using Genstat *for Windows*.

Results

Phenotypic characteristics, TSS and total lipids of berries

Healthy and infected berries differed in phenotypic characteristics and total lipid content (Table 1). Diameter of intact berries, weight with and without seeds, and the number of seeds/berry decreased with increasing severity of powdery mildew ($P < 0.001$). Berries were mostly spherical (Figure 1b) and the surface area to volume ratio increased with powdery mildew severity (Figure 2a). The concentration of total lipids (% of fresh weight) was greater in fully-infected berries than in half-infected and healthy berries ($P < 0.001$). Density of deseeded berries, seed weight and TSS remained similar among healthy and infected berries (Table 1). The density of deseeded berries, described by their weight/volume ratio (volume being adjusted for the volume of seeds), was unaffected by colonization by *E. necator* (Figure 2b).

MIR spectroscopic analysis

Spectral features of *E. necator* conidia collected from berries were in the main fingerprint region (1800–800 cm^{-1}) (Figure 3a). Absorption bands of range I (1780–1700 cm^{-1}) and IV (1480–1400 cm^{-1}) can be attributed to fatty acid esters and lipids due to ester (C=O) and CH_2, CH_3 (CH deformation) functional groups, respectively. Proteins were identified from their secondary amide absorption at regions II (1695–1625 cm^{-1}) and III (1560–1525 cm^{-1}) due to amide I (C=O stretching) and amide II (N–H bending and C–N stretching) bands. Nucleic acids were the main contributors to absorption bands in range V (1300–1200 cm^{-1}) due to phosphate stretching. Range VI (1185–900 cm^{-1}) was attributed to polysaccharides due to the vibrations of the functional group C–O–C (C–O stretching) (Williams and Fleming 1995).

IR absorption spectra of visually healthy and infected berry matrices were similar, with water (1634 cm^{-1}) and polysaccharides (region VI) the main components, and fatty acid esters, proteins, lipids and nucleic acids evident in regions I–V (Figure 3b). The region assigned to water (O–H overtone band) contains soluble proteins and overlaps with region II (amide I, 1695–1625 cm–1).

PCA was performed on profiles of the second derivative of smoothed ATR-MIR spectra of 136 berries including 707 wavenumbers in the main fingerprint region (1800–800 cm^{-1}). The score plot of the first two components (PC1 explained 85% of the variation, PC2 explained 2%) showed that visually healthy berries were less diverse than infected berries (data not presented). The corresponding loading variables for PC1, which may be attributed to glucose, fructose, ribose, glycogen, phenols, esters and nucleic acids (1185–900 cm^{-1}), were the main contributors to variation. No clear separation of visually healthy and powdery mildew severity groups was observed in relation to PC1 and PC2.

To tease out differences between visually healthy, half- and fully-infected berries, a region (1800–1185 cm^{-1}) including 435 wavenumbers and indicative of a mixture of lipid moieties, amide I and II, protein carboxyls, nucleic acids and fatty acid esters was analysed. The first 15 PCs explained 81% of the total variation among 136 berries. No separation was observed in relation to PC1 (30% of variation explained) (data not shown). In the PC2-PC3 scores plot (PC2 explained 16% of the variation, PC3 explained 7%), a clear separation of the majority of fully-infected (n = 32) from other berries (n = 104) was observed in the direction of PC3 and, to a lesser extent, PC2 (data not shown). Additionally, a group of 15 healthy berries from visually healthy bunches was separated from the other healthy berries by PC2 > 0.

Following dimension reduction by PCA, LDA applied to 15 PCs differentiated the three groups of berries with 86% success. PC2 had the best classification success rate (50%). PC2 loading for 136 berries indicated that the fatty acid esters peak (1760 cm^{-1}) and region 1665–1529 cm^{-1}, which mainly correspond to water and proteins (amide I and II), contributed most to separation of the majority of fully-infected berries from the rest (data not shown).

For the subset of 61 berries used subsequently for fatty acid analysis, the first 7 PCs explained 69% of the total variation. A PCA plot showing distribution of healthy (n = 20), half- (n = 21) and fully- (n = 20) infected berries with PC2 and PC3 corresponding to 14% and 5% of the variation, respectively, demonstrated separation of 14 fully-infected berries from the remainder (Figure 3c). LDA applied to these seven PCs differentiated the three groups of berries with 82% success. PC3 had the greatest discriminatory power (58%), misclassifying < 2% of fully-infected berries as healthy, and correctly classifying 69% of visually healthy berries (Table 3). The PC3 loadings showed five main peaks in the region 1697–1520 cm^{-1} and one non-assigned peak, 1789 cm^{-1}, separating 14 fully-infected berries from the remainder (Figure 3c,d). The main region corresponds to water and proteins (amide I and II) and the non-assigned peak may relate to carboxylic acids.

Fatty acid composition of conidia

Twelve fatty acids comprising C14-C24 were quantified in freeze-dried conidia collected from berries that were infected early (E-L 23–26) and late (E-L 33) in the season and concentrations were similar in both collections (Table 2). One saturated (C14:0) and three unsaturated (C18:3n–6, C20:3n–6, C22:1n–9) fatty acids were below the limit of quantification in some of the samples (data not shown).

Saturated fatty acids (6) were 6–7 fold more abundant than unsaturated acids (6) (data not shown). The combined concentration of the six main saturated fatty acids was 2303–5015 mg/100 g in conidia collected from early infected, and 1977–6839 mg/100 g in conidia collected from late infected berries. Arachidic acid (C20:0) was dominant, making up half of the total saturated fatty acids (C14-C24) detected in conidia [1115–2993 mg/100 g (E-L 23–26) and 916–3482 mg/100 g (E-L 33)], followed by stearic (C18:0) and palmitic (C16:0) acids. The mean concentration of arachidic acid was similar in both collections of E. necator (P = 0.48).

Six unsaturated fatty acids were identified in *E. necator* conidia. Their total concentration ranged from 333 to 642 mg/100 g in conidia collected from early infected berries, and from 213 to 1504 mg/100 g for late infected berries; these concentrations were not significantly different ($P > 0.05$). Oleic (C18:1n–9), linoleic (C18:2n–6) and α–linolenic (C18:3n–3) acids were the most abundant unsaturated fatty acids present and concentrations were similar ($P > 0.05$) in both collections of conidia (data not shown).

Individual saturated fatty acids (C14-C24) in both collections of *E. necator* did not show rate-limited behaviour and the concentration of each subsequently synthesized fatty acid correlated well with the concentration of its precursor fatty acid (Figure 4a). Three dominant unsaturated fatty acids (C18:1n–9, C18:2n–6, C18:3n–3) showed similar behaviour and each synthesized fatty acid was correlated with its precursor acid (r > 0.70) (Figure 4b).

Eight fatty acids, C14-C20, were quantified in freeze-dried conidia and conidiophores of *B. cinerea* from Chardonnay berries (Table 2); unsaturated fatty acids (4) were 2–3 fold more abundant than saturated fatty acids (4). Linoleic acid (C18:2n–6) and palmitic acid (C16:0) were the most abundant unsaturated and saturated fatty acids, respectively. Arachidic (C20:0), behenic (22:0) and lignoceric (C24:0) acids were not detected.

Fatty acid composition of grape berries

A total of 15 fatty acids, 7 saturated and 8 unsaturated, were identified and quantified in visually healthy and infected deseeded berries (Table 2). The abundance of total saturated and total unsaturated fatty acids was similar. The total concentrations of all saturated (C14:0, C15:0, C16:0, C18:0, C20:0, C22:0 and

C24:0) and of four unsaturated (C18:1n–9, C18:2n–6, C18:3n–3 and C18:1n–7) fatty acids differed significantly between visually healthy and infected berries ($p < 0.01$) (Table 2).

Arachidic acid was the only acid to become consistently more abundant as severity of powdery mildew increased, ranging from 0.61 to 1.69 mg/100 g in healthy berries, 1.23 to 4.05 mg/100 g in half- and 1.61 to 7.09 mg/100 g in fully-infected berries. On average, its concentration significantly increased with powdery mildew severity, by almost 2-fold in half-infected and 4-fold in fully-infected compared with healthy berries ($P = 0.001$).

The concentration of individual even-chain saturated fatty acids in healthy and infected berries was not substrate-specific or rate-limited by infection, given that the concentration of each subsequently synthesized fatty acid correlated well with the concentration of its precursor (Figure 5a). The only odd-chain fatty acid, pentadecanoic acid (C15:0), was present in small amounts in healthy and infected berries (Table 2). Three prevalent unsaturated acids (C18:1n–9, C18:2n–6 and C18:3n–3) (Table 2) were continuously synthesized in all groups of berries (Figure 5b).

The SLDA conducted for the seven saturated fatty acids showed that four (C20:0, C14:0, C15:0 and C22:0) had the greatest discriminatory power with the overall success rate of 77%, assigning 97% of healthy, 75% of half- and 73% of fully-infected berries to their original visual groups (Table 4). Healthy berries were rarely predicted to be half- or fully-infected, < 2% and < 1%, respectively. Prediction of half- and fully-infected berries as healthy was < 8%.

Arachidic acid alone separated the three groups of berries with overall success rate of 70%, differentiating 90% of healthy, 71% of half-infected and 67% of fully-infected berries. Healthy berries were infrequently predicted to be half-infected (< 10%) and no healthy berry was predicted to be fully-infected. Most incorrect predictions concerned half-infected berries (Table 4).

Discussion

Powdery mildew affected grape berry development and was associated with fewer seeds and increased surface area-to-volume ratio; the latter possibly contributed to increased concentration (% w/w) of total lipids in fully infected berries (Table 1). Powdery mildew also altered the biochemical composition, *e.g.* water content and/or soluble/insoluble proteins (MIR data) and fatty acid profile (GC data), of berries, which supports previous reports that fungal infection leads to modification of existing grape substrates or *de novo* synthesis of compounds (Steel et al. 2013). Arachidic acid was identified as an indicator of powdery mildew on grape berries and correlated well with increasing disease severity in the set of 61 berries. To our knowledge this is the first research to profile fatty acids in conidia of *E. necator* and powdery mildew-affected berries.

Fully-infected berries covered with mycelia and conidia were smaller and lighter than healthy and half-infected berries, due either to lack of growth and expansion of the epidermis or fewer seeds per berry, given that mature berry size is related to the number of seeds (Goffinet and Pratt 2015). The decreased weight of deseeded diseased Chardonnay berries is in agreement with results for Sauvignon Blanc berries classified as having low and high levels of scarring associated with powdery mildew (Tian et al. 2015). In our study, the density (weight/spherical volume) of healthy and infected berries was similar (Table 1). Furthermore, accumulation of TSS was unaffected by *E. necator* as was also reported for 'low-scarred' and 'high-scarred' individual Sauvignon Blanc berries infected at E-L 31 (pea size) and harvested at 20 °Brix (Tian et al. 2015), and for bunches of Chardonnay with 1–100% surface area affected (Stummer et al. 2003). These results suggest that the physiological activity of healthy and diseased berries was similar, which is relevant when considering threshold values for a powdery mildew biomarker for assessment of crop harvested.

IR absorption spectra of E. necator conidia, and healthy and infected berries were comparable to similar biological samples (Hill et al. 2013, Lecellier et al. 2014). Qualitative and quantitative changes in MIR spectra (1800–1185 cm^{-1}) were related to the occurrence and severity of powdery mildew. The spectra informative for powdery mildew were distinct from that identified by Hill et al. (Hill et al. 2013) as specific for Botrytis bunch rot, 1141–1050 cm^{-1} (*i.e.* 8760–9520 nm), and indicative of the presence of glycogen and other polysaccharides. MIR spectroscopy in the range 1800–1185 cm^{-1}, followed by LDA of the first 15 PCs for 136 berries and 7 PCs for the subset of 61 berries, may be considered a promising method for classification of berries, with an overall success rate of 87% and 82%, respectively. The SLDA selected

PC3, explaining 5% of the total variation and loaded in the protein and water region, as the optimal discriminator of infection for the subset of 61 berries. However, using PC3 only 69% of berries originally assigned to the healthy group were predicted to be healthy (Table 3), which is less than the success rate of prediction based on arachidic acid (90%) or four saturated fatty acids (97%) (Table 4). As PC3 was driven largely by water, protein content and carboxylic acids (Figure 3d), further investigation is needed to identify specific spectral bands or regions corresponding to *E. necator* compounds that may have greater power to predict healthy and half-infected berries when chemometrics are applied. Protein-related regions (1695–1300 cm^{-1}) may indicate pathogenesis-related proteins, which increase in grape skin and pulp in response to powdery mildew (Tian et al. 2015). The peak at 1789 cm^{-1} may be attributed to the carboxylic acid functional group arising from grape organic acids (*e.g.* tartaric, malic and citric acids), which have been reported to increase in bunches having more than 10% of the surface area affected by powdery mildew (Stummer et al. 2003). Modification of methods for sample preparation might reduce or eliminate spectral interference due to water and provide more information about amide I region, which overlaps with the water peak.

The dominance and abundance of saturated fatty acids in *E. necator* conidia collected from berries infected at E-L 23–33 was demonstrated here (Table 2). Powdery mildew fungi, such as *Erysiphe* and *Sphaerotheca* species, contain large amounts of saturated fatty acids (Tulloch and Ledingham 1960, Losel 1988). The prevalence of C20-C24 fatty acids in *E. necator* conidia (68% of the total saturated fatty acids) is somewhat less than that reported for conidia of *E. graminis* f.sp. *hordei* (91%), *Sphaerotheca humuli* var. *fuliginea* (86%) and *Blumeria graminis* f.sp. *tritici* (92%) (Tulloch and Ledingham 1960, Senior et al. 1993, Muchembled et al. 2006); this may be related to the age of conidia and/or the presence of mycelia and conidiophores of *E. necator* from berries. In comparison, young conidia of *B. graminis* f.sp. *tritici* contained mainly medium-chain fatty acids (C12-C18) whereas old conidia had mostly long-chain fatty acids (C22-C24) (Muchembled et al. 2000, 2005).

Arachidic acid was the predominant (45% of total) fatty acid in both collections of *E. necator*, in contrast to the general view in the literature that most fungal species contain, in order of abundance, oleic (C18:1n–9), palmitic (C16:0) and linoleic acids (C18:2n–6) (Akpinar-Bayizit 2014). Application of paraffinic oil did not affect the abundance of arachidic acid in *E. necator* conidia, as the oil did not contain C20-C24 fatty acids. The predominance of arachidic acid has not been reported previously for any obligate, including powdery mildew species, or facultative fungal pathogens. In conidia harvested from leaves, arachidic acid was either not detected (*B. graminis* f.sp. *tritici*), detected in traces (*E. graminis* f.sp. *hordei*) or in moderate amount (13% of total fatty acids in *S. humuli* var. *fuliginea*) (Tulloch and Ledingham 1960, Senior et al. 1993, Muchembled et al. 2000, 2006). The content of behenic (C22:0) and lignoceric (C24:0) acids (14% of total identified in our study) was less in conidia of *E. necator* than was reported for *B. graminis*, *S. humuli* var. *fuliginea* and *E. graminis* f.sp. *hordei* (Tulloch and Ledingham 1960, Senior et al. 1993, Muchembled et al. 2005).

The similar concentration of arachidic acid in two collections of *E. necator* from berries indicated that, in the vineyard management system used here, the synthesis and/or accumulation of arachidic acid in conidia might be independent of the stage at which berries become infected, post-infection growth and sporulation on the berry. The high concentration of arachidic acid in *E. necator* and its absence from *B. cinerea* collected from berries in the present study (data not shown) make arachidic acid a potential component for characterizing *E. necator* and for quantifying powdery mildew on grapes.

The fatty acid composition of Chardonnay berries changed in response to powdery mildew. Alteration of fatty acid profiles or concentrations of individual fatty acids has been documented for facultative interactions such as grape berries-*Botrytis cinerea* (Agudelo-Romero et al. 2013, 2015), wheat-*Fusarium culmorum* (Stuper-Szablewska et al. 2014) and potato-*Phytophthora infestans* (Hamzehzarghani et al. 2016). Eleven fatty acids quantified in the visually healthy berries occurred in significantly different concentrations in powdery mildew-affected berries analysed at E-L 37 (Table 2). This contrasts with findings for Botrytis bunch rot-affected berries analysed at E-L 33 and E-L 35 where the occurrence of five fatty acids (C17:0, C23:0, C18:1n–9, C18:2n–6 and C18:3n–3) was exclusively associated with infection (Agudelo-Romero et al. 2015). Arachidic acid was the only fatty acid showing significant correlation with increase of powdery mildew severity (*i.e.* half- and fully-infected berries). Although this fatty acid was prevalent in conidia of *E. necator* collected from berries and present in small amounts in visually healthy berries (Table 2), it is possible that arachidic acid is synthesized upon infection by *E. necator*, perhaps analogous to pathogenesis-related proteins in the same pathosystem (Tian et al. 2015).

Arachidic (C20:0), myristic (C14:0), pentadecanoic (C15:0) and behenic (C22:0) acids showed the greatest power in distinguishing among visually healthy, half- and fully-infected berries at harvest (E-L 37), allowing reliable classification of 19 healthy berries (97%) with only one berry (<3%) predicted as half-infected (Table 4). Except for pentadecanoic acid, the concentrations of these acids have been reported to increase naturally during berry ripening (E-L 35, E-L 38) (Millan et al. 1992, Agudelo-Romero et al. 2013, 2015). Increase in arachidic and behenic acids during ripening may also be the result of accumulation of superficial waxes that have long-chain saturated fatty acids as major constituents (Loureiro et al. 2012, Agudelo-Romero et al. 2013). Overall, our results suggest saturated fatty acids to be a suitable indicator of powdery mildew infection.

The concentration of arachidic acid aligned well with powdery mildew severity and could detect traces of infection, *e.g.* two visually healthy berries (approx. 10%) with atypical concentration of arachidic acid were predicted to be half-infected. These berries were assumed to have been infected prior to ontogenic resistance, then *E. necator* killed or inhibited by fungicide applications. Sparse, dead colonies may have been overlooked due to their resemblance to white waxy threads on the surface of berries, however, initial parasitism by *E. necator* may have caused increased concentration of arachidic acid. The discrepancy between the percentage of predicted and visually assigned half- and fully-infected berries (Table 4) may reflect heterogeneity of fungal biomass on the berry or the time of infection relative to berry development.

Analysis of medium chain fatty acids is suggested as a new approach to objective measurement of powdery mildew. Berries in this study were deseeded before analysis. However, grape seeds contain negligible quantities of arachidic acid (Rubio et al. 2009), so would not confound the use of arachidic acid as a biomarker for powdery mildew and thresholds for arachidic acid could be calculated per kg of grapes. On the other hand, MIR analysis did not discriminate between degrees of infection, although the protein region changed in response to severe disease, suggesting that an MIR-based method may be feasible if proteins are extracted in a suitable manner.

Further research is needed to elucidate if arachidic acid alone or in combination with C14:0, C15:0 and C22:0 can be used to assess powdery mildew in the vineyard and if arachidic acid is related to other indicators of powdery mildew, such as accumulation of pathogenesis-related proteins. Such research might involve comparison with other approaches, such as quantitative PCR. Abiotic (e.g. heat, UV radiation, fungicides) or biotic (other microorganisms) stress in the vineyard may affect growth of *E. necator*, its metabolic activity including abundance of arachidic acid, and may lead to quantitative and qualitative alterations of fatty acid profiles of healthy and powdery mildew–affected berries. Conversion of arachidic acid to unsaturated fatty acids is known to occur in response to environmental stress (Velazquez-Becerra et al. 2013). Investigation of fatty acid profiles of white and red grape varieties from vineyards with various management practices, agroclimatic regions and vintages is also required. Furthermore, the severity of powdery mildew that results in specific sensory characters in wines needs to be defined to ensure that thresholds for disease are well matched to the quality of wine so that critical concentrations of fatty acids can be identified.

Conclusions

Powdery mildew affected development but not physiological activity of Chardonnay berries. The density of berries, growth of seeds and accumulation of TSS were unaffected, suggesting that healthy and infected berries were equally physiologically active, which is important for setting thresholds for the presence of powdery mildew in grape harvests.

Specific MIR spectral bands or regions need to be identified to allow prediction of healthy and half-infected berries when multivariate methods are applied. Discriminatory analysis applied to the selected PCs for 136 berries and the subset of 61 berries allowed healthy, half- and fully-infected berries to be distinguished with > 80% success. Water content and/or proteins were the main contributors to separation of the three groups of berries using PCA.

E. necator conidia were rich in saturated fatty acids, arachidic acid (C20:0) being the most abundant. Powdery mildew altered the fatty acid profile and concentrations of individual fatty acids in berries. Discriminatory analysis showed that saturated fatty acids provide an indicator of powdery mildew severity in grape berries. Four fatty acids (C20:0, C14:0, C15:0, C22:0) assigned 97% of healthy and two thirds of half- and fully-infected berries to their original visual groups. Arachidic acid was the only fatty acid that

discriminated healthy, half- and fully-infected berries and, therefore, is proposed as a specific and quantitative marker for powdery mildew of berries.

References cited in this section

Agudelo-Romero, P., Erban, A., Sousa, L., Pais, M.S., Kopka, J. and Fortes, A.M. (2013) Search for transcriptional and metabolic markers of grape pre-ripening and ripening and insights into specific aroma development in three Portuguese cultivars. PLoS ONE **8**, e60422

Agudelo-Romero, P., Erban, A., Rego, C., Carbonell-Bejerano, P., Nascimento, T., Sousa, L., Martinez-Zapater, J.M., Kopka, J. and Fortes, A.M. (2015) Transcriptome and metabolome reprogramming in *Vitis vinifera* cv. Trincadeira berries upon infection with *Botrytis cinerea*. Journal of Experimental Botany **66**, 1769-85

Akpinar-Bayizit, A. (2014) Fungal lipids: The biochemistry of lipid accumulation. International Journal of Chemical Engineering and Application **5**, 409-14

Baker, M.J., Trevisan, J., Bassan, P., Bhargava, R., Butler, H.J., Dorling, K.M., Fielden, P.R., Fogarty, S.W., Fullwood, N.J., Heys, K.A., Hughes, C., Lasch, P., Martin-Hirsch, P.L., Obinaju, B., Sockalingum, G.D., Sule-Suso, J., Strong, R.J., Walsh, M.J., Wood, B.R., Gardner, P. and Martin, F.L. (2014) Using Fourier transform IR spectroscopy to analyze biological materials. Nature Protocols **9**, 1771-91

Birchmore, W., Scott, E.S., Zanker, T., Emmett, B. and Perry, W. (2015) Smart-phone app field assessment of powdery mildew. Australian and New Zealand Grapegrower & Winemaker **622**, 46-47.

Coombe, B.G. (1995) Adoption of a system for identifying grapevine growth stages. Australian Journal of Grape and Wine Research **1**, 104-10

Corte, A.D., Chitarrini, G., Gangi, I.M.D., Masuero, D., Soini, E., Mattivi, F. and Vrhovsek, U. (2015) A rapid LC-MS/MS method for quantitative profiling of fatty acids, sterols, glycerolipids, glycerophospholipids and sphingolipids in grapes. Talanta **140**, 52-61

Debieu, D., Corio-Costet, M.F., Steva, H., Malosse, C. and Leroux, P. (1995) Sterol composition of the vine powdery mildew fungus, *Uncinula necator*: comparison of triadimenol-sensitive and resistant strains. Phytochemistry **39**, 293-300

Evans, K.J., Whisson, D.L. and Scott, E.S. (1996) An experimental system for characterizing isolates of *Uncinula necator*. Mycological Research **100**, 675-80

Evans, K.J., Palmer, A.K. and Metcalf, D.A. (2013) Effect of aerated compost tea on grapevine powdery mildew, botrytis bunch rot and microbial abundance on leaves. European Journal of Plant Pathology **135**, 661-73

Ficke, A., Gadoury, D.M., Seem, R.C. and Dry, I.B. (2003) Effects of ontogenic resistance upon establishment and growth of *Uncinula necator* on grape berries. Phytopathology **93**, 556-63

Ficke, A., Gadoury, D.M., Seem, R.C., Godfrey, D. and Dry, I.B. (2004) Host barriers and responses to *Uncinula necator* in developing grape berries. Phytopathology **94**, 438-45

Gadoury, D.M., Seem, R.C., Wilcox, W.F., Henick-Kling, T., Conterno, L., Day, A. and Ficke, A. (2007) Effects of diffuse colonization of grape berries by *Uncinula necator* on bunch rots, berry microflora, and juice and wine quality. Phytopathology **97**, 1356-65

Gadoury, D.M., Cadle-Davidson, L., Wilcox, W.F., Dry, I., Seem, R.C. and Milgroom, M.G. (2012) Grapevine powdery mildew (*Erysiphe necator*): a fascinating system for the study of the biology, ecology and epidemiology of an obligate biotroph. Molecular Plant Pathology **13**, 1-16

Gee, C.T., Gadoury, D.M. and Cadle-Davidson, L. (2008) Ontogenic resistance to *Uncinula necator* varies by genotype and tissue type in a diverse collection of *Vitis* spp. Plant Disease **92**, 1067-73

Goffinet, M.C. and Pratt, C. (2015) Grapevine structure and growth stages. Wilcox, W.F., Gubler, W.D. and J.K. Uyemoto, eds. Compendium of grape diseases, disorders, and pests. 2nd ed (APS Press: Minnesota, USA) pp. 5-15

Guilpart, N., Calonnec, A., Raynal, M., Coulon, T., Debord, C., Gary, C. and Metay, A. (2014) Bunch closure is a relevant threshold for grapevine susceptibility to powdery mildew (*Erysiphe necator*) in field conditions. Diez-Navajas, A.M., Ortiz-Barredo, A., Menendez, C., Emmett R., Gadoury, D.M., Gubler, W.D., Kassemeyer, H.-H., Magarey, P. and Seem, R., eds, Proceedings of the seventh international workshop on grapevine downy and powdery mildew, 30 June-4 July 2014 (Arabako Foru Aldundia, Vitoria Gasteiz, Spain), pp. 77-9

Hamzehzarghani, H., Vikram, A., Abu-Nada, Y. and Kushalappa, A.C. (2016) Tuber metabolic profiling of resistant and susceptible potato varieties challenged with *Phytophthora infestans*. European Journal of Plant Pathology **145**, 277-87

Hill, G.N., Evans, K.J., Beresford, R.M. and Dambergs, R.G. (2013) Near and mid-infrared spectroscopy for the quantification of botrytis bunch rot in white wine grapes. Journal of Near Infrared Spectroscopy **21**, 467-75
Iland, P., Proffitt, T., Dry, P. and Tyerman, S. (2011) The grapevine: from the science to the practice of growing vines for wine. (Patrick Iland Wine Promotions Pty Ltd: Adelaide, Australia)
Lecellier, A., Mounier, J., Gaydou, V., Castrec, L., Barbier, G., Ablain, W., Manfait, M., Toubas, D. and Sockalingum, G.D. (2014) Differentiation and identification of filamentous fungi by high-throughput FTIR spectroscopic analysis of mycelia. International Journal of Food Microbiology **168-169**, 32-41
Loeffler, R.S.T., Butters, J.A. and Hollomon, D.W. (1992) The sterol composition of powdery mildews. Phytochemistry **31**, 1561-63
Losel, D.M. (1988) Fungal lipids. Ratledge, C. and Wilkinson, S.G., eds. Microbial Lipids (Academic Press: London, UK) pp. 699-806
Losel, D.M. (1991) Synthesis and functioning of membrane lipids in fungi and infected plants. Pesticide Science **32**, 353-62
Loureiro, V., Malfeito Ferreira, M., Monteiro, S. and Ferreira, R.B. (2012) The microbial community of grape berry. Gerós, H., Chaves, M.M. and Delrot, S, eds. The biochemistry of the grape berry. (Bentham Science Publishers: SAIF Zone Sharjah, U.A.E) pp. 241-68
McMullin, D., Mizaikoff, B. and Krska, R. (2015) Advancements in IR spectroscopic approaches for the determination of fungal derived contaminations in food crops. Analytical and Bioanalytical Chemistry **407**, 653-60
Millan, C., Vargas, A., Rubio, A., Moreno, J. and Ortega, J.M. (1992) Fatty acid content of unripe and ripe 'Pedro Ximénez' *Vitis vinifera* Grapes. Journal of Wine Research **3**, 235-40
Moore, J.P., Zhang, S.-L., Nieuwoudt, H., Divol, B., Trygg, J. and Bauer, F.F. (2015) A multivariate approach using attenuated total reflectance mid-infrared spectroscopy to measure the surface mannoproteins and β-glucans of yeast cell walls during wine fermentations. Journal of Agricultural and Food Chemistry **63**, 10054-63
Muchembled, J., Sahraoui, A.L.H., Grandmougin-Ferjani, A. and Sancholle, M. (2000) Effect of age on the fatty acid content of *Blumeria graminis* conidia. Biochemical Society Transactions **28**, 875-7
Muchembled, J., Sahraoui, A.L.H., Laruelle, F., Palhol, F., Couturier, D., Grandmougin-Ferjani, A. and Sancholle, M. (2005) Methoxylated fatty acids in *Blumeria graminis* conidia. Phytochemistry **66**, 793-96
Muchembled, J., Sahraoui, A.L.H., Grandmougin-Ferjani, A. and Sancholle, M. (2006) Changes in lipid composition of *Blumeria graminis* f.sp. *tritici* conidia produced on wheat leaves treated with heptanoyl salicylic acid. Phytochemistry **67**, 1104-9
Naumann, A. (2009) A novel procedure for strain classification of fungal mycelium by cluster and artificial neural network analysis of Fourier transform infrared (FTIR) spectra. Analyst **134**, 1215-23
Porep, J.U., Erdmann, M.E., Korzendorfer, A., Kammerer, D.R. and Carle, R. (2014a) Rapid determination of ergosterol in grape mashes for grape rot indication and further quality assessment by means of an industrial near infrared/visible (NIR/VIS) spectrometer - a feasibility study. Food Control **43**, 142-9
Porep, J.U., Walter, R., Kortekamp, A. and Carle, R. (2014b) Ergosterol as an objective indicator for grape rot and fungal biomass in grapes. Food Control **37**, 77-84
Rubio, M., Alvarez-Orti, M., Alvarruiz, A., Fernandez, E. and Pardo, J.E. (2009) Characterization of oil obtained from grape seeds collected during berry development. Journal of Agricultural and Food Chemistry **57**, 2812-15
Senior, I.J., Hollomon, D.W. and Holloway, P.J. (1993) Unusual long-chain monoenoic fatty acids in conidia of *Erysiphe graminis*. Phytochemistry **34**, 65-8
Stahl, P. and Klug, M. (1996) Characterization and differentiation of filamentous fungi based on fatty acid composition. Applied and Environmental Microbiology **62**, 4136-46
Steel, C.C., Blackman, J.W. and Schmidtke, L.M. (2013) Grapevine bunch rots: impacts on wine composition, quality, and potential procedures for the removal of wine faults. Journal of Agricultural and Food Chemistry **61**, 5189-206
Stransky, K., Jursik, T. and Vitek, A. (1997) Standard equivalent chain length values of monoenic and polyenic (methylene interrupted) fatty acids. Journal of High Resolution Chromatography **20**, 143-58
Stummer, B.E., Francis, I.L., Markides, A.J. and Scott, E.S. (2003) The effect of powdery mildew infection of grape berries on juice and wine composition and on sensory properties of Chardonnay wines. Australian Journal of Grape and Wine Research **9**, 28-39
Stummer, B.E., Francis, I.L., Zanker, T., Lattey, K.A. and Scott, E.S. (2005) Effects of powdery mildew on the sensory properties and composition of Chardonnay juice and wine when grape sugar ripeness is standardised. Australian Journal of Grape and Wine Research **11**, 66-76

Stuper-Szablewska, K., Busko, M., Goral, T. and Perkowski, J. (2014) The fatty acid profile in different wheat cultivars depending on the level of contamination with microscopic fungi. Food Chemistry **153**, 216-23

Tian, B., Harrison, R., Jaspers, M. and Morton, J. (2015) Influence of ultraviolet exclusion and of powdery mildew infection on Sauvignon Blanc grape composition and on extraction of pathogenesis-related proteins into juice. Australian Journal of Grape and Wine Research **21**, 417-24

Tu, W.C., Muhlhausler, B.S., Yelland, L.N. and Gibson, R.A. (2013) Correlations between blood and tissue omega-3 LCPUFA status following dietary ALA intervention in rats. Prostaglandins, Leukotrienes and Essential Fatty Acids **88**, 53-60

Tulloch, A.P. and Ledingham, G.A. (1960) The component fatty acids of oils found in spores of plant rusts and other fungi. Canadian Journal of Microbiology **6**, 425-34

Velazquez-Becerra, C., Macias-Rodriguez, L.I., Lopez-Bucio, J., Flores-Cortez, I., Santoyo, G., Hernandez-Soberano, C. and Valencia-Cantero, E. (2013) The rhizobacterium *Arthrobacter agilis* produces dimethylhexadecylamine, a compound that inhibits growth of phytopathogenic fungi in vitro. Protoplasma **250**, 1251-62

Waterhouse, A.L., Sacks, G.L. and Jeffery, D.W. (2016) Understanding wine chemistry (John Wiley & Sons, Ltd: Chichester, West Sussex, UK)

Williams, D.H. and Fleming, I. (1995) Spectroscopic methods in organic chemistry. 5th ed (McGraw-Hill Education: NY, USA)

Table 1. Phenotypic characteristics of healthy and powdery mildew-affected Chardonnay grape berries

Characteristics	Berries							*P* value
	Healthy			Infected				
				Half		Fully		
	Healthy	E-L 23–26	E-L 33	E-L 23–26	E-L 33	E-L 23–26	E-L 33	
	n = 5	n = 12	n = 3	n = 13	n = 8	n = 10	n = 10	
Diameter of seeded berry (mm)	12.7 ± 0.19[†]	12.9 ± 0.48	12.5 ± 0.17	10.7 ± 0.18	11.4 ± 0.16	9.8 ± 0.3ab	10.1 ± 0.3a	< 0.001
Weight of seeded berry (mg)	1433 ± 73d	1372 ± 132d	1294 ± 44d	858 ± 39d	1050 ± 39c	680 ± 52a	686 ± 54ab	< 0.001
Weight of deseeded berry (mg)	1329 ± 70d	1228 ± 127d	1202 ± 41d	778 ± 34b	962 ± 34c	609 ± 45a	614 ± 49ab	< 0.001
Volume of deseeded berry (μL)	955 ± 43d	958 ± 121d	916 ± 33d	543 ± 29b	680 ± 26c	421 ± 36a	473 ± 43ab	< 0.001
Density of deseeded berry (mg/μL)	1.37 ± 0.029b	1.30 ± 0.063b	1.32 ± 0.028b	1.45 ± 0.04ab	1.43 ± 0.03ab	1.50 ± 0.059a	1.32 ± 0.035b	0.06
Seed weight (mg)	42 ± 1.2	46 ± 2.5	45 ± 1.3	44 ± 1.3	43 ± 1.0	43 ± 2	44 ± 1.8	0.86
Number of seeds/berry	2.6 ± 0.14a	3.2 ± 0.36a	2.1 ± 0.14b	1.9 ± 0.15bc	2.1 ± 0.15b	1.6 ± 0.18c	1.7 ± 0.17bc	< 0.001
TSS (°Brix) ‡	19.1 ± 0.38	15 ± 2.22	18.2 ± 0.43	18.2 ± 1.54	18.4 ± 0.4	18.8 ± 1.26	19.8 ± 0.94	0.54
Total lipids (%)	0.44 ± 0.05bc	0.45 ± 0.07bc	0.36 ± 0.03c	0.45 ± 0.04bc	0.46 ± 0.03bc	0.58 ± 0.04a	0.54 ± 0.04ab	< 0.001

[†] Data expressed as the mean ± standard error (SE) of 20 visually healthy, 21 half- and 20 fully-infected berries; Values within rows with the same superscript letter are not significantly different ($P < 0.05$); ‡ TSS, total soluble solids; E-L, grapevine growth stage (Coombe 1995).

Table 2. Mean log-concentration[†] of fatty acids in deseeded healthy and powdery mildew infected-berries of Chardonnay grapes, conidia of *Erysiphe necator* from naturally infected Chardonnay berries, and conidia and conidiophores of *Botrytis cinerea* from inoculated Chardonnay berries

	Berries								***E. necator***			***B. cinerea***
	Healthy			**Infected**								
				Half		**Fully**						
Fatty acid	**Healthy n = 5**	**E-L 23–26 n = 12**	**E-L 33 n = 3**	**E-L 23–26 n = 13**	**E-L 33 n = 8**	**E-L 23–26 n = 10**	**E-L 33 n = 10**	***P*[‡] value**	**E-L 23–26 n = 3**	**E-L 33 n = 4**	***P* value**	
C14:0	–1.18±0.08	–1.40±0.10	–1.34±0.05	–1.27±0.06	–1.24±0.05	–0.91±0.06	–1.01±0.06	0.001	1.03±1.18	1.65±1.12	0.27	3.43±0.06
C15:0	–1.93±0.10	–2.04±0.11	–2.03±0.07	–1.83±0.08	–1.79±0.07	–1.53±0.08	–1.66±0.08	0.010	ND[¶]	ND		1.86±0.43
C16:0	2.27±0.07	2.21±0.09	2.28±0.04	2.34±0.05	2.36±0.04	2.60±0.05	2.59±0.05	0.010	6.13±0.02	6.41±0.17	0.42	5.54±0.02
C18:0	0.43±0.09	0.23±0.11	0.33±0.06	0.59±0.07	0.58±0.05	0.98±0.06	0.90±0.06	0.001	6.24±0.22	6.50±0.19	0.60	4.36±0.19
C20:0	0.08±0.17	–0.26±0.21	–0.11±0.10	0.77±0.13	0.74±0.10	1.35±0.12	1.19±0.12	**0.001**[§]	7.43±0.33	7.61±0.28	0.48	ND
C22:0	0.08±0.10	0.00±0.13	0.03±0.07	0.38±0.08	0.40±0.06	0.83±0.07	0.72±0.07	0.001	5.63±0.34	5.90±0.29	0.83	ND
C24:0	0.00±0.11	0.06±0.13	0.02±0.07	0.28±0.08	0.29±0.07	0.69±0.07	0.60±0.07	0.001	5.34±0.30	5.68±0.26	0.92	ND
C18:1n–9	1.21±0.08	1.18±0.12	1.30±0.07	1.31±0.01	1.36±0.06	1.55±0.07	1.69±0.06	0.001	5.17±0.28	5.17±0.27	0.94	5.10±0.10
C18:2n–6	2.57±0.06	2.51±0.08	2.58±0.04	2.63±0.05	2.64±0.04	2.84±0.07	2.80±0.04	0.001	5.10±0.43	5.20±0.30	0.99	6.62±0.15
C18:3n–3	1.32±0.09	1.31±0.11	1.31±0.06	1.43±0.07	1.38±0.06	1.70±0.06	1.67±0.06	0.001	4.56±0.35	4.80±0.30	0.79	4.81±0.24
C18:3n–6	–2.02±0.20	–2.47±0.25	–2.28±0.13	–2.17±0.16	–2.18±0.12	–1.78±0.14	–2.06±0.16	0.147	ND	ND		ND
C18:1n–7	–1.22±0.09	–1.32±0.11	–1.10±0.06	–1.09±0.07	–1.04±0.06	–0.86±0.06	–0.90±0.06	0.002	ND	ND		ND
C20:1n–9	–1.99±0.07	–2.12±0.09	–2.11±0.05	–2.11±0.06	–2.16±0.05	–1.92±0.06	–2.12±0.06	0.045	ND	ND		ND
Number of berries with fatty acids under the limit of quantification												
C16:1n–7	1	2	1	3	1	2	3	0.980	NA††	NA		3.04±0.05
C20:2n–6	4	5	3	9	4	8	8	0.270	NA	NA		ND

[†] Data expressed as the natural logarithm LN of the mean ± standard error (SE); [‡] Statistical significance; [§] Statistically significant for healthy, half- and fully-infected berries; [¶] Not detected; †† Not applicable; E-L, grapevine growth stage (Coombe 1995).

Table 3. Classification of 61 berries based on PC3 that had the greatest discriminatory power in stepwise linear discriminant analysis

Visual category of berries	**% of berries predicted to be:**		
	Healthy	**Half-infected**	**Fully-infected**
Healthy	69.47	11.65	18.88
Half-infected	38.58	44.34	17.08
Fully-infected	1.69	38.00	60.30

Table 4. Classification of 61 berries based on four saturated acids (C20:0, C14:0, C15:0, C22:0) and arachidic acid (C20:0) alone

Visual category of berry	**% of berries predicted to be:**		
	Healthy	**Half-infected**	**Fully-infected**
	C20:0, C14:0, C15:0, C22:0		
Healthy	97.46	1.69	0.85
Half-infected	7.61	75.41	16.99
Fully-infected	4.95	22.37	72.68
	Arachidic acid (C20:0)		
Healthy	90.27	9.73	0.00
Half-infected	10.31	71.43	18.26
Fully-infected	0.00	32.78	67.22

(a)

Alverstoke Vineyard											◄ North											
Total Area (ha)	0.3																					
Vine Spacing (m)	2.7																					
Row Width (m)	3																					
Vines per panel	**2**							Panel identified as 'non-hot spot'							Panel identified as 'hot spot'							
											Panel											
Variety	22	21	20	19	18	17	16	15	14	13	12	11	10	9	8	7	6	5	4	3	2	1
Petit Verdot 97V1																						
Chardonnay I10V1 (length 63m)																						
Chardonnay I10V1 (length 73m)																						
Grenache SA137																						

(b)



(c)

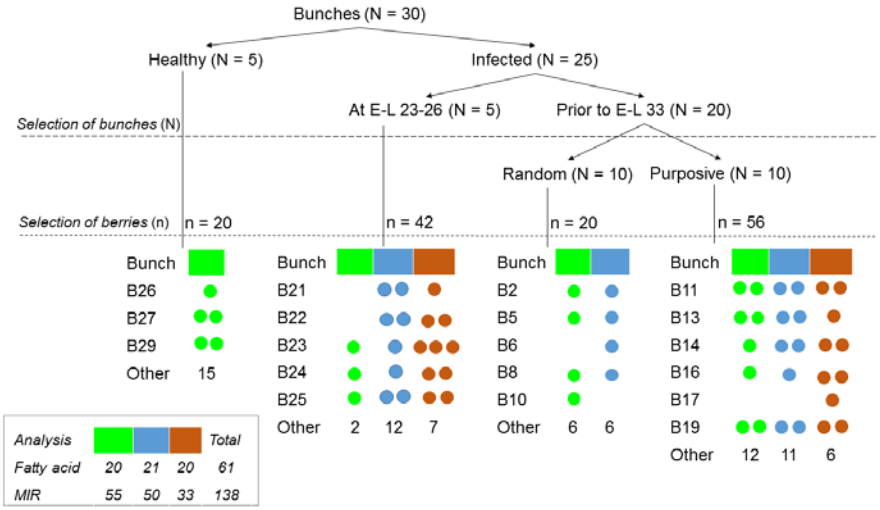


Figure 1. (a) Spatial distribution of panels of Chardonnay vines in the Alverstoke vineyard where sampling was conducted; (b) Powdery mildew-affected bunch with berries representing each of three categories selected for analysis based on visual assessment of surface area affected with powdery mildew: healthy (top), half-infected (middle) and fully-infected (bottom); (c) Sampling strategy for bunches (N = 30) and berries (n = 138), and subsampling strategy per bunch to obtain individual berries for fatty acid analysis: healthy (green), half-infected (blue) and fully-infected (brown). Berries from bunches designated “Other” were used in MIR but not fatty acid analysis. The inset shows the total number of berries used in fatty acid analysis and MIR scanning

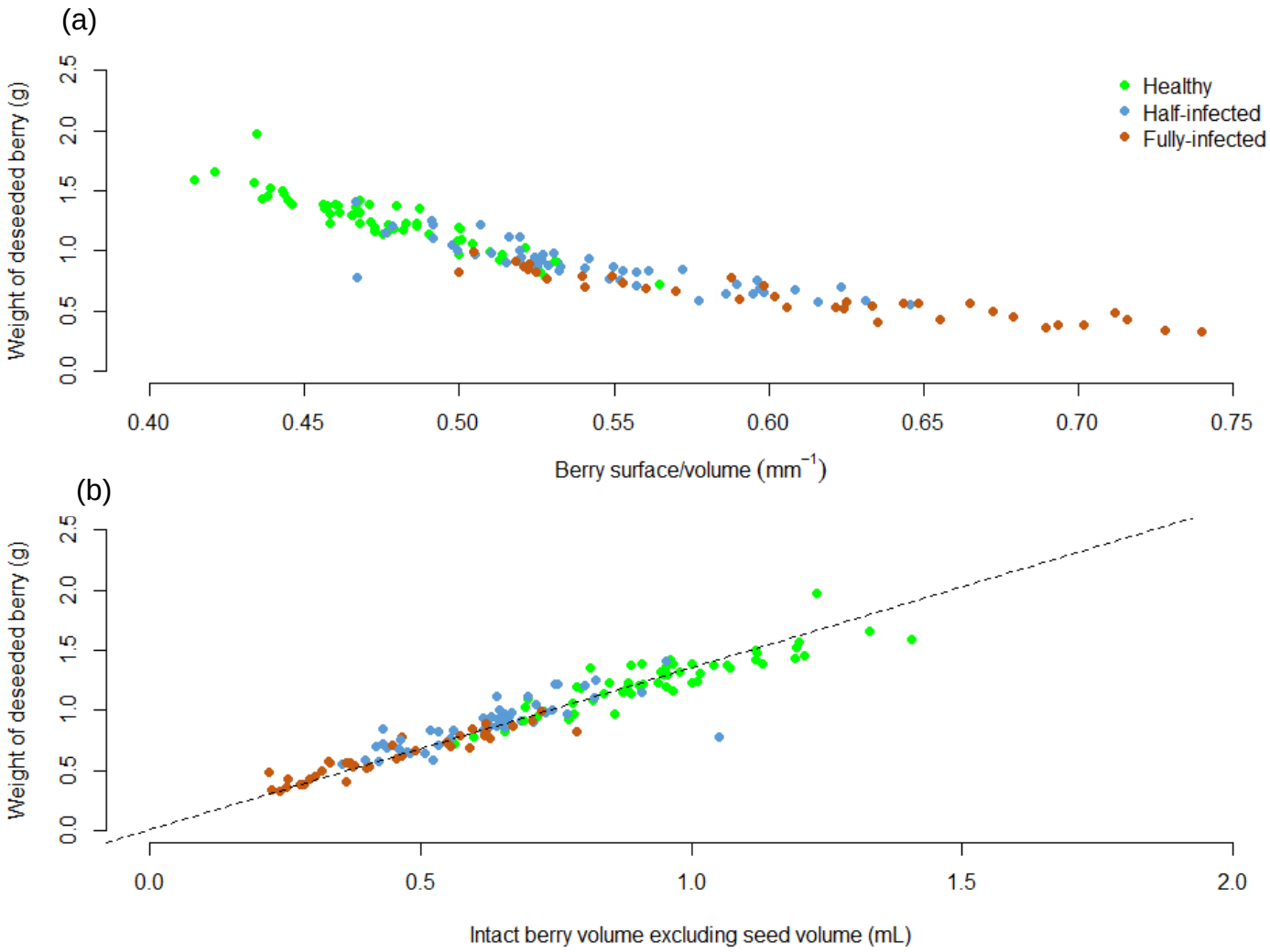
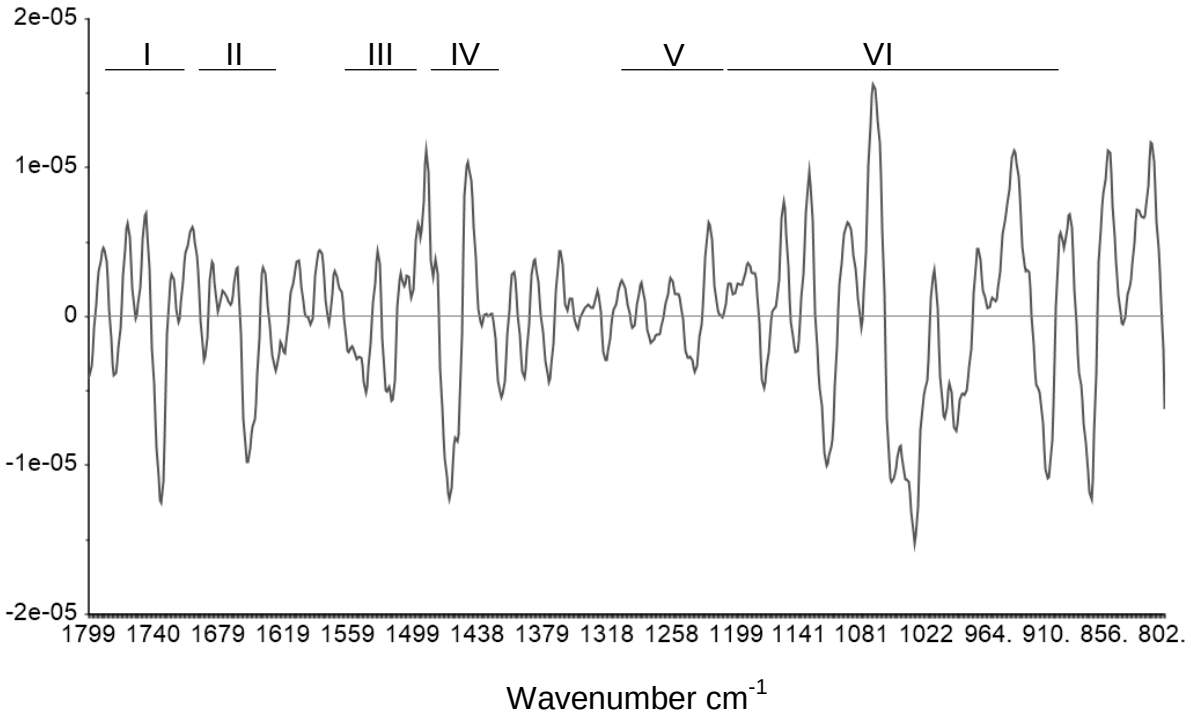
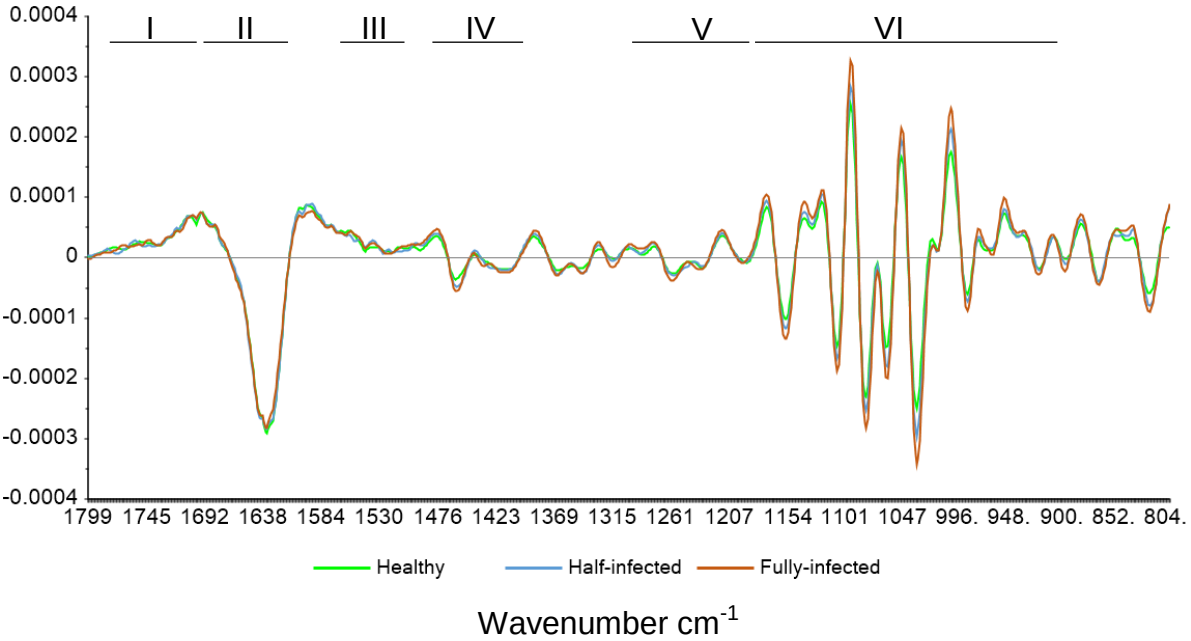


Figure 2. Relationships between weight of deseeded berry and (a) berry surface area to volume ratio, and (b) intact berry volume excluding seed volume

(a)


2e-05
1e-05
0
-1e-05
-2e-05
I
II
III
IV
V
VI
1799 1740 1679 1619 1559 1499 1438 1379 1318 1258 1199 1141 1081 1022 964. 910. 856. 802.
Wavenumber cm-1

(b)


0.0004
0.0003
0.0002
0.0001
0
-0.0001
-0.0002
-0.0003
-0.0004
I
II
III
IV
V
VI
1799 1745 1692 1638 1584 1530 1476 1423 1369 1315 1261 1207 1154 1101 1047 996. 948. 900. 852. 804.
Healthy
Half-infected
Fully-infected
Wavenumber cm-1

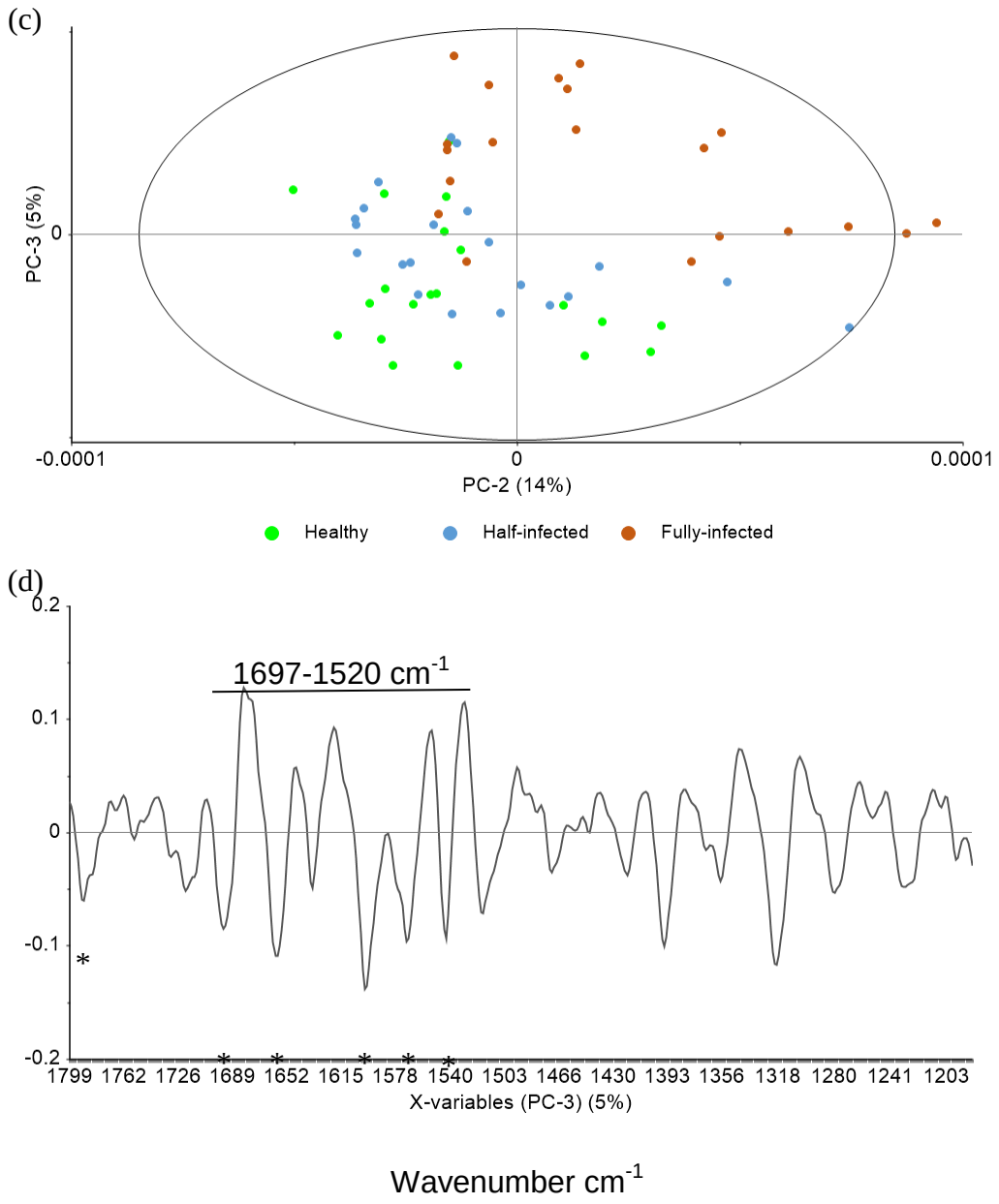
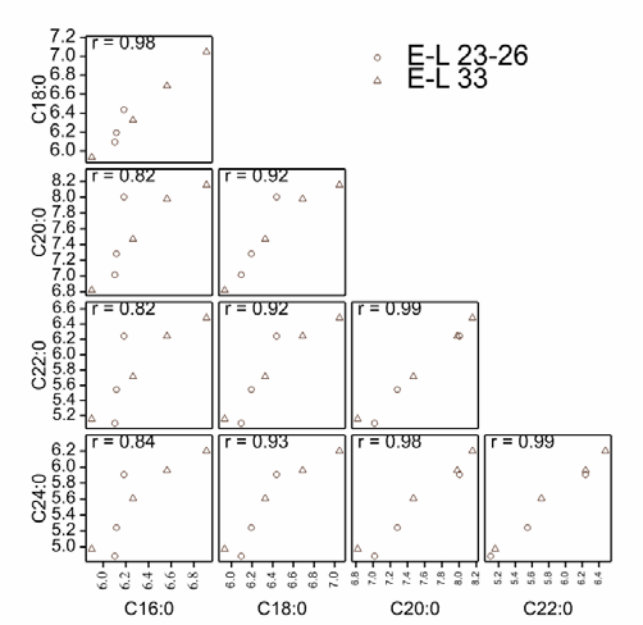


Figure 3. Mid-infrared (MIR) spectroscopic analysis of grape powdery mildew. Second derivative of MIR spectra (1800–800 cm^{-1}) of (a) freeze-dried conidia of *Erysiphe necator* collected from berries and (b) representative visually healthy (green), half- (blue) and fully-infected (brown) berries, main regions of MIR spectra: I fatty acid esters (1780–1700 cm^{-1}), II amide I (1695–1625 cm^{-1}), III amide II (1560–1525 cm^{-1}), IV lipids (1480–1400 cm^{-1}), V nucleic acids (1300–1200 cm^{-1}), and VI polysaccharides (1200–900 cm^{-1}); (c) PCA plot with 95% confidence ellipse showing the distribution of 61 berries and separation of the majority of fully-infected berries (brown) from the half-infected (blue) and healthy berries (green) along PC2 and PC3; (d) the PC3 loadings showing six main peaks that contributed most to separation of the majority of fully-infected from the remaining berries

(a)



(b)

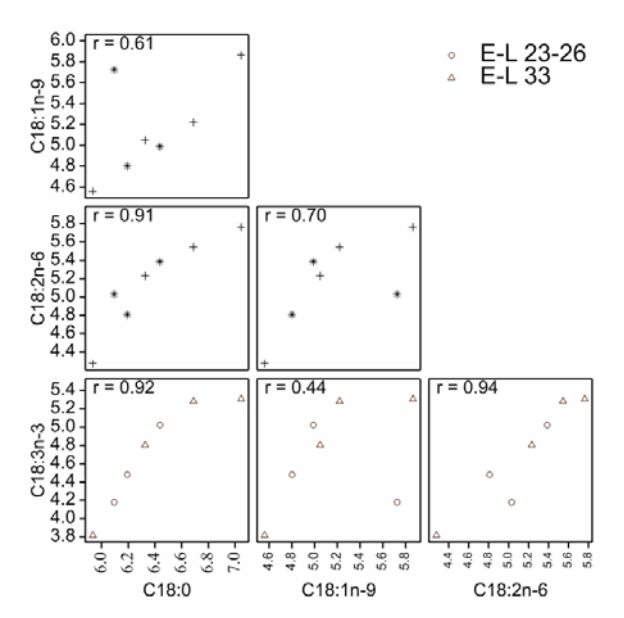
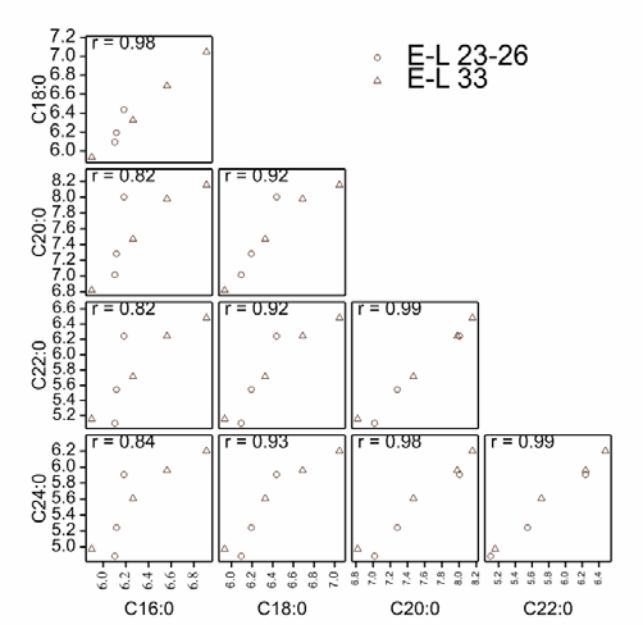


Figure 4. Correlation matrix of log–concentrations for (a) six saturated fatty acids quantified from conidia of *Erysiphe necator* collected from berries infected early (E-L 23–26) and late (E-L 33) in the growing season combined, and (b) C18 and three most abundant unsaturated fatty acids in those conidia. The Pearson correlation coefficient (r) is reported for each pair

(a)



(b)

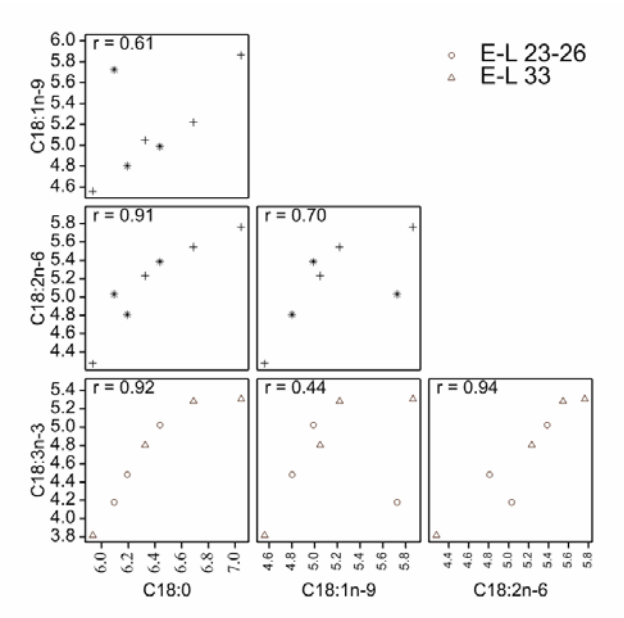
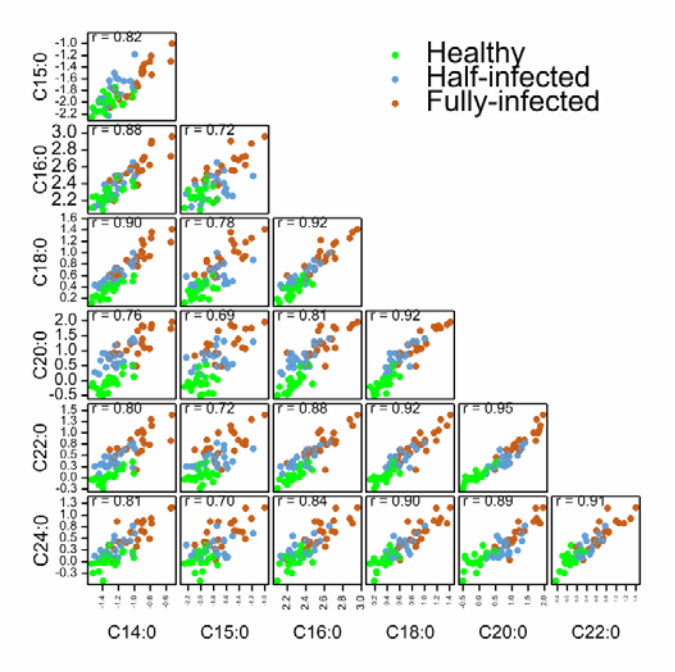


Figure 4. Correlation matrix of log–concentrations for (a) six saturated fatty acids quantified from conidia of *Erysiphe necator* collected from berries infected early (E-L 23–26) and late (E-L 33) in the growing season combined, and (b) C18 and three most abundant unsaturated fatty acids in those conidia. The Pearson correlation coefficient (r) is reported for each pair

(a)



(b)

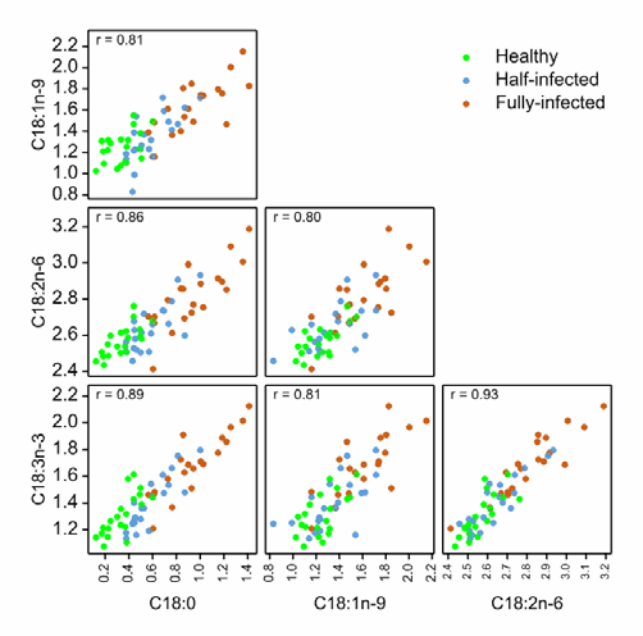


Figure 5. Correlation matrix of log-concentrations for (a) six saturated fatty acids and (b) C18 and three most abundant unsaturated fatty acids quantified in healthy and powdery mildew-infected Chardonnay berries. The Pearson correlation coefficient (r) is reported for each pair

7. Outcome/Conclusion

Improving visual assessment of powdery mildew

The outputs set out in the original application and the project variations instigated by the Project Steering Group in consultation with Wine Australia were achieved. Development of the diagrammatic key, iPhone app and vineyard best practice powdery mildew assessment guide (original application) led logically to preparing the app for Android devices and online resources to support diagnosis and assessment of powdery mildew (variations).

Development of the diagrammatic key with 2% increments in severity at the low end of the scale drew on the considerable experience of the Steering Group through a series of rigorously designed exercises. Although there was no strong evidence that the key improved the quality of powdery mildew assessment in the vineyard, a standardised key is now widely and readily available, through PMapp and the online resource, to assessors who like to use a key.

Development of PMapp drew on the experience of the Steering Group and others, who provided guidance on the components and their design, and tested and provided invaluable feedback on prototypes. That app developer, Wade Perry, had prior experience of working with the wine sector greatly enhanced the process. Simultaneous release of the Apple and Android versions in Australia in time for vintage 2016 resulted in up to 1000 downloads and numerous enquiries from wine sector personnel in New Zealand, Europe, and North and South America indicated that global release in November 2016 will lead to widespread uptake. Feedback from leaders in the Australian wine sector following adoption of PMapp during vintage 2016 has been extremely positive and the app has been credited with improving the agreement between assessments made in the vineyard and at the winery. Although it is designed for assessing powdery mildew, it being used to assess bunch rots; while the images were designed to represent powdery mildew, the components that provide guidance on area assessment and allow efficient recording of severity are applicable to estimating severity of bunch diseases and disorders in general. Quotes provided by users for the joint media release by the University of Adelaide and Wine Australia (Appendix 5.3) attest to the practical benefits of PMapp.

The online resources were designed at the request of the Steering Group, who provided feedback on content and prototypes. The computer code was developed by the most cost-effective and, arguably, least experienced of the developers who provided quotations. While the researchers and developers gained considerable experience through this process, the resource was not ready for release before Australian vintage 2016. The project leader worked closely with Arris to achieve global release in November 2016. While it is too early to gauge uptake and benefits of the online resource, user traffic and feedback will be provided to Wine Australia in due course. The resource has been used in teaching at the University of Adelaide and Charles Sturt University.

Objective measures for powdery mildew

A specific, sensitive and reliable qPCR assay was developed for measuring the biomass of the powdery mildew fungus on grapes. While this proceeded more slowly than planned, in part due to provision of contaminated primers by a supplier which was established only after intensive trouble-shooting, the assay is a robust and accurate research tool and a means of calibrating an industry-friendly objective measure. This aspect of the project is being written up for publication in a scientific journal.

Near and mid-infrared spectroscopy did not prove sufficiently sensitive to discriminate between bunches of grapes with small increments in powdery mildew severity. The encouraging results obtained in the CRC for Viticulture and GWRDC project UA08/05 were based on relatively broad severity categories and, when batches of grapes with increments of 0.5-2% severity at the low end of the scale (0-12%) were manufactured in the laboratory on a weight for weight basis (diseased berries being lighter than healthy berries), critical severities, e.g. 3 and 5%, could not be distinguished from neighbouring categories. This was true of MIR applied to Chardonnay, Riesling, Grenache and Pinot Noir berries. NIR proved problematic as expertise for reading spectra was no longer available in Adelaide and an attempt to conduct analyses in a commercial setting at Berri was unsuccessful due to equipment failure. However, MIR analysis suggested that fatty acid ester content changed in powdery mildew-affected berries, prompting fatty acid profiling.

The fatty acid, arachidic acid, was identified as a biomarker for powdery mildew on grape berries, and reliably differentiated healthy, moderately and severely diseased grape berries. Arachidic acid is not found in the pathogens which cause downy mildew, botrytis bunch rot or ripe rot. Medium to long-chain fatty acids were chosen as the biochemical component to measure in place of ergosterol, which

is absent from the grapevine powdery mildew fungus. The work was facilitated by the expertise, close proximity and invaluable assistance of staff at the Waite Lipid Analysis Facility. A paper on this work has been submitted for publication in the Australian Journal of Grape and Wine Research.

Training

Dr Tijana Petrovic was appointed to the postdoctoral position vacated by Dr Belinda Stummer 2 months after the project began. Dr Petrovic began work in July 2013, alongside Mr Timothy Zanker. Both staff expanded their skills in qPCR and Dr Petrovic acquired new skills in conducting spectroscopy and analysing MIR and NIR spectra as well as in interpreting results of fatty acid analysis. She attended a CAMO Software course “Multivariate Data Analysis 1 with The Unscrambler X” (Sydney, 29-30 September 2015). Mr Zanker attended an ImageJ Workshop (Adelaide, 7-8 July 2015).

Ms Dilhani Perera undertook honours on aspects of this research and, at the suggestion of collaborator Dr Daniel Cozzolino, conducted preliminary work on fatty acid analysis, under the supervision of project staff Drs Tijana Petrovic, Olena Kravchuk and Eileen Scott, and with guidance from Dr Cozzolino. She also gained skills in preparing grape samples for MIR spectroscopy and in writing both her thesis and a draft manuscript. After completing her honours year in June 2015, she conducted some further work on the project then was successful in obtaining a PhD scholarship at Charles Sturt University.

Ms Jessamy Bennett undertook a University of Adelaide summer scholarship in 2014-15 and gained experience in plant pathology, microscopy and culturing *Botrytis cinerea* as well as contributing to a manuscript.

8. Recommendations

The principal recommendations arising from the outcomes of research project UA1202 are below.

Objective measures and effects of precisely known powdery mildew severity on wine quality:

- Investigate the use of arachidic acid, alone or in combination with behenic, myristic and pentadecanoic acids, to quantify powdery mildew on bunches, in must and free-run juice of popular white and black grape varieties when calibrated using the qPCR assay, including
    - Abundance of fatty acids in grapes with powdery mildew when exposed to abiotic (heat, UV radiation, fungicides) and biotic (other microorganisms) stresses
- Investigate the role of arachidic and related fatty acids in negative sensory attributes of wines, such as oily-viscous and irritating mouth-feel identified in Chardonnay wines made from powdery mildew-affected grapes. Arachidic acid is an obvious candidate as it imparts (as free fatty acid) such mouth-feel characteristics to food and can be precisely quantified.
    - Define relationship between arachidic acid content of grape must, juice and wine and sensory characters of juice and wine (tasting panel with identified sensitivity to arachidic acid);
    - Study effects of vinification process on content and perception of arachidic acid content in wine made from grapes with powdery mildew (quantified using the qPCR assay);
    - Explore assay for arachidic acid from juice and wine collected on “blood spot paper” patented and being developed by Waite Lipid Analysis Services for medical use.

Improvements in visual estimation of disease, pending adoption of objective measures:

- Maintain the currency of PMapp by investing resources to upgrade the software. The app developer advises that the current version will function for several years before major upgrade is required to comply with continual upgrading of operating systems.
- Support development of version 2 of PMapp to encompass improvements and additions suggested by the Project Steering Group and participants in workshops as follows:
    - The severity assessment screen can be customised so that frequently-used buttons stand out and to record if disease is active or inactive and rachi and micro-berries are symptomatic;
    - Link PMapp to Google maps to allow distribution of disease in the vineyard to be captured in a “heat map”;
    - Add to PMapp a sampling design functionality for simple random sampling of vines for assessment;
    - Develop materials for parallel assessment of diseases (e.g. bunch rots, leaf powdery and downy mildew) and disorders (e.g. sunburn, bird damage). This would require additional assessment screens in different colours and creating images that show entire berries affected, as well as leaf area affected.
- Support improvements to the online resources that support PMapp:
    - Improve user engagement by making the disease recognition exercise more interactive, e.g. ask the user to outline berries/areas of the bunch with symptoms;
    - Exploit developments in technology that will allow the use of 3-dimensional images of bunches to improve experience of recognising powdery mildew so that spore-bearing structures on the berry surface can be seen more clearly;
    - Expand the website to include materials to support assessment of other diseases and disorders (as noted above) that might be added to the app in future.
- Investigate the use of ranked set sampling, using the vineyard assessment guide and PMapp, to improve the accuracy, efficiency and cost-effectiveness of in-field disease assessment.

Appendix 1: Communication

Publications

Petrovic T, Perera D, Cozzolino D, Kravchuk O, Zanker T, Bennett J, Scott ES. Discrimination of powdery mildew-affected grape berries at harvest using mid-infrared attenuated total reflection spectroscopy and fatty acid profiling. Submitted to Australian Journal of Grape and Wine Research

Knauer U, Matros A, Petrovic T, Zanker T, Scott E, Sieffert U. Improved classification accuracy of powdery mildew infection levels of vine grapes by spatial-spectral analysis of hyperspectral images. Submitted to BMC Plant Methods

Petrovic T, Zanker T, Kravchuk O, Scott ES. Development and evaluation of a TaqMan duplex quantitative real-time PCR assay for quantifying *Erysiphe necator* (powdery mildew) on grape bunches. Prepared for submission to Australian Journal of Grape and Wine Research

Petrovic T, Zanker T, Scott ES (2015) Pathogen of the month (April): *Erysiphe necator* Schwein on grapevine. http://www.appsnet.org/Publications/potm/pdf/apr15.pdf

Petrovic T, Bartlett L, Bennett J, Scott ES (2016) Pathogen of the month (January): *Plasmopara viticola* (Berk. & Curtis) Berl. & de Toni. http://www.appsnet.org/Publications/potm/pdf/Jan16.pdf

Articles in industry journals

Birchmore W, Scott ES, Emmett RW, Perry W and Zanker T (2015). Update on smart-phone app for field assessment of powdery mildew. The Australian and New Zealand Grapegrower and Winemaker **622**, 46-47

Emmett R, Scott E, Petrovic T, Zanker T, Evans K, Kravchuk O, Perry W (2015). A diagrammatic key to assist assessment of powdery mildew severity on grape bunches. The Australian and New Zealand Grapegrower and Winemaker, **623**, 46-49

Conference proceedings

Petrovic T, Emmett RW, Zanker T, Evans KJ, Kravchuk O and Scott ES (2014) Improving diagrammatic keys for the assessment of powdery mildew on grape bunches. Proceedings of the 7th International Workshop on Grapevine Downy and Powdery Mildew, Vitoria-Gasteiz, Spain, 30 June -4 July, pp. 23-4

Petrovic T, Zanker T, Perera D, Stummer BE, Cozzolino D and Scott ES (2014) Development of qPCR and mid-infrared spectroscopy to aid objective assessment of powdery mildew on grape bunches. Proceedings of the 7th International Workshop on Grapevine Downy and Powdery Mildew, Vitoria-Gasteiz, Spain, 30 June - 4 July, pp. 122-4

Perera D, Petrovic P, Kravchuk O, Cozzolino D and Scott ES (2014) Quantification of powdery mildew on grape berries. Paper presented at Crush 2014, Adelaide, 25-26 September

Petrovic T, Zanker T, Perera D, Stummer BE, Cozzolino D and Scott ES (2014) Mid-infrared spectroscopy and qPCR as tools to detect and quantify powdery mildew on grape bunches. Paper presented at Crush 2014, Adelaide, 25-26 September

Petrovic T, Kravchuk O, Zanker T, Cozzolino D and Scott ES (2015) Quantitative PCR (qPCR) and mid-infrared spectroscopic (MIR) analyses of powdery mildew on grape bunches. Paper presented at the 20th Biennial Australasian Plant Pathology Society Conference, Perth, Western Australia, 14-16 September, p. 36

Petrovic T, Zanker T, Stummer BE, Cozzolino D and Scott ES (2015) Discrimination of fungi associated with grape bunches using Attenuated Total Reflection Mid-Infrared (ATR-MIR) spectroscopy. Poster presented at the 20th Biennial Australasian Plant Pathology Society Conference, Perth, Western Australia, 14-16 September, p. 162

Scott, ES, Birchmore, W, Emmett, RW, Perry, W, Zanker, T, Petrovic T, Kravchuk O, Evans, KJ (2015) An app for assessing powdery mildew – challenges and next steps. Paper presented at Crush 2015, Adelaide, 20 November

De Bei R, Fuentes S, Scott E, Tyerman S, Gilliham M, Collins C (2016) Grower and research friendly digital tools for vineyard management and assessment. Poster presented at the 10th International Symposium on Grapevine Physiology and Biotechnology, Verona, Italy, 13-18 June

Emmett RW, Scott ES, Petrovic T, Zanker T, Evans KJ, Kravchuk O, Perry W (2016) A diagrammatic key for assessing powdery mildew severity on grape bunches. Poster presented at the 16th Australian Wine Industry Technical Conference, Adelaide, 24-28 July

Scott ES, Birchmore W, Emmett RW, Perry W, Zanker T (2016) PMapp: a new tool to facilitate assessing powdery mildew on grape bunches. Poster presented at the 16th Australian Wine Industry Technical Conference, Adelaide, 24-28 July

Other Presentations

Scott ES. Research on objective measures for powdery mildew. Presentation to Treasury Wine Estates Technical Viticulture Team, Penfolds Magill Estate, 20 July 2015

Scott ES. PMapp: a tool to facilitate assessing grape powdery mildew. Presentation in Workshop 7, Canopy management using grower-friendly digital tools, 16th Australian Wine Industry Technical Conference, Adelaide, 24 July 2016

Scott ES. PMapp: a tool to facilitate assessing grape powdery mildew. McLaren Vale Grape Wine and Tourism Association Viticulture Conference, 13 September 2016. *This presentation led to an invitation to review the McLaren Vale Viticulture Guide, Pest and Disease Management section*

Scott ES. PMapp and supporting website: tools to facilitate assessing grape powdery mildew. National Wine and Grape Industry Centre Workshop on Recent research on major grape diseases and new disease resistant grape varieties, Wagga Wagga, NSW, 16 November 2016

Scott ES and Petrovic T. Updates on progress to Project Steering Group on 10 January 2013, January 2014, 8 January 2015, 10 June 2015, 25 November 2015, 14 September 2016

Other Communications

PMapp, an application for smart-phones and tablet devices released as free download via Apple iTunes Store (https://appsto.re/au/qe-e5.i) and Google Play (https://play.google.com/store/apps/details?id=com.lemursoftware.pmapp).

Website supporting PMapp: pmassessment.com.au

2% increment key (see Appendix 5.1)

Vineyard powdery mildew best practice assessment guide (see Appendix 5.2)

Appendix 2: Intellectual Property:

PMapp and the supporting online resources were made free to access. This was agreed in consultation with the Project Steering Group, including Wine Australia project managers and a representative of Adelaide Research and Innovation. As such, there is no commercialisable project intellectual property associated with these outputs.

Appendix 3: References

References are provided at the end of each section

Appendix 4: Staff

Project staff

Eileen Scott	University of Adelaide (project leader)
Olena Kravchuk	University of Adelaide
Tijana Petrovic	University of Adelaide (Wine Australia research fellow)
Timothy Zanker	University of Adelaide (Wine Australia research officer)
Dilhani Perera	University of Adelaide (Wine Australia honours scholarship holder)
Jessamy Bennett	University of Adelaide (University summer scholarship holder)
Bob Emmett	RW Emmett Horticultural Pathology Research
Katherine Evans	Tasmanian Institute of Agriculture, University of Tasmania

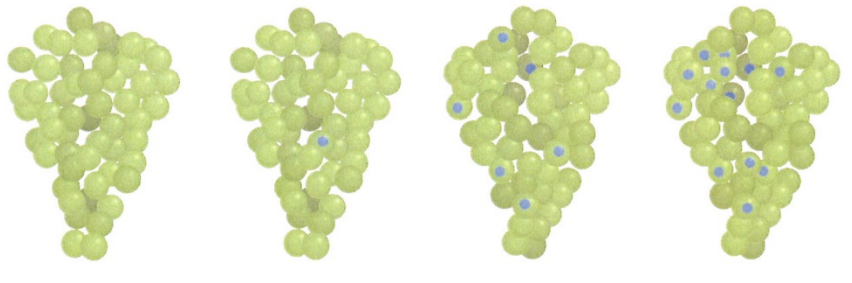
Bob Dambergs	Wine TQ (formerly of the Australian Wine Research Institute)
Warren Birchmore	Accolade Wines
Chris Bevin	formerly of Accolade Wines
Wies Cynkar	Australian Wine Research Institute

Software development for PMapp and online resource

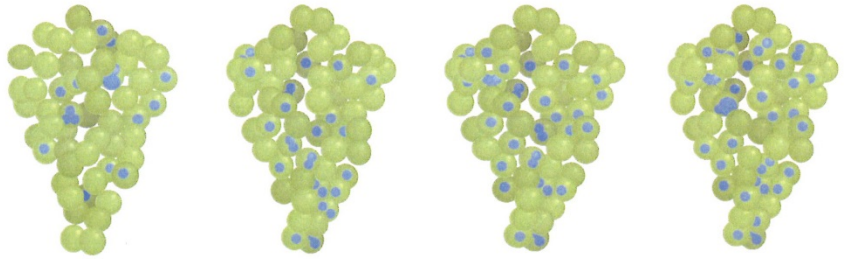
Wade Perry	Lemur Software (app development)
Petros Bakopoulos	GrapeBrain (formerly Seer Insights) (coding for online resource)
Harry Lucas	GrapeBrain (formerly Seer Insights)
Bruno Carrocci	Arris Marketing and Communications (online resource)
Edward Bittner	Arris Marketing and Communications
Bahareh Dehghanian	Arris Marketing and Communications

Appendix 5.1: Diagrammatic key with 2% increments in severity at low end of the scale

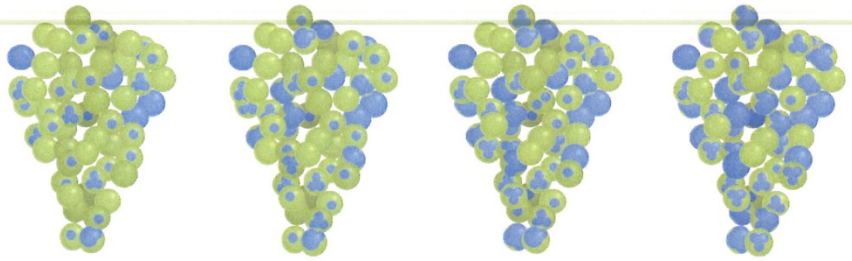
Grape powdery mildew severity assessment key (2% increments in low range)



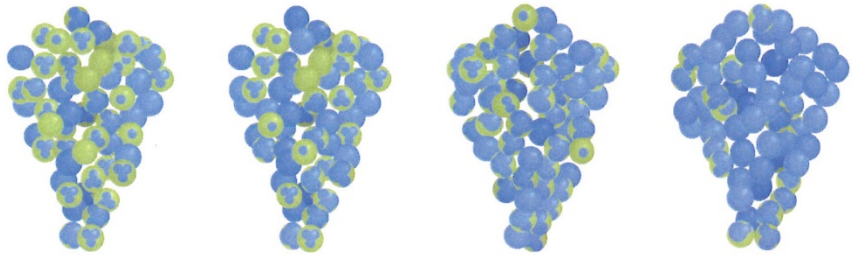
0% (0) 0.5% (0.4) 2% (2) 4% (4)



6% (6) 8% (8) 10% (10) 12% (12)



20% (20) 30% (32) 40% (41) 50% (49)



60% (58) 70% (70) 80% (78) 90% (92)

Note: Name of each image = category percentage and percentage blue measured by ImageJ© analysis in brackets.

© R Emmett, E Scott, T Petrovic, T Zanker, K Evans, O Kravchuk, W Perry

Appendix 5.2. Best practice guide for vineyard powdery mildew assessment

THE UNIVERSITY of ADELAIDE

RWE Horticultural Pathology Research

Wine Australia for Australian Wine

Best Practice Guide for Vineyard Powdery Mildew Assessment

Introduction

This guide provides a summary of information required for the assessment of powdery mildew severity on grapes in patches of vines in vineyards (vineyard patches).

In-field assessments of disease on grapes in vineyard patches are conducted normally in the period from pre-bunch closure to just before harvest. Assessments of powdery mildew severity may be conducted either alone or in combination with assessments of severity of other diseases (e.g. Botrytis bunch rot) or damage affecting the quality of grapes for wine production, depending on wine company protocols. Diagrammatic keys may facilitate assessment of disease severity (Emmett et al., 2015).

Knowledge of powdery mildew history and/or presence and distribution in vineyard patches before field assessments are conducted can be important because it may influence sampling strategies. A review of records of disease severity during crop assessments in previous seasons and/or records of disease appearance and incidence during monitoring (Appendix 1) earlier in the current season may identify parts of patches with disease 'hot spots' that need to be treated differently during field assessment (Allan 2003).

Vineyard assessment flow chart

Key steps for assessors

1. Ability to recognise powdery mildew on grape bunches reliably?

    (a) No – Go to 2.

    (b) Yes – Go to 3.

2. Review symptoms of powdery mildew on grape bunches and other symptoms commonly confused with powdery mildew (powdery mildew recognition tool).

    (a) Yes – Go to 3.

3. Ability to assess severity of powdery mildew on bunches consistently[1] ?

    (a) No – Go to 4.

    (b) Yes – Go to 5.

4. Undertake bunch powdery mildew area assessment training, evaluation and in-field mentoring to develop ability to assess bunch powdery mildew severity consistently. A diagrammatic key is available to assist with area assessment.

    (a) Yes – Go to 5.

[1] Consistently = concordance value ≥ 0.9 in results from area assessment training tool, where concordance value indicates agreement of estimated with actual area of the images assessed.

5. Knowledge of procedures for vineyard patch assessment and calculation of disease incidence and severity scores?

(a) No – Go to 6.

(b) Yes – Go to 7.

6. Review procedures for vineyard patch powdery mildew assessment (Procedure A) and calculation of crop disease incidence and severity scores (Procedure B).

(a) Yes – Go to 7.

7. Conduct vineyard patch powdery mildew assessment and calculate crop disease incidence and severity scores. A free app, PMapp, [Apple products, Android products], has been developed to facilitate recording powdery mildew in the vineyard.

Procedures

A. Vineyard patch powdery mildew assessment

- Select vines and bunches for assessment according to the wine company's protocol, or use the following procedure to make at least 200 observations per patch (Allan 2003):
    - For every 10 ha, select at random at least 200 typical bunches from vines evenly distributed across the patch.
        - Randomly select rows in each patch. For example, if there are 20 rows, select 4 rows (row numbers 2, 7, 12 and 17), 5 rows (row numbers 2, 6, 10, 14 and 18) or 6 rows (row numbers 2, 5, 8, 11, 14 and 17)
        - Walk down each selected row and assess (or collect) a similar number of bunches to give a total of at least 200 bunches from all rows. For example, about 50 bunches from each of 4 rows, or about 33 bunches from each of 6 rows.
        - Bunches to be assessed should be selected relatively evenly but randomly along each row. Where possible, angle each bunch to sunlight so that the fungus can be seen on the berry surface.
    - Rows at the edge of patches, atypical rows and vines in panels at the end of rows should be excluded from sampling and assessments.

B. Calculation of crop disease incidence and severity scores

- Calculation of crop disease incidence (percentage of bunches diseased) and severity (mean percentage of each bunch diseased) should be done using MS Excel spreadsheets or similar software provided by the wine company or vineyard enterprise. PMapp allows the user to view cumulative incidence and severity during the assessment and to email to a nominated email account the assessment data and a summary.

References and further reading (Guide and Appendix)

Allan W. (2003). Winegrape assessment in the vineyard and at the winery. Winetitles, Adelaide SA. pp 7-8.

Emmett R, Scott E, Petrovic T, Zanker T, Evans K, Kravchuk O, Perry W. 2015. A diagrammatic key to assist assessment of powdery mildew severity on grape bunches. Australian and New Zealand Grapegrower and Winemaker, 623, 46-49.

Viti-notes (2010). Monitoring powdery mildew. Australian Wine Research Institute, Adelaide SA. 3 pp.

Appendix 1

Monitoring vineyard patches for powdery mildew appearance and incidence

Early to mid-season (bud burst to just before pre-bunch closure)

Use the wine company's monitoring protocol to select rows and vines for assessment, or use the following procedure (Viti-notes 2010).

- Select vine rows randomly across the patch for inspection.
- Slowly walk along the selected rows and inspect each side of at least 200 vines for disease symptoms, taking up to 30 seconds per vine.
- Record the number of vines inspected.
- If powdery mildew is detected, record the number of vines with symptoms of powdery mildew on any organ(s), i.e. leaves, stems, flowers, berries.
- Determine the proportion of vines with disease, i.e. disease incidence, by dividing the number of vines with disease by the number inspected.
- Inspect vineyards every 2 weeks commencing at E-L Growth Stage 12 (around 2 weeks after bud burst). Combine inspections with other disease monitoring where appropriate.
- Conduct initial inspections in the most disease prone parts of vineyard patches and/or parts with a history of disease, i.e. potential 'hot spots'.
- Early in the season, when vine canopies are open, look for isolated diseased leaves and shoots.
- As the season progresses, focus inspections on dense vine foliage where air movement is poor or where disease occurred last season.

Glossary of Terms

Disease incidence – the percentage of *bunches* affected of the total number of bunches assessed

Disease severity – the percentage of *bunch surface area* affected

Hot spot – a disease-prone area of vines within a patch.

Patch – a defined area of vines within a vineyard.

Appendix 5.3. Media release November 2016

THE UNIVERSITY of ADELAIDE

Wine Australia

Media Release

www.adelaide.edu.au/news

Thursday 17 November 2016

Winegrape powdery mildew app goes global

Grape growers and winemakers around the world will be able to easily assess powdery mildew in the field with the help of a mobile application just released globally.

PMapp, which supports decisions about grape quality, has been developed by the University of Adelaide in close collaboration with the Australian grape and wine sector, and supported by Wine Australia.

“Powdery mildew is a serious disease that affects grapevines worldwide and can cause off flavours and aromas in wine if it is not controlled,” says project leader Eileen Scott, Professor of Plant Pathology at the University of Adelaide’s School of Agriculture, Food and Wine.

“It’s a costly disease for wine sectors across the world through loss of yield and cost of control and, because of the serious quality issues for wine, there is little tolerance of powdery mildew in the winery. But it’s hard to assess – the symptoms can be hard to distinguish from dust or spray residue.

“PMapp is a simple tool that facilitates efficient assessment and recording of the severity and incidence of powdery mildew.”

A local version of PMapp was released in Australia in December 2015 and proved its worth for the grape and wine community during the 2016 Australian vintage. It has now been made available to download outside Australia.

Powdery mildew is assessed in the vineyard as the percentage surface area of grape bunches affected, which gives a measure of disease severity. PMapp allows the user to visually assess the severity by matching it with computer-generated images.

The app allows assessors to enter disease data quickly in the vineyard, email the results and then analyse the resulting spreadsheet, which records GPS coordinates and other details of the assessment.

There is also a suite of online resources to support PMapp. This can be used to train or up-skill wine sector personnel and students to recognise powdery mildew symptoms and estimate disease severity.

Wine Australia’s General Manager Research, Development and Extension Dr Liz Waters says that PMapp is a valuable tool for the grape and wine community. “The PMapp and training website

developers have taken the findings of this comprehensive research project funded by Wine Australia and produced two useable tools for the wine sector," Dr Waters says.

Comments from Australian users over the 2015/2016 season include:

Ian Macrae, CCW Cooperative Ltd: "Although PMapp was developed for assessing the severity of powdery mildew, we used the app for bunch rot assessment as well. Accurate assessment of severity is required when the patch is facing possible rejection. PMapp was a great tool in making decisions acceptable to both grower and winery."

Andrew Weeks, CEO, Australian Vignerons: "PMapp offers potential for a uniform and reliable assessment procedure for powdery mildew, which in turn provides a consistent market signal for winegrowers. This may lead to better understanding of disease control, and ultimately benefits in wine."

Alex Sas, Chief Viticulturist of Accolade Wines: "PMapp will quickly become part of the standard operating procedures of large wine companies in Australia and worldwide."

The PMapp is now available on Apple's App Store or Google Play. The online resources can be found at pmassessment.com.au.